

1	Table des matières	
2	Introduction	6
3	I. Functionalization of PLA via reactive extrusion	9
4	1. Chemical modification of PLA	10
5	1) Peroxide-mediated modification.....	10
6	2) Peroxide-mediated modification of PLA for foaming	15
7	3) Alternatives to peroxide initiated modification	18
8	2. Blend Compatibilization.....	23
9	1) PLA / ABS Compatibilization.....	24
10	2) PLA / PA Compatibilization	26
11	3) PLA / PHBV / PBAT compatibilization.....	27
12	4) PLA / PE compatibilization.....	27
13	5) PLA / PGSMA compatibilization.....	29
14	6) Compatibilization induced by plasticizers.....	30
15	7) PLA / PCL blend compatibilization	34
16	8) Other blend compatibilization.....	35
17	3. Composite Compatibilization	39
18	1) PLA / Carbon fibers or carbon nanotubes composites.....	39
19	2) PLA / food industry byproduct composites.....	40
20	3) Biobased nanocomposites (PLA / CNC or SNC, PLA / CNF)	42
21	4) PLA / lignin or tannin composites.....	46
22	5) PLA / thermoplastic starch composites	49
23	6) Other composites.....	49
24	II. Ring-opening polymerization of lactide via reactive extrusion.....	54
25	1. PLA arising from other catalysts.....	56
26	2. Copolymers	57
27	3. Nanocomposites and complexed PLA	59

1	4. Flame Retardancy.....	62
2	Conclusion	65
3	Bibliography	67
4		
5	Figure 1 Global plastics production from 2016 to 2020 (1).....	7
6	Figure 2 From starch to poly(lactic acid)	8
7	Figure 3 Chemical structure of dicumyl peroxide (DCP) (a) and benzoyl peroxide	
8	(BPO) (b).....	10
9	Figure 4 Chemical structure of used coagents: TAM (a), TMPTMA (b), TMPTA (c),	
10	PETA (d) (19).....	11
11	Figure 5 PMMA-g-PLA (A) and PMMA-g-PHB (B) syntheses by exchange reactions	
12	(21).....	12
13	Figure 6 Grafting of NTA onto PLA via REX (22)	13
14	Figure 7 Grafting reaction of A PLA with MA and B PLA-MA with PEI (25)	14
15	Figure 8 Mass loss as a function of hydrolysis time for low molecular weight unmodified	
16	PLA (PLA1), high molecular weight unmodified PLA (PLA2), low molecular weight PLA	
17	modified with 0.1 wt % DCP and 0.1 wt % TAM (PLA1/0.1/0.1) and with 0.1 wt % DCP	
18	and 0.3 wt % TAM (PLA1/0.1/0.3) (24).....	14
19	Figure 9 SEM images, foam density and cell sizes of neat and modified PLA samples	
20	(14).....	17
21	Figure 10 Schematic mechanism for the free radical initiated grafting of VTMOs on	
22	PLA and mechanism showing the hydrolysis of the methoxy groups and the	
23	condensation resulting in siloxane crosslinked PLA (32).....	19
24	Figure 11 Mechanisms of PLA decomposition and grafting condensation reaction	
25	between PLA and GTMS(33)	20
26	Figure 12 Schematic representation of the chemical structure of acrylated epoxidized	
27	soybean oil (AESO) obtained by acrylation of epoxidized soybean oil (ESO) with	
28	acrylic acid (AA) (41).....	23
29	Figure 13 Cardanol and functionalized cardanol monomers (49).....	25
30	Figure 14 Joncryl structure(51)	26
31	Figure 15 TGA analysis of PLA/HDPE_A and PLA/C2/HDPE and DSC thermograms	
32	of PLA, HDPE and different blends (53).....	28

1	Figure 16 Stress vs strain curves indicating fracture toughness (UT) and appearance	
2	of (A) neat PLA, (B) 80/20 RPLA/PGSMA1 (reaction temperature = 180°C), and (C)	
3	80/20 RPLA/PGSMA2 (reaction temperature = 150°C) (56)	30
4	Figure 17 Schematic representation of physical compatibilization of PLA and EPDM	
5	with EMAGMA and possible chemical reactions and (a) coalescence of dispersed	
6	particles without compatibilizer and (b) inhibition of coalescence with compatibilizer	
7	and possible agglomeration (57)	31
8	Figure 18 Processing and reprocessing procedures of (p)PLA including the main	
9	experimental conditions (61)	33
10	Figure 19 Complex viscosities as a function of angular frequency, $\tan\delta$ curves as a	
11	function of angular frequency, normalized transient stress relaxation moduli, $G^*(t)/G^*(t=0)$,	
12	(measured at 190°C) for PLA, PCL, and compatibilized and non-compatibilized	
13	PLA/PCL (80/20) blends (64)	35
14	Figure 20 Log (σ_{AC}) of nanocomposites at different frequencies (76).....	40
15	Figure 21 Mechanism of chemical reaction among PLA, wood flour and MAH (80).	41
16	Figure 22 (a) Mechanism of thermal decomposition of the DCP into peroxide radicals	
17	during extrusion at $T \frac{1}{4} 180^\circ\text{C}$ (initiation step), (b) Generation of CNC and PLA radicals	
18	followed by reactive extrusion at screw speed $\frac{1}{4} 50$ rpm and recycle time $\frac{1}{4} 2$ min	
19	(propagation step) leading to the formation of PLA grafted CNC structures (termination	
20	step). (c) Pictorial representation of the grafting mechanism of initiation, propagation	
21	and termination of the reactive extrusion process for PLA-g-CNC along the different	
22	zones of the extruder (82)	43
23	Figure 23 (a) Molecular weight distribution, weight average (M_w) and number average	
24	(M_n) and (b) polydispersity index (PDI) of extruded PLA, reactively extruded PLA/CNC	
25	nanocomposites (PLAD, PLADCNC1, PLADCNC2 & PLADCNC3) and reprocessed	
26	PLA-g-CNC gels (rPLA, rPLACNC1(1.35), rPLACNC2(3.33) & rPLACNC3(5.15)) (82)	
27	44
28	Figure 24 Possible reaction mechanism of DCP-initiated grafting of PLA onto CNF (91)	
29	46
30	Figure 25 Tannic acid, a specific compound from the tannin family; is widely applied	
31	to any large polyphenolic compound containing sufficient hydroxyls and other suitable	
32	groups (such as carboxyls)	47
33	Figure 26 Production of tannin-grafted PLA via REX (85)	48

1	Figure 27 Illustration of proposed permeation mechanism through TPS / MTPS and	
2	TPS / MTPS with nanoclays and PLA coating (93)	49
3	Figure 28 Schematic diagram of the manufacturing process including main	
4	manufacturing conditions per stages (98)	51
5	Figure 29 (a) Thermogravimetric analysis (TGA) curves with inset zooming the onset	
6	of degradation; and (b) first derivate thermogravimetric (DTG) and evolution as a	
7	function of temperature of the (c) storage modulus and (d) dynamic damping factor	
8	(tan δ) of the poly(lactic acid) (PLA)/flaxseed fiber (FF) pieces compatibilized with (3-	
9	glycidyloxypropyl) trimethoxysilane (GPTMS), epoxy-based styrene-acrylic oligomer	
10	(ESAO), poly(styrene-co-glycidyl methacrylate) (PS-co-GMA), and maleinized linseed	
11	oil (MLO)(102)	53
12	Figure 30 Reactive extrusion process	55
13	Figure 31 Chemical structure of D,L-lactide (a), glycolide (b) and PLGA (c)(11).....	57
14	Figure 32 Effect of the presence of enzymes in the hydrolysis of the samples for 30	
15	days(119)	59
16	Figure 33 Scheme of the nanocomposites preparation procedure(114)	60
17	Figure 34 Schematic representation of the St-g-PLA/organoclay nanocomposite	
18	synthesis via a shear mixer and reactive extrusion(125).....	62
19	Figure 35 Three-step synthetic pathway to 9,10-dihydro-oxa-10-	
20	phosphaphenanthrene-10-oxide (DOPO)-poly(lactic acid) (PLA) PUs: (A) Synthesis	
21	of DOPO-diamine; (B) DOPO-initiated bulk ring-opening polymerization (ROP) of L,L-	
22	lactide (L,L-LA); (C) chain coupling reaction(127)	64
23		

24

ABSTRACT

25

26

27 Poly(lactic acid) (PLA) is a bio-based, bio-compostable and bio-compatible aliphatic
 28 polyester which derives from lactic acid. The interest for this bioplastic has increased
 29 in the last decade, as search for alternatives to oil-based plastics such as
 30 poly(ethylene) and poly(styrene), becoming compelling. PLA can be manufactured via
 31 two different routes: poly-condensation or ring-opening polymerization. The latter has
 32 been conducted successfully in combination with reactive extrusion (REX) to produce

1 high molecular weight poly(L-lactide) (PLLA) with good mechanical properties.
2 Reactive extrusion is a "green" process, which allows for continuous production
3 without the use of toxic organic solvents. This technique can be paired with in situ
4 chemical modification of PLA and compatibilization with other polymers. This includes
5 the formation of copolymers, branched PLA and composites. The aim of this review is
6 to provide an update on the last eight years of research dedicated to reactive extrusion
7 applications on PLA.

8

9

10

11

Recent advances on reactive Extrusion of Poly(lactic acid)

1
2
3

4 Marie-Odile Augé,^a Daniele Roncucci,^b Serge Bourbigot,^{a,c} Fanny Bonnet,^a
5 Sabyasachi Gaan,^c Gaëlle Fontaine ^{a*}

6 ^a University of Lille, CNRS, INRAE, Centrale Lille, UMR 8207 - UMET - Unité Matériaux
7 et Transformations, F-59000 Lille, France

8 ^b Advanced Fibers, Empa Swiss Federal Laboratories for Material Science and
9 Technology, Lerchenfeldstrasse 5, 9014, St. Gallen, Switzerland

10 ^c Institut Universitaire de France (IUF)

11

12 Introduction

13 Since the 50s, the production of plastics worldwide has skyrocketed to achieve 368
14 million tons in 2019 (Figure 1) but stagnated in 2020 due to the pandemic (1). A huge
15 part of this plastics production is dedicated to short life applications, mainly in
16 packaging industry (40.5 % in Europe) (1), with 150 million tons in 2015 (2). The other
17 part concerns long-life applications such as electronic, transportation, building and
18 construction. As the demand for plastics and their production is growing, the waste
19 plastics production is also increasing and reached 300 million metric tons in 2015 (2).
20 Moreover, a large majority of the plastics are arising for petroleum sources which are
21 in a limited supply. This taken into account, and due to the environmental concerns,
22 more and more academic and industrial studies are dedicated to the development of
23 bioplastics.

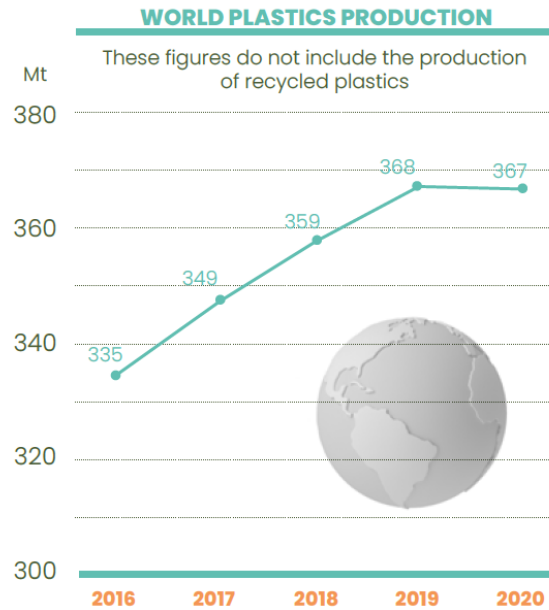


Figure 1 Global plastics production from 2016 to 2020 (1)

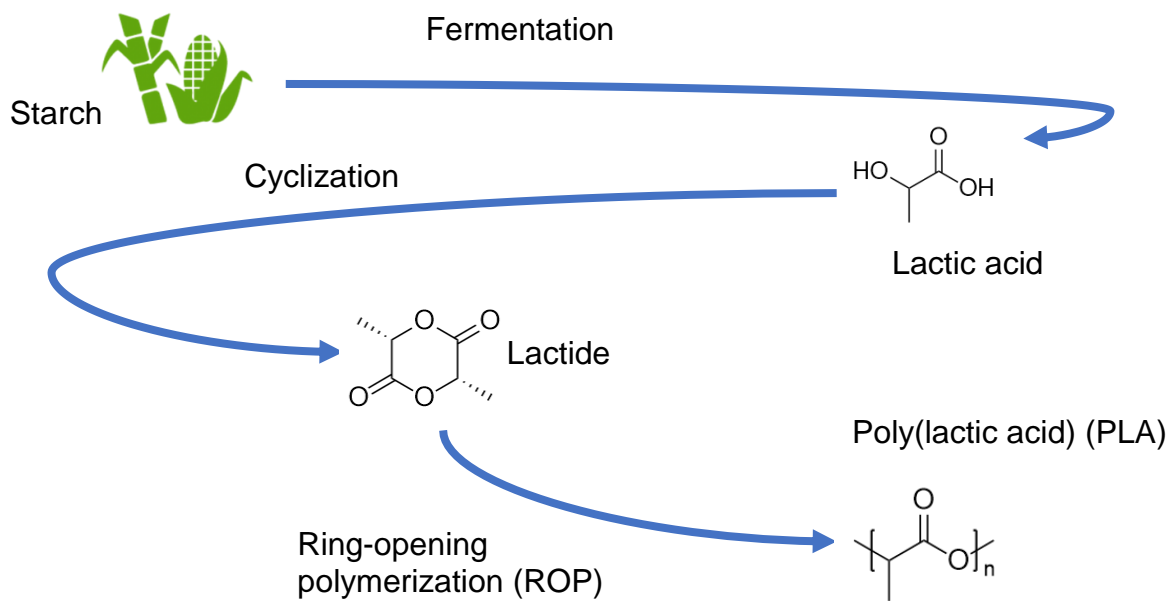
1

2

3 Although they only represent a minor part of the plastic production (circa 1 %),
 4 bioplastics are in a growing phase (3). Their use is still limited due to economic
 5 considerations, such as high production costs, and also inferior mechanical
 6 performances compared to usual fossil-based plastics (3). However, some biobased
 7 polyesters including poly(lactic acid) (PLA) and polybutylene succinate (PBS) have the
 8 potential to replace fossil-based polymers while fulfilling the requirements for circular
 9 economy, sustainability and properties (mechanical, processability and gas barrier
 10 performance) (3).

11 Among bioplastics, poly(lactic acid) also called polylactide is a bio-based,
 12 biocompatible and compostable thermoplastic polymer. It can be produced from
 13 renewable resources such as cellulose or starch (Figure 2) (3). PLA is synthesized
 14 either by direct polycondensation of lactic acid or by the ring-opening polymerization
 15 (ROP) of lactide (LA), a cyclic ester obtained by the di-cyclisation of lactic acid (Figure
 16 2). Lactide monomer can be either L-lactide, D-lactide or *rac*-lactide (racemic mixture
 17 of L- and D-isomer) but L-lactide remains the most used as poly(L-lactide) (PLLA) is
 18 an isotactic semi-crystalline polymer which displays the best thermomechanical
 19 properties among polylactides. Therefore, as the present review focuses on PLLA
 20 exclusively, PLA will refer to PLLA all along the text. Regarding the polycondensation
 21 process, it requires a continuous removal of water under high pressure, high

1 temperatures and long reaction time, leading to PLA with relatively low or medium
 2 molecular weights. On the other hand, the ROP process can be performed under
 3 milder experimental conditions, in solution or in bulk, giving rise to high molecular
 4 weight polymers in a few minutes without any by-products, making it faster, safer, and
 5 cheaper. Thus, ROP is the most current process involved in the industry for the
 6 production of PLA (4). The production of PLA by ROP can also be conducted by
 7 reactive extrusion (REX) (5,6), a process that requires the use of an extruder as a
 8 reactor where the polymerization reaction takes place in a continuous way.



9
 10 *Figure 2 From starch to poly(lactic acid)*

11 PLA displays properties similar to some petroleum-based polymers such as
 12 polystyrene (PS) and polyethylene terephthalate (PET) (7) in terms of mechanical
 13 strength and elastic recovery (8,9). Moreover, this thermoplastic polymer has a glossy
 14 optical appearance and displays good barrier properties toward water, oxygen and
 15 carbon dioxide (10). Thus, PLA can be used as an alternative to polyethylene (PE),
 16 polypropylene (PP), PS for short-life applications such as food packaging or single use
 17 cutlery (8,10). Moreover, its biocompatibility makes it an interesting material for
 18 medical applications such as suture, bone tissue engineering, skin regeneration or
 19 controlled release systems (10–13) in particular, poly(lactic-co-glycolic acid) is a
 20 copolymer that has been studied for its potential medical applications (11–13). PLA is
 21 also used in the textile industry to manufacture household and industrial wipes,

1 diapers, feminine hygiene products, and disposable garments (9). However, its inferior
2 thermal properties, heat distortion temperature, high flammability, and poor elongation
3 at break limit its use (8,13). Commercial PLA often exhibits susceptibility to hydrolysis
4 during processing and low crystallization rate (14). It also has to be noticed that within
5 a few month at 58°C *i.e.* composting conditions, PLA degrades quickly (13).

6 Researches on improving PLA properties mainly focuses on blending PLA with other
7 polymers or fillers to develop blends or composites. Commonly, the PLA blends with
8 other polyesters are immiscible and necessitate the use of chemical compatibilizers.
9 Some research also investigates a more challenging way to chemically modify PLA
10 from lactide which can be done in many ways such as static mixing (15), autoclave
11 (16) or reactive extrusion (6). However, in recent years, reactive extrusion is
12 considered as the most economically viable and environmentally friendly modification
13 technique in polymer processing (4).

14 This review will summarize the state of the art of the chemical modifications of PLA
15 via reactive extrusion. This processing technique is the most used to modify PLA as
16 its implementation is less challenging than the conventional chemical modification
17 starting from lactide. The synthesis of PLA itself via reactive extrusion is also reviewed.
18 This work will focus on the research developed after the publication of the book chapter
19 “*Reactive Extrusion of PLA-based Materials: from Synthesis to Reactive Melt-*
20 *blending*” (4). Indeed, since 2014, the number of publications related to this topic has
21 skyrocketed. Although there exist other reviews on the chemical modification of PLA
22 using reactive extrusion, they primarily focused on more specific topics such as *e.g.*
23 the foaming of chemically modified PLA (16) or the use of maleic anhydride
24 functionalized PLA as a coupling agent (17). Therefore, a more general review on this
25 topic is both relevant and timely.

26 I. Functionalization of PLA via reactive extrusion

27 As already mentioned, PLA displays good gas barrier properties as well as mechanical
28 strength but also inherently low melt strength and other drawbacks. Thus, in order to
29 enhance its properties various routes have been developed to perform PLA chemical
30 modification such as radical-mediated chemical modification, blending PLA with other
31 polymers or adding fillers to develop PLA-based composites.

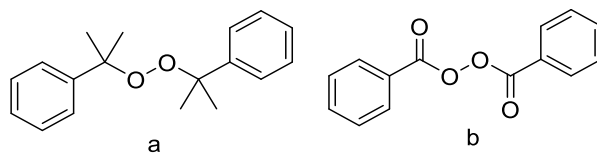
1

2 1. Chemical modification of PLA

3 The most studied method to introduce branching in PLA is the use of peroxide initiators
4 (18–27) that can introduce branching and cross-linking in the PLA macromolecules as
5 well as promote the grafting of acrylate coagents (20–22). Some research on these
6 coagents is based on the development of PLA “green” foams (14,16,28–33). In order
7 to avoid the use of peroxide initiators, several researches are conducted on silanes
8 (34–37), N-acetoxy-phthalimide (NAPI) (18,19), UV-irradiation (38,39) or epoxy-
9 functionalized reagents (40–43).

10 1) Peroxide-mediated modification

11 PLA can be functionalized during the REX process with the help of peroxide initiators
12 such as dicumyl peroxide (DCP) or benzoyl peroxide (BPO) (Figure 3). The
13 macroradicals are formed by H-abstraction from the PLA backbone which allows the
14 grafting of molecules onto PLA (18,19).

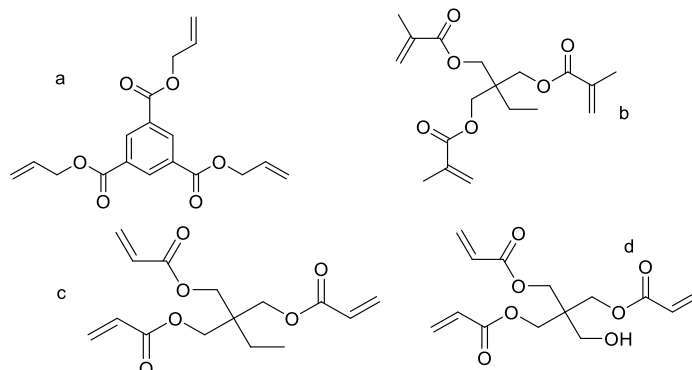


15

16 *Figure 3 Chemical structure of dicumyl peroxide (DCP) (a) and benzoyl peroxide (BPO) (b)*

17 Kontopoulou *et al.*(20–22) investigated the properties of branched PLA through
18 different approaches. In a first study, the same branching strategy *i.e.* using triallyl
19 trimesate (TAM) and DCP, was used to determine the structure-property relationship
20 of branched PLA (20). The branching of PLA via peroxide-mediated REX provides a
21 way to obtain PLA with enhanced crystallization kinetics and melt strength (20).
22 Moreover, this process does not affect mechanical properties, nor the short-term
23 decomposition profiles. Branched PLA displays high molecular weights resulting in an
24 unnotched Izod impact strength twice higher than neat PLA (34 kJ.m⁻² vs 17 kJ.m⁻²)
25 (20). This study also demonstrated that various branched PLA can be designed by
26 changing the amount of cross-linking agent. Therefore, branched PLA could be
27 specifically designed to display properties that can meet the requirements of various
28 industrial processes (20). Finally, a comparison was made between co-agent modified
29 PLAs where peroxide-mediated REX was performed with allylic coagent (TAM) and

1 acrylate coagents *i.e.* trimethylolpropane trimethacrylate (TMPTMA),
2 trimethylolpropane triacrylate (TMPTA) and pentaerythritol triacrylate (PETA) (Figure
3 4) (21).

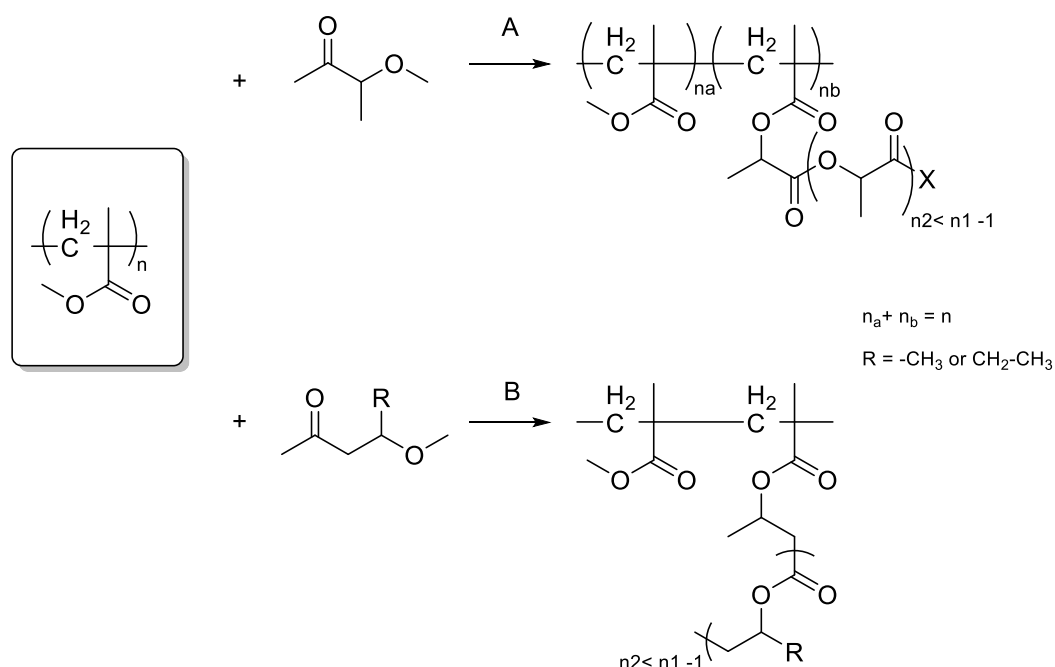


4
5 *Figure 4 Chemical structure of used coagents: TAM (a), TMPTMA (b), TMPTA (c), PETA (d) (21)*

6 Thus, the use of PETA as crosslinker led to low branch densities and a small increase
7 of the activation energy for flow whereas TMPTMA was not able to increase the
8 activation energy (21). Usually, the activation energy values are related to the branch
9 density (21). Therefore, values around 75 kJ.mol⁻¹ witness lower levels of branching
10 (21). Moreover, due to the steric hindrance of its methyl groups and its tendency to
11 homopolymerize, TMPTMA displayed poor grafting efficiency (21). TMPTA crosslinker
12 was able to introduce branching but larger quantities were needed compared to TAM.
13 Thus, the allylic coagent seems to be a better solution than the use of the acrylate-
14 based crosslinkers. Long-chain branched PLA modified with TAM exhibited higher
15 zero shear viscosity (2700 Pa.s), higher M_w (130 kg.mol⁻¹) and higher activation energy
16 (112 kJ.mol⁻¹) resulting from a higher branching rate (21). Recently, the same group
17 reported advances in peroxide-initiated graft modification (22). Coagents were used in
18 combination with Joncryl ADR 4368 (a commercial chain-extender containing epoxy
19 groups) to perform the chain extension of PLA. Among the tested coagents (TAM,
20 PETA, TMPTA, TMPTMA and triallyl cyanurate (TAC)) TAM was found to be the most
21 effective one (22) inducing higher branching degree with 25 % enhanced impact
22 strength compared to neat PLA. The obtained PLA also displays 48 % crystallinity and
23 has a lower crystallization half time of 0.6 min at 135°C instead of 9.3 min for PLA
24 extended with Joncryl ADR 4368 (22).

25 Another work by Taha *et al.*(23) described the grafting of PLA and poly(3-
26 hydroxybutyrate) (PHB) onto poly(methyl methacrylate) (PMMA). The grafting

1 efficiency is influenced by the temperature, the catalyst and its concentration (23).
 2 Results showed that tin(II) octoate ($\text{Sn}(\text{Oct})_2$) gave rise to blends with the highest
 3 grafting degree compared to those obtained with 1,5,7-triazabicyclodec-5-ene (TBD)
 4 (Figure 5) (23). In another study, the grafting of itaconic anhydride (IA) onto PLA via
 5 REX was done using dicumyl peroxide (DCP) (10). PLA grafted IA displayed altered
 6 thermal properties indeed, the glass transition temperature (T_g) was reduced from 5 to
 7 15 % depending on both IA and DCP contents. Moreover, the crystallinity of PLA
 8 increases depending on the degree of grafting (0-0.75 % determined by titration) (10).
 9 The grafted PLA obtained in the previous two cases (10,23) may be used as a
 10 compatibilizer in blends of PLA with another polymer such as acrylonitrile butadiene
 11 styrene (ABS) or polyamide (PA).



12

13

Figure 5 PMMA-g-PLA (A) and PMMA-g-PHB (B) syntheses by exchange reactions (23)

14 The peroxide-mediated grafting of PLA is also used to obtain long chain-branched
 15 (LCB) PLA (24,25). For example, metal-chelating nitrilotriacetic acid (NTA) ligands
 16 were grafted onto PLA via REX using DCP as peroxide initiator (Figure 6). This method
 17 was developed to produce non-migratory antioxidant PLA-based packaging. The
 18 obtained LCB PLA displayed hydrophobic properties e.g. a contact angle close to 90°
 19 as well as an ability to delay ascorbic acid decomposition which demonstrate its
 20 antioxidant properties.

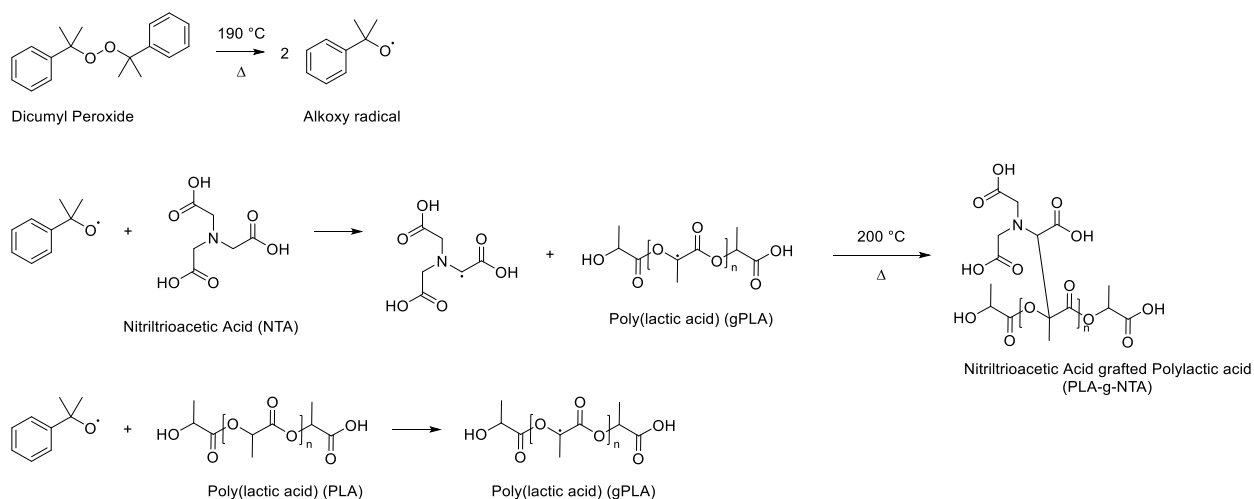


Figure 6 Grafting of NTA onto PLA via REX (24)

1
2
3 Khajeheian *et al.*(25) used the REX process to develop branched PLA in the presence
4 of peroxides *e.g.* tertbutyl-peroxybenzoate (TBPB), 2,5-dimethyl-2,5-di-
5 (tertbutylperoxy)-hexane, Lupersol 101 (L101) and BPO (25). In addition, itaconic
6 anhydride was used as a chain-extender. Depending on the chosen peroxide and the
7 REX conditions (190°C or 235°C), branched and partially cross-linked PLAs were
8 obtained. Due to their enhanced thermal stability, they were proved to be able to
9 withstand several heat treatments which make them re-meltable (25) and tend to
10 suggest that they may be recyclable. The use of L101 to functionalize PLA was
11 recently published by Tachaboonyakiat *et al.*(27) The aim was to graft
12 polyethyleneimine (PEI) onto PLA via *in situ* REX in order to add functional groups
13 along the polymer chain. Therefore, PLA was first modified with maleic anhydride
14 (MAH) using L101 as initiator and then to types of PEI (PEI₈₀₀ and PEI_{25k}) reacted by
15 the ring opening reaction of both anhydride and amino groups (Figure 7) (27). DSC
16 analysis gave insights on the thermal properties of the modified PLA indeed the
17 addition of PEI lowered the T_g compared to neat PLA (56°C vs 58°C). Moreover, the
18 PLA-PEI₈₀₀ exhibited an enhanced crystallinity rate (24% vs 9%). The authors expect
19 PLA-PEI₈₀₀ to display enhanced mechanical properties compared to neat PLA; it
20 should be assessed in another study. Another goal of this work was to study the
21 biological properties of PLA-PEI_x since a few research assessed the antimicrobial
22 activity of PEI and its use in coating for medical devices and drug carriers (27). Results
23 showed that PLA-PEI displayed antibacterial activity against the representative Gram-
24 positive bacterium *S. aureus*. Further research should be done to confirm these first
25 results which may open a wider range of application for PLA in the medical field (27).

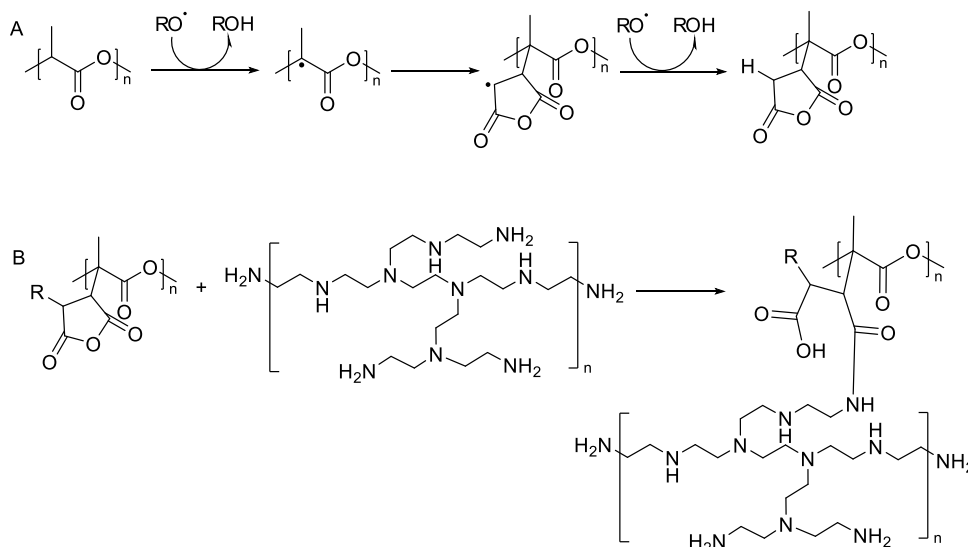


Figure 7 Grafting reaction of **A** PLA with MA and **B** PLA-MA with PEI (27)

Long chain-branched PLA may degrade differently than neat PLA. A study investigated the hydrolytic decomposition of LCB PLA with TAM and DCP as peroxide initiators (26). Mass loss and thermal properties of LCB PLA and neat PLA were evaluated during their exposition at 60°C in an environmental chamber with controlled pH using phosphate buffer solution (26). It turned out that the branching does not delay the hydrolytic decomposition of PLA (Figure 8) (26). However, the mass loss of the modified samples differs from the one of the unmodified PLA. Indeed, low and high molecular weight segments are preferentially degraded and the resulting oligomers have a counter-diffusion effect (26).

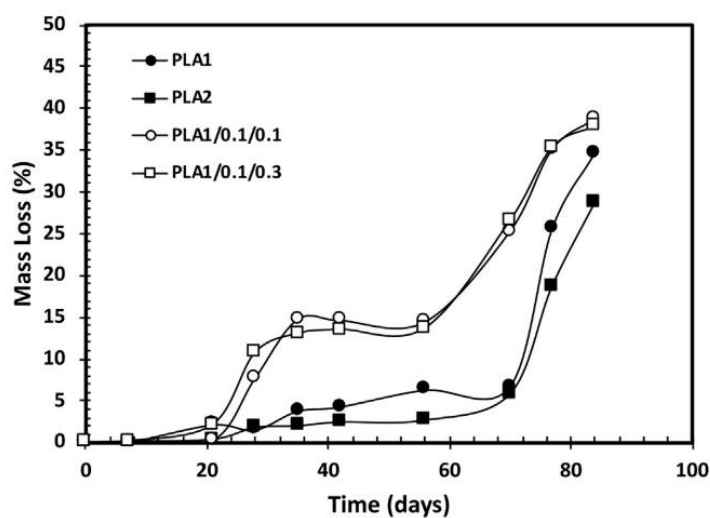


Figure 8 Mass loss as a function of hydrolysis time for low molecular weight unmodified PLA (PLA1), high molecular weight unmodified PLA (PLA2), low molecular weight PLA modified with 0.1 wt % DCP and 0.1 wt % TAM (PLA1/0.1/0.1) and with 0.1 wt % DCP and 0.3 wt % TAM (PLA1/0.1/0.3) (26)

1 Thus, LCB PLA may find applications in fields that require degradable biopolymers
2 with enhanced mechanical properties. Indeed, the previous studies (20–26) showed
3 that introducing branching in the PLA matrix provides a better impact strength but also
4 higher thermal stability. Therefore, since its biodegradability is not hindered by the
5 chemical modification, LCB PLA becomes an interesting material, especially in the
6 medical field or for single-use cutlery. However, a limitation to these studies is the
7 biocompatibility of the used coagents (TAM, PETA, TMPTA, TMPTMA). Indeed, the
8 incorporation of chain extenders may hinder this property of PLA.

9 2) Peroxide-mediated modification of PLA for foaming

10 Industrial sectors including thermal and acoustic insulation, packaging and upholstery
11 are interested in PLA as a green alternative to polymer foams (29). However, the
12 foamability of PLA is poor due to its low melt strength but also due to its semi-rigid
13 molecular structure that induces poor crystallization (28). Therefore, the following
14 studies focus on the improvement of PLA foamability (14,16,28–33).

15 In 2017, a paper presented PLA functionalization via REX using DCP and a multi-
16 functional co-agent triallyl-trimesate (TAM) to develop high density foams (29). The
17 obtained PLA was then foamed using supercritical nitrogen. The results showed that
18 the modified PLA displayed enhanced nucleation activity allowing the production of
19 foams with higher cell densities (10^{11} cells/cm³) and lower cell sizes than unmodified
20 foamed PLA (29).

21 The aim of Kong *et al.*(30) study was to develop long-chain branched PLA that could
22 meet the requirement of applications above 50°C. Thus, they investigated the use of
23 low-content (0.3 wt %) cyclic organic peroxides (COP) initiators combined to acrylate
24 coagents *i.e.* 1,4-butanediol diacrylate (BDDA), trimethylolpropane triacrylate
25 (TMPTA) and pentaerythritol tetraacrylate (PETA). The results showed that the
26 addition of coagents prevents the formation of byproducts and led to LCB-PLA with
27 enhanced branching degree (30). The heat resistance assessment of the obtained
28 LCB-PLA highlighted an increased crystallinity (24 % vs 8 % for neat PLA) leading to
29 an improved heat resistance *e.g.* the Vicat softening temperature increased up to
30 153°C whereas it is only 60°C for neat PLA. Since its melt strength and crystallinity
31 were improved, LCB-PLA also displayed improved foaming properties. Indeed,

1 polymers with high extensional viscosity and high melt extensivity as well as high melt
2 strength are required for foaming (33).

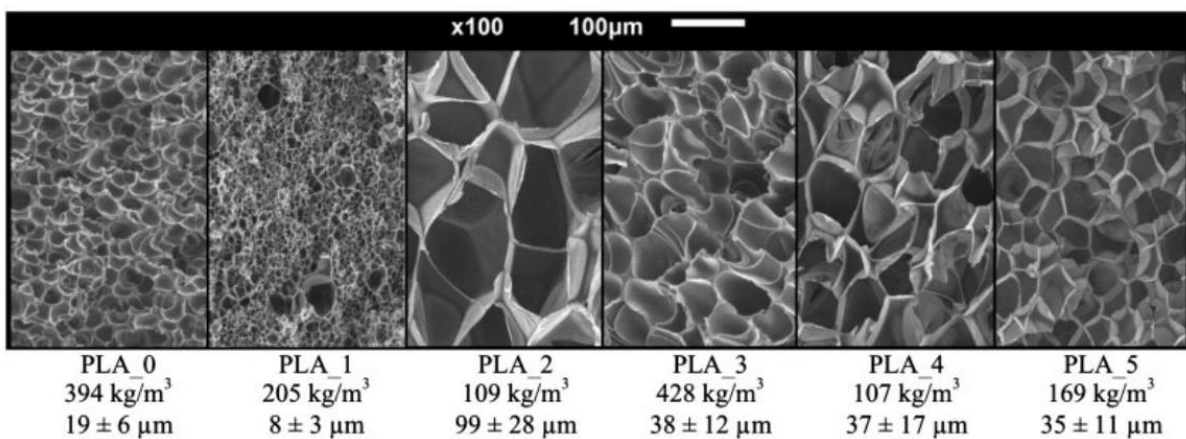
3 Another study used soybean oil (SO) to introduce long-chain branching into PLA (28).
4 Indeed, SO has the advantage to be renewable, biodegradable and non-toxic, thus,
5 the obtained long-chain branched PLA keeps its biodegradability. The branching
6 reaction was initiated by low amount of cyclic peroxide during a REX process. LCB-
7 PLA was foamed via extrusion foaming using supercritical carbon dioxide (28).

8 The foaming properties of chemically modified PLA using REX were also studied by
9 Göttermann *et al.*(31) Tris(2,3-epoxypropyl) isocyanurate (TGIC), hexamethylene
10 diisocyanate (HDI), 1,3-Phenylene-bis-oxazoline (PBO), styrene maleic anhydride
11 (SMA) copolymer, organic peroxide (DCUP), were used as different chain extenders
12 and dicumyl peroxide as the peroxide initiator. The highest molecular weight of
13 $237.600 \text{ g.mol}^{-1}$ was reached using dicumyl peroxide at 0.2 % weight concentration,
14 vs. $130,000 \text{ g.mol}^{-1}$ for unmodified PLA. This resulted in better results than those
15 obtained with Joncryl (multifunctional epoxy) (31). All the reactive blends (except the
16 one modified with TGIC and HDI) display a lower crystallinity compared to neat PLA
17 (25 %). Modification of the backbone hinders the packing of the chains. The lower the
18 crystallinity, the larger the modifier chains and the more PLA chains are hindered in
19 their crystallization. The best thermal or crystallization properties were observed for
20 the DCUP modified PLA (PLA2) even if its crystallinity is just slightly lower than in the
21 neat PLA (20 % compared to 25 %). It is also the only blend that crystallizes during
22 the cooling process. This phenomenon is due to a higher crystallization speed
23 resulting from the branched chains that have a nucleating effect. This leads to a
24 significantly higher melt strength, which is fundamental for extrusion foaming, as it
25 allows the building of a stable foam structure by reducing cell collapse (31).

26 Magaraphan *et al.*(32) reported the use of ethoxylated bisphenol A dimethacrylates
27 (Bis-EMA), which have a rigid difunctional structure and exhibit low water absorption,
28 as a cross-linking agent (32). When introduced with DCP in the PLA matrix, it induces
29 cross-linking of the obtained polymer resulting in the improvement of the storage
30 modulus (up to 3500 MPa at 30°C vs 1900 MPa for neat PLA) and the complex
31 viscosity of PLA. Unfortunately, thermal properties decrease while increasing the
32 amount of Bis-EMA. Indeed, the maximum decomposition temperature ranges from

1 389°C for PLA with 0.3 % of DCP to 385°C for PLA with 0.1 % of DCP and 7 % of Bis-
2 EMA (32).

3 In others studies, Altstädt et al.(14,16,33) investigated the influence of chain extension
4 onto foamed PLA. In a first study, chain extended PLA was prepared with five different
5 chain extenders (CE) (multifunctional epoxide (PLA_1), organic peroxide (PLA_2),
6 styrene maleic anhydride (PLA_3), bis-oxazoline and diisocyanate (PLA_4),
7 isocyanurate and diisocyanate (PLA_5)) using DCP as peroxide initiator (16). The
8 obtained PLAs were then foamed in autoclave (Figure 9). The use of multifunctional
9 epoxide CE or organic peroxide CE led to the highest molecular weights. In particular,
10 organic peroxide allowed the formation of larger cells while foaming due to a high
11 elongation viscosity of the branched polymer. However, the rheological study revealed
12 a viscosity reduction for all modified PLAs due to the onset of degradation after 15 min
13 (16). In a more recent study, the results highlighted the influence of the molecular
14 weight and D-lactide content in commercial PLA. This D-lactide content is usually low
15 *i.e.* from 0.5 to 4% but some commercial PLA can reach 12% of D-lactide content. A
16 suitable foaming of PLA requires, a slow and low crystallization and is dependent of
17 the D-lactide content, the melt strength and the zero complex viscosity of PLA (14).
18 Moreover, the rheological study in the presence of carbon dioxide (CO₂) showed an
19 inhibition of the CE as well as a higher gas diffusion. These parameters need to be
20 taken into account to perform the reactive foam extrusion of the branched PLA (33).



21

22

Figure 9 SEM images, foam density and cell sizes of neat and modified PLA samples (16)

23

24

The previous studies aim to enhance the foamability of PLA in order to develop bio-based foams that will find a use as insulation materials. However, even though the

1 foamability of PLA is assessed, its insulation capacity should be studied as well with
2 a comparison between PLA foam and usual insulation foams.

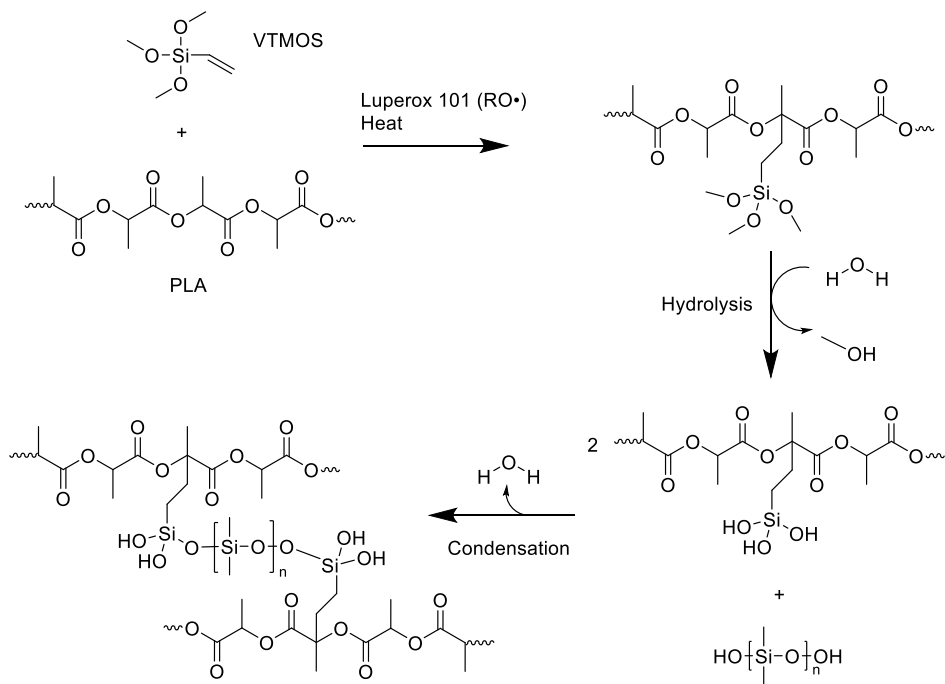
3 3) Alternatives to peroxide initiated modification

4 *Silane mediated modification*

5 The crosslinking of PLA with the help of silane is energy saving (34) compared to usual
6 techniques such as peroxides or high energy radiation initiation. Moreover, it displayed
7 higher productivity and the hybrid polymers contain stable siloxane (Si–O–Si)
8 bonds.(34)

9 Through a free-radical grafting reaction that creates both grafting and cross-linking,
10 Narayan *et al.*(34) produced PLA-grafted vinyltrimethoxysilane (VTMOS). The grafting
11 results from the vinyl function of VTMOS while crosslinks are formed through moisture
12 curing thanks to the alkoxysilane group (Figure 10).(34) The addition of silanol-
13 terminated poly(dimethylsiloxane) allowed the formation of longer siloxane crosslinks
14 (Figure 10). It results in an enhancement of the tensile toughness as well as other
15 mechanical properties *e.g.* elongation at break and impact toughness (28 J.m^{-1} vs 22
16 J.m^{-1} for neat PLA). SEM analysis pointed out that the siloxane crosslinks improved
17 the ability of the hybrid PLA to deform and absorb energy leading to the enhanced
18 toughness.(34) Indeed this technique allows the study of the sample morphology.
19 Therefore, the fractured surfaces of samples that went through tensile and impact
20 testing were analyzed. The SEM pictures showed the presence of white strands
21 corresponding to the siloxane linkage.(34)

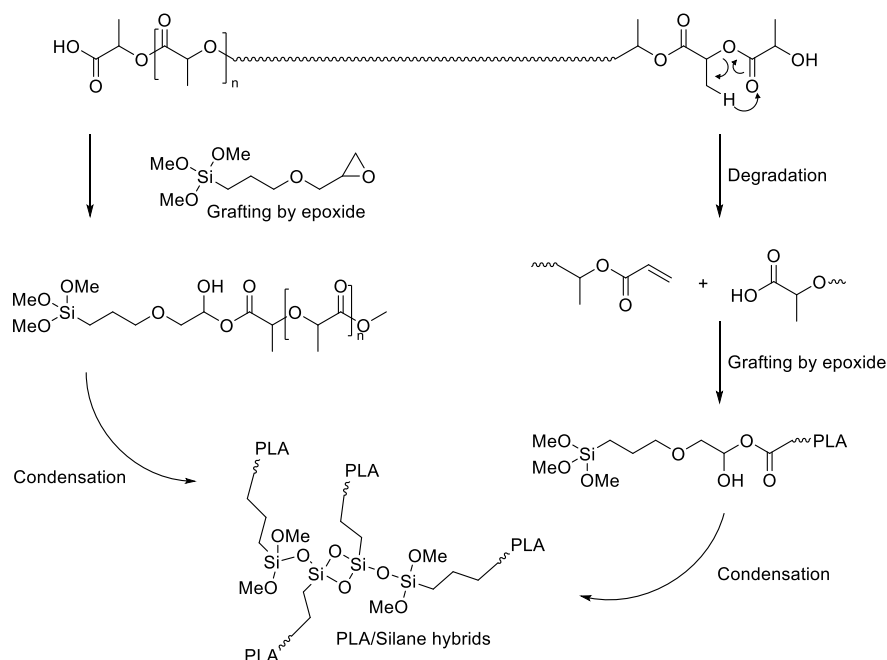
22



1

2 *Figure 10 Schematic mechanism for the free radical initiated grafting of VTMS on PLA and mechanism showing*
 3 *the hydrolysis of the methoxy groups and the condensation resulting in siloxane crosslinked PLA (34)*

4 Ha *et al.*(35,36) prepared hybrid PLA via REX using functionalized silica. In a first
 5 study, epoxide-functionalized alkoxy silanes (GTMS) were grafted onto PLA through a
 6 chemical reaction between the cyclic epoxide groups and the nucleophilic end groups
 7 of PLA (Figure 11). The results of the mechanical tests highlighted the improved
 8 toughness of the hybrid PLA. Especially the complex viscosity of the modified polymer
 9 was increased probably as a result of enhanced topological interactions induced by
 10 GTMS.(35) Moreover, differential scanning calorimetry (DSC) thermograms showed
 11 that the crystalline fraction of the hybrid PLA was doubled in the presence of GTMS
 12 (39 % vs 18 %).(35)



1
2 *Figure 11 Mechanisms of PLA decomposition and grafting condensation reaction between PLA and GTMS(35)*

3 In a second study, tetraethoxysilane (TEOS) was used with a fixed amount of GTMS
4 to functionalize PLA (36). High molecular weights ($M_n = 130\ 000\ \text{g}\cdot\text{mol}^{-1}$) hybrid PLA
5 were obtained and displayed crystallinity rates up to 57 % depending on the amount
6 of TEOS (36). Mechanical properties of the hybrid polymer were positively affected as
7 well as its thermal properties (36). Indeed, the maximum decomposition temperature
8 of PLA hybrids reached 370°C which is slightly better than neat PLA (355°C).
9 Moreover, the storage modulus of the hybrids was increased up to 200 MPa at low
10 angular frequencies vs 80 MPa for neat PLA (36).

11 Alkoxy-modified silanes (phenyltriethoxysilane ($\text{Ph-Si}(\text{OEt})_3$) and *N*-
12 octyltriethoxysilane ($\text{Oct-Si}(\text{OEt})_3$)) were studied to enhance PLA thermal properties
13 as well as its hydrophobicity (37). The contact angle of LCB-PLA was increased (82°
14 vs 69°) indicating better water resistance achieved with the incorporation of Oct-
15 $\text{Si}(\text{OEt})_3$. Moreover, the best results for mechanical properties were obtained by using
16 1.3 % of silane chain-extender *i.e.* Oct- $\text{Si}(\text{OEt})_3$. With these conditions, the elongation
17 at break of LCB-PLA was about 30 %, its tensile strength reached 240 MPa and
18 achieved a Young's modulus close to 5 GPa.(37) However for sample with Ph-
19 $\text{Si}(\text{OEt})_3$, except for the Young's modulus, the same parameters were found to be
20 lower *e.g.* the tensile strength dropped to 177 MPa and the elongation at break was

1 only of 23 % (37). Finally, the TGA analysis shows that the addition of both silane
2 chain-extenders does not hinder PLA thermal properties (37).

3 *NAPI initiated modification*

4 The grafting of PLA with maleic anhydride or itaconic anhydride (10) have been
5 reported in the literature. It is usually initiated by conventional peroxides *e.g.* dicumyl
6 peroxide (DCP) or benzoyl peroxide (BPO) that has the drawback to induce side
7 reactions such as PLA chain scission, branching or cross-linking (18). Monge *et*
8 *al.*(18,19) investigated the use of N-acetoxy-phthalimide (NAPI) as an alternative
9 initiator to the usual peroxides for grafting of PLA via REX. Under heating, NAPI breaks
10 down into nitroxide radicals that combine with the macroradicals of PLA and led to a
11 better control of PLA structure while avoiding the side reactions (18,19). Moreover, the
12 obtained grafting rates were similar to those obtained with the use of peroxides (0.4
13 mol %). However, the optimal concentration of NAPI was proven to be 50 times higher
14 than the one of the reference peroxide initiator (Luperox 101) (19) under similar
15 experimental condition, *i.e.* 200°C (2.5 mol % vs 0.05 mol %) (19). Therefore, the
16 needed amount of NAPI could be questionable. Indeed, peroxide initiated modification
17 requires smaller amount of peroxide initiator.

18 *UV-induced modification*

19 To avoid the use of peroxide initiator, Liao *et al.*(38) developed an ultraviolet-induced
20 REX process that allowed a better control on the side reactions *e.g.* chain scission
21 and branching reactions of PLA. A long-chain branched (LCB) PLA was obtained
22 thanks to the addition of trimethylolpropane triacrylate (TMPTA) into the PLA matrix
23 during the REX process (38). The LCB structure displays nucleating effect resulting in
24 higher crystallization rates for LCB PLA compared to neat PLA (38) which may extend
25 the application field of PLA. Moreover, the obtained LCB polymers are free from
26 peroxides residues. Li *et al.*(39) studied the foaming using supercritical CO₂ of LCB-
27 PLA prepared with the above mentioned protocol. The effect of the long-chain
28 branching structure on the cell morphologies of PLA foams was investigated. The
29 stronger matrix strength and higher nucleation potential of LCB-PLA turned out to be
30 the main reason of its better foaming behavior (39).

1 *Epoxy functionalized coagents*

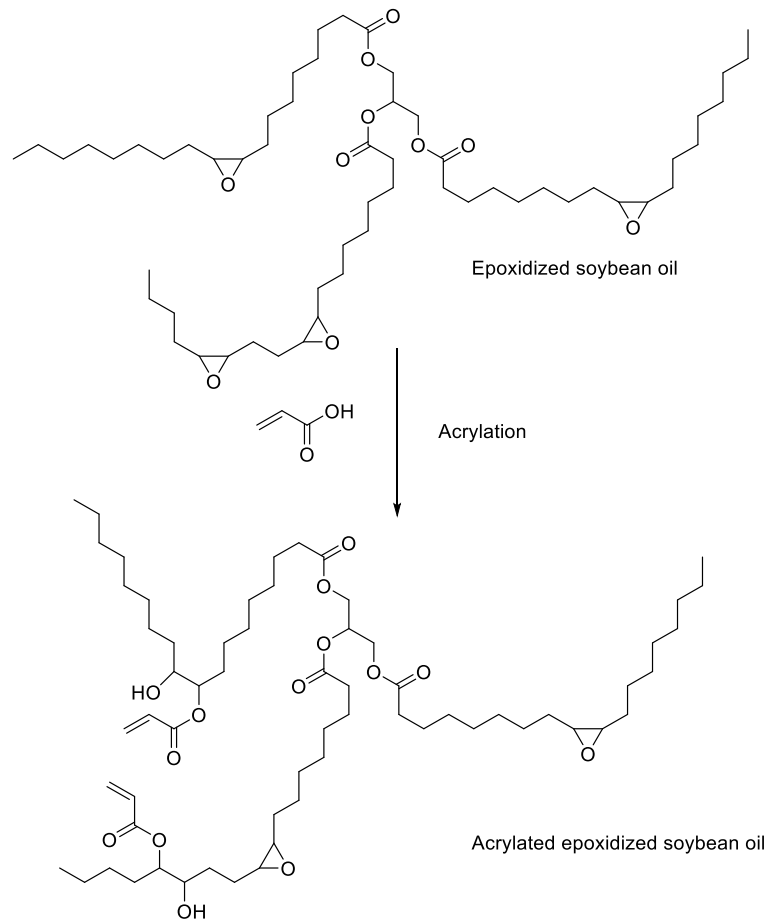
2 The development of chain-extension strategies of PLA may be a solution to overcome
3 PLA tendency to degrade after reprocessing and make it recyclable (40). PLA was
4 modified with a micro lamellar talc as mineral filler, Joncryl ADR 4368 as chain
5 extender (CE) and an aliphatic polyester derived from succinic acid which was
6 supposed to increase the flexibility of the PLA-based blend (40). Chain-extended PLA
7 was then subjected to successive compounding processes. Characterizations of the
8 obtained polymers were performed to assess their rheological, thermal and
9 mechanical properties (40). Results showed that the addition of CE contributed to
10 increase the elongation at break (up to 350 %), to restore partially the molecular weight
11 when reprocessing (40). However, the process need to be improved in order to
12 develop completely recyclable PLA.

13 Tzetzis *et al.*(44) also investigated the use of an epoxy chain extender (Joncryl ADR
14 4400) and studied its influence on 3D printed PLA. Joncryl-modified PLA exhibited
15 enhanced melt flow index (0.37 vs 4.29 g/10 min) and complex viscosity (4000 vs 2500
16 Pa.s). The chain extension also allowed the increase of the molecular weight from
17 75,000 up to 125,000 g/mol. Moreover, mechanical tests revealed that the addition of
18 2 wt% of Joncryl afforded better performances to the modified PLA (44). Indeed, the
19 elastic modulus was increased by almost 400 MPa (3945 vs 3572 MPa) and the
20 hardness went from 142 MPa up to 157 MPa. The chain extension of PLA using
21 Joncryl allowed this research group to print the obtained polymer using the fused
22 deposition modelling process (44).

23 A one-step REX-calendering process was designed by Carrasco *et al.*(41) Their goal
24 was to modify linear PDLLA using a styrene-acrylic multifunctional epoxide oligomeric
25 agent (SAmfE) as reactive agent. The physical ageing and the properties of the
26 obtained LCB-PLA was impacted by the long-chain branching induced by SAmfE.
27 Indeed, the aged samples displayed a slightly enhanced strain at break (2.5 % vs
28 2.2%). The same group also investigated the optimization of the REX parameters and
29 developed an analytical equation. It was designed for the modelling of the kinetic
30 parameters related to the thermal decomposition of branched PLA (42).

31 Quiles-Carrillo *et al.*(43) prepared various blends of PLA / acrylated epoxidized
32 soybean oil (AESO) using REX. The content of AESO (Figure 12) in the blends varied

1 from 2.5 up to 10 %, with 2.5 % increments. After melt compounding, the formulations
2 were injection molded. A slight decrease of tensile strength was observed for
3 specimen with higher load of AESO (the highest decrease was observed for 10 %
4 AESO content having a tensile strength below 60 MPa). However, the elongation at
5 break of modified PLA reached a maximum for the blend containing 10 % AESO (*ie*
6 10.6 % increase) (43).



7

8 *Figure 12 Schematic representation of the chemical structure of acrylated epoxidized soybean oil (AESO)*
9 *obtained by acrylation of epoxidized soybean oil (ESO) with acrylic acid (AA) (43)*

10 2. Blend Compatibilization

11 Reactive and unreactive blending of PLA with other polymer can be an interesting
12 technique in terms of cost, scalability and environmental friendliness (45,46). Using
13 different strategies such as plasticization, rubber toughening, or dynamic
14 vulcanization, PLA with improved properties can be achieved. It can be blended with
15 various oil-based polymers (acrylonitrile-butadiene-styrene (ABS) (46–52), polyamide
16 (PA) (53,54), polyethylene (PE) (55,56)) however it often displays a limited
17 compatibility with them. Therefore, different compatibilization strategies were studied

1 e.g. the incorporation of epoxy agents (53), the use of functionalized soybean oil
2 (43,57) or the addition of cardanol (46,51).

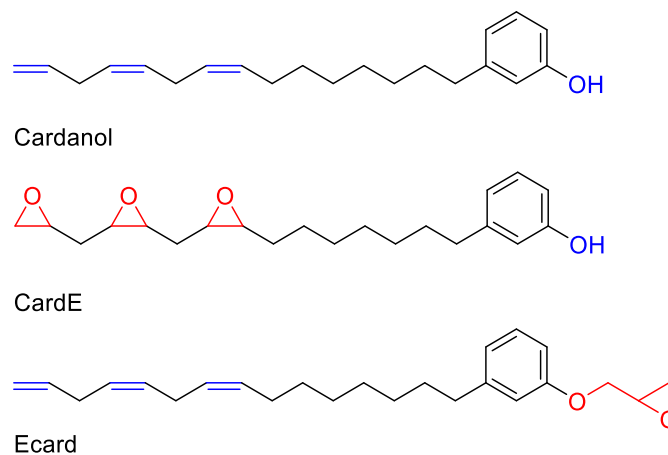
3 1) PLA / ABS Compatibilization

4 When PLA is blended with ABS the interfacial interaction is poor, leading to lower
5 mechanical properties than neat PLA (47). In order to increase the bio-based content
6 in ABS, the latter was blended with PLA (50 / 50 ratio) (48). Both an acrylic copolymer
7 (Biostrenght 9000) and Joncryl chain extenders (ADR-4368C with epoxy functionality)
8 were used to improve the interfacial adhesion between ABS and PLA. The blend
9 containing the acrylic copolymer displays an elongation at break increased up to 140
10 % (vs 5 % for neat PLA and unmodified PLA / ABS blend) (48). The blend containing
11 also Joncryl displayed a lower value while impact strength was increased to 250
12 J/m.(48) In another study, the same group used statistical analysis in order to find the
13 best loadings of each component to improve the mechanical properties. The optimized
14 blend contains 3.6 wt % of acrylic copolymer and 1.2 wt % of chain extender. This led
15 to an increase of the impact strength by over 600 %, the elongation at break by over
16 1000 %, the tensile strength increased by 11 %, while the tensile modulus was
17 increased by over 7 % (49).

18 Carrasco *et al.*(47) produced a PLA / ABS (70 / 30) blend compatibilized by adding
19 styrene-acrylic multi-functional epoxide oligomeric agent (SAmfE). Initially PLA was
20 reacted with SAmfE while ABS was processed with maleic anhydride (MAH). This
21 enables the reaction of the hydroxyl and acid functions of the modified polymers and
22 allows chain extension. Thermal decomposition analysis of the blends showed that
23 temperature decomposition for PLA-REX, ABS and the blend were 335°C, 386°C and
24 303 °C, respectively (47). The same group, in a later study, assessed the
25 decomposition kinetics during polymer processing (50). They compared PLA / ABS
26 and PLA / ABS-g-MAH blends produced via reactive extrusion *i.e.* PLA-REX / ABS
27 (70 / 30) to PLA-REX / ABS / ABS-g-MAH (70 / 24 / 6).(50) The decomposition
28 temperature was increased by 90°C (from 463°C to 553°C) (50) when the
29 compatibilizer was added.

30 In an another work conducted by Verge *et al.*(46) the compatibility of PLA / ABS blend
31 was improved by the addition of cardanol (Figure 13), a bio-based phenolic compound,
32 during the REX process. The authors proved that cardanol is able to react with the

1 polybutadiene segments of ABS via radical pathway. Contrary to what was believed,
2 cardanol grafting occurs on the aromatic ring thanks to the phenolic moiety and does
3 not involve the double bonds of the alkyl chain (46). This group also studied the use
4 of two different epoxidized cardanol monomers *i.e.* CardE and Ecard (Figure 13) to
5 compatibilize the blend of PLA / ABS. CardE was produced by epoxidizing the double
6 bounds while Ecard was obtained by reaction of epichlorohydrin at the phenolic
7 hydroxyl group. Initially, studies were conducted to assess the reactivity of the two
8 different compounds.



9
10

Figure 13 Cardanol and functionalized cardanol monomers (51)

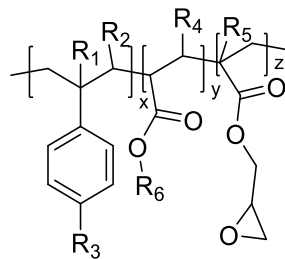
11 These two compounds interact differently with ABS and PLA. PLA / CardE (5 wt %)
12 and ABS / CardE (5 wt %) blends were prepared by extrusion in order to elucidate the
13 mechanism of grafting. For the blend of PLA / CardE no reaction between the
14 carboxylic end groups of PLA and the oxirane ring was observed (51). In turn, this
15 does not result in a simultaneous reaction of the three components. CardE promotes
16 the dispersion of ABS within PLA, however, at content above 5 % neat cardanol had
17 detrimental effect. Trials were also conducted using a mixture of Ecard and cardanol
18 which can both react with PLA and ABS (51). Results shown that with 10 wt. % of a
19 50 / 50 mixture, the PLA / ABS blends displayed an elongation at break up to 82.9 %
20 and an impact resistance of 7.9 kJ.m⁻² (51).

21 The blending of PLA and ABS using maleic-anhydride-modified ABS as the
22 compatibilizer was studied by Abt *et al.*(52) These blends were prepared in three
23 different steps. Modified PLA was first prepared by adding 0.6 wt % of Joncryl via a
24 reactive extrusion process. Then, this PLA was pelletized and mixed with or without
25 ABS / ABS-g-MAH in various proportions (70 / 30 / 0, 70 / 27 / 3 and 70 / 24 / 6). The

1 blends were then extruded, pelletized and injection molded. ABS dispersed in the PLA
2 matrix forms rod-like dispersed morphology which led to a 30 % increase in the energy
3 absorbed up to rupture compared to neat PLA (52).

4 2) PLA / PA Compatibilization

5 PLA / PA11 (polyamide 11) blends were prepared using reactive extrusion (53). These
6 two polymers being immiscible, compatibilization is necessary and was done using
7 Joncryl epoxide (Figure 14) (53). The blends PLA / PA11 (80 / 20 weight %) were
8 elaborate with different amounts of Joncryl. This was conducted by firstly reacting PLA
9 with 4 wt. % Joncryl. Modified PLA was then blended with PLA / PA11 giving blends
10 with 0-3 wt. % of Joncryl. A reduction in PA11 dispersed phases diameter was
11 observed, indicating compatibilization through coalescence suppression. Elongation
12 at break was improved by 3.4 % for blends containing 2-3 % of Joncryl (53).



13 $R_1-R_5 = H, CH_3, \text{higher alkyl or combinations}$
14 $R_6 = \text{alkyl}$
15 $1 < x, y, z < 10$

16 *Figure 14 Joncryl structure(53)*

17 The work of Maazouz *et al.*(54) focused on improving the processability of PLA by
18 reactive extrusion with PA11 with a chain extender (Joncryl ADR®-4368). Two
19 different approaches were used: (i) all the components were added in the micro
20 compounder at the same time or (ii) PLA and the chain extender are pre-mixed in the
21 micro compounder prior to the addition of PA11 (54). Also, different ratios (100 / 0, 80
22 / 20, 60 / 40, 40 / 60, 20 / 80 and 0 / 100) (54) of PLA / PA11 were blended. For the
23 one-step process, the SEM images show a reduction in particle size of the dispersed
24 phase, compared to the blends without Joncryl. However, for the blends obtained in
25 two steps process, there is a better adhesion between the polymer and the dispersed
phases resulting in a reduced interfacial tension (1.37 vs. 2.57 mN/m for
uncompatibilized blend) (54). It was shown that the incorporation of Joncryl in the

1 blend allows a significant improvement of mechanical properties (viz. the elongation
2 at break) increases from 20 % for the PLA / PA11 (80 / 20) blend to 260 % for the PLA
3 / PA11 / Joncryl (80 / 20 / 0.7), however for the pre-modified PLA, the blend PLA-
4 Joncryl /PA11 (80 / 0.7 / 20) showed an increase of 355 %. This was explained by the
5 reaction of the two polymers with the chain extenders allowing better compatibilization
6 of the two phases (54).

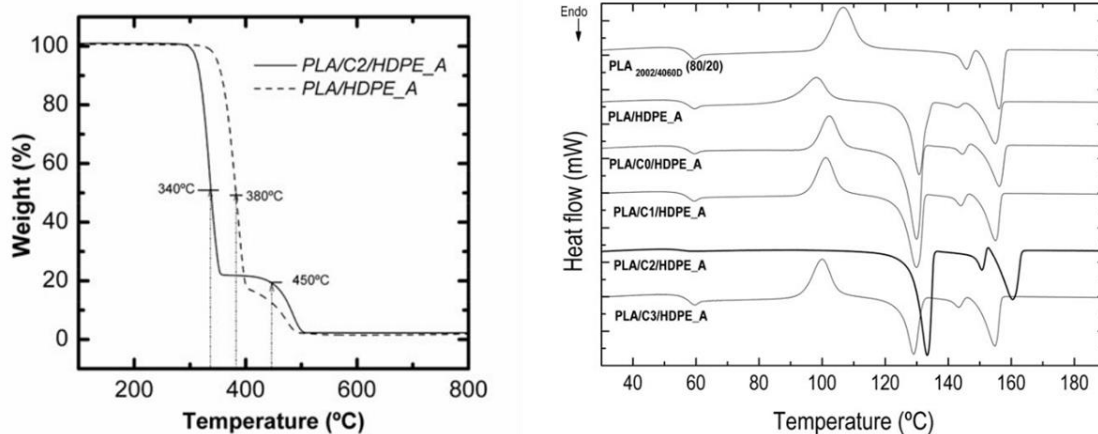
7 3) PLA / PHBV / PBAT compatibilization

8 Quiles-Carrillo *et al.* used reactive extrusion to produce ternary blends of poly(3-
9 hydroxybutyrate-co-3-hydroxyvalerate) (PHBV), PLA, and polybutylene adipate
10 terephthalate (PBAT) (57). These blends were made miscible by adding an epoxy-
11 based styrene–acrylic oligomer (ESAO, Joncryl) which react during melt
12 compounding. Each individual polymer was premixed with Joncryl and then fed in the
13 extruder, subsequently films were made using a press. Different blends were produced
14 with various quantities of each component. The scanning electron microscope (SEM)
15 images, show that for the neat biopolymers blend, small droplets were present in each
16 phase indicating the thermodynamical immiscibility of the polymers. With the addition
17 of Joncryl these phases are still present, however they are reduced in size (600 nm vs
18 in the range of 2-10 μm without ESAO) indicating a better interfacial adhesion. This
19 enhancement is rationalized by the formation of a block copolymer and terpolymer of
20 PHBV-*b*-PLA-*b*-PBAT.(57) After the addition of low-functionality ESAO to the PHBV /
21 PLA / PBAT 1:1:1 blend, the E (elastic modulus) and σ_y (tensile strength at yield)
22 values were improved by more than 10 % and 35 %, respectively, while ϵ_b value was
23 almost 8 times higher. Blends containing the highest amount of PHBV could be used
24 as compostable food packaging. Indeed, they display similar properties to oil-based
25 polymers such as PET, PS and polycarbonate (PC) *i.e.* PLA and PHBV can produce
26 rigid films with an E about 800-1200 MPa and a σ_y about 30-40 MPa (57).

27 4) PLA / PE compatibilization

28 The production of PLA / PE block copolymers by REX using two different reaction
29 pathways was investigated (55). Compatibilizer C1, was prepared by reacting
30 oligomers of PLA with PE-*g*-MAH (polyethylene grafted maleic anhydride).
31 Compatibilizer C2 involves the preparation of polyethylene containing a carboxylic
32 moiety (PE-OH) obtained by polymerizing of ethylene with 10-undecenoic acid. Then,
33 this pre-polymer was reacted with L-lactide via ROP using tin octoate as the catalyst.

1 This route is further developed in the ROP section. Compatibilizer C3 resulted of the
 2 polycondensation reaction of L-lactide with PE-g-MAH. All three synthesized
 3 compatibilizers were compared to a commercial one (C0) which was PE-g-MAH
 4 (Fusabond E226). The blends were then prepared via REX varying the amount of
 5 components: compatibilizer, PLA and HDPE (55). By TGA analysis, a two steps curve
 6 is observed witnessing the immiscibility of the two polymers (Figure 15). This
 7 statement is confirmed by the DSC results (Figure 15). Indeed, the compatibilized
 8 blend show a thermogram close to the one of PLA whereas uncompatibilized blends
 9 displays a 10°C lower cold crystallization exotherm (T_{cc}). Moreover, it can be noticed
 10 that C2 compatibilizer induces a significant shift of the melt endotherm of PLA / C2 /
 11 HDPE_A blend compared to all the other blends. According to the authors, this change
 12 is due to the synthetic pathway of C2 compatibilizer which created a different linkage
 13 between PLA and HDPE. The TGA analysis also show that the decomposition of each
 14 component catalyzes the decomposition of the other. This could be an advantage for
 15 the waste disposal, as a higher degradation rate is observed when the compatibilizer
 16 is present. Regarding the mechanical properties of the PLA / HDPE (80 / 15) blend,
 17 the one containing C2 compatibilizer displayed an elongation at break of 7 % which
 18 represents a 5 % improvement compared to the uncompatibilized blend (55).



19

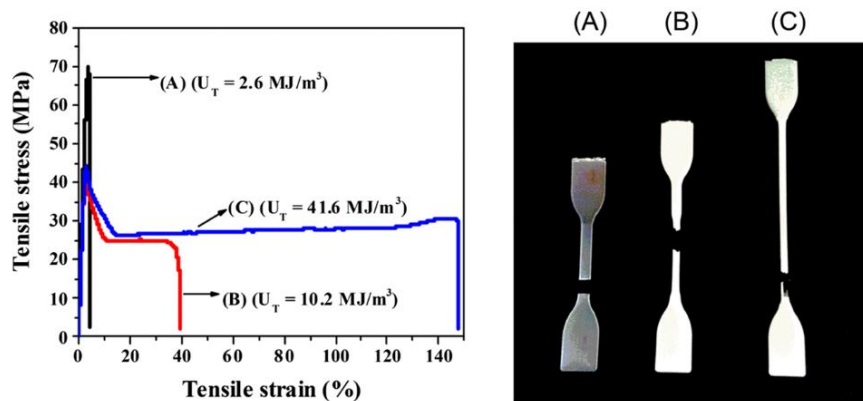
20 *Figure 15 TGA analysis of PLA/HDPE_A and PLA/C2/HDPE and DSC thermograms of PLA, HDPE and different*
 21 *blends (55)*

22 Bäckström *et al.*(56) developed a plasticizer, derived from oxidation of HDPE,
 23 composed of succinic / glutaric and adipic acid. This mixture was obtained by a
 24 microwave-assisted hydrothermal process; this involves oxidation of HDPE in a
 25 solution of a nitric acid with microwave heating. The resulting mixture contains succinic

1 / glutaric / adipic acid in 0.49 / 0.39 / 0.12 ratio. To the acid mixture, 1,4-butanediol is
2 added and polymerization is initiated by heating to 190 °C in order to produce the
3 oligo-ester plasticizer. Then crotonic acid was subsequently added as end-capping
4 group with a molar ratio of plasticizer/crotonic acid of 1/2. The blends were produced
5 by pre-mixing 20 % of the 'recycled plasticizer' with PLA and solution casted.
6 Afterwards, 0.19 mm thickness films were formed using a hot press. Then, Luperox101
7 (0.5 % weight) was added to the films and the resulting products were subsequently
8 fed in the extruder. For the grafted blend the strain at break was increased from 6 %
9 for PLA to 156 %, which corresponds to an increase of 26 times (56).

10 5) PLA / PGSMA compatibilization

11 The elongation at break of PLA was increased by blending with various formulations
12 of poly(glycerol succinate) (PGS) and poly(glycerol succinate co maleate) (PGSMA).
13 (45,58) PGSMA was synthesized using different ratios of glycerol, succinic acid and
14 maleic anhydride.(58) Different parameters such as monomers molar ratio, reaction
15 temperature and time, were varied to obtain a PGS gel and different end-chain
16 moieties. Firstly, PLA / PGS (80 / 20) blends were prepared using REX and their
17 mechanical properties tested resulting in an slightly improved elongation at break (10
18 vs 5 % for neat PLA) (58) and an enhanced crystallinity rate (22 vs 15 % for neat PLA)
19 (58). These results confirm that while using a stoichiometric balance of monomers for
20 the synthesis of PGS, a higher toughness of the PLA / PGS blend can be achieved. It
21 is shown that higher M_w of the PGS enables entanglement with the PLA leading to a
22 higher elongation at break and toughness (Figure 16). Combination of REX and a free
23 radical initiator allowed the grafting and crosslinking of the PLA matrix forming PLA-g-
24 PGSMA copolymers. For an effective toughening of PLA by reactive melt blending
25 with glycerol-based polyesters, the best conditions found for the synthesis of PGSMA
26 were 1 / 0.5 / 0.5 mol glycerol / succinic acid / maleic anhydride synthesized at 150°C
27 for 5 h (58).



1

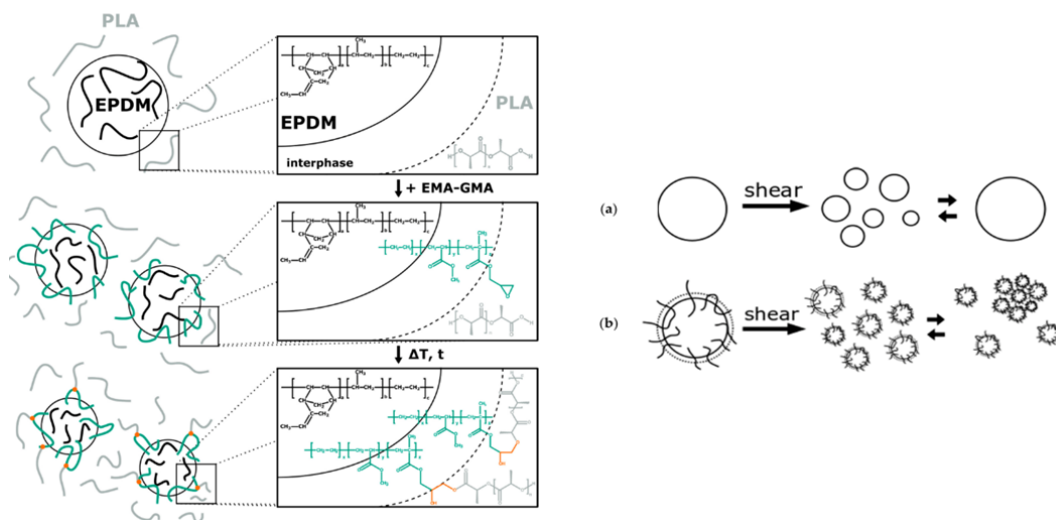
2 *Figure 16 Stress vs strain curves indicating fracture toughness (U_T) and appearance of (A) neat PLA, (B) 80/20*
 3 *RPLA/PGSMA1 (reaction temperature = 180°C), and (C) 80/20 RPLA/PGSMA2 (reaction temperature = 150°C)*
 4 *(58)*

5 Another way to compatibilize PLA with PGSMA is the use of dynamic vulcanization
 6 process.(45) This technique involves both the melt blending and the chemical reaction
 7 between PLA and a secondary polymer as well as the creation of a cross-linked
 8 elastomeric phase in the PLA matrix.(45) The preparation of the blends was done
 9 through reactive extrusion and cross-linking was initiated by Luperox101 peroxide.
 10 Different formulations of PGSMA were produced by varying glycerol, succinic acid and
 11 maleic anhydride amounts. This allowed the increase or decrease of unsaturation on
 12 the copolymer, which will affect the cross-linking density. Thus, it can be concluded
 13 that the main reactions taking place during the dynamic vulcanization of PLA and
 14 PGSMA are the PGSMA self-crosslinking and PLA-*g*-PGSMA formation. In addition,
 15 it was proven that a stronger interfacial adhesion was obtained with increasing of
 16 maleic anhydride amount due to higher PLA-*g*-PGSMA formation. Then a series of
 17 blends of PLA / PGSMA were obtained with a fixed of initiator of 1 % (note that a higher
 18 load of initiator did not improve the toughness). The tensile strength and modulus of
 19 the blends were decreased linearly with the addition of PGSMA due to its elastomeric
 20 properties. The blend of 60 / 40 PLA / PGSMA displayed an enhancement of 53 and
 21 175 % on the elongation at break and notched Izod impact respectively as compared
 22 to neat PLA.(45)

23 6) Compatibilization induced by plasticizers

24 Piontek *et al.*(59) studied the compatibilization effect of bio-based ethylene-propylene-
 25 diene-rubber (EPDM) on PLA. The blends were prepared at different ratios of radical
 26 initiator (poly(ethylene-co-methyl acrylate-co-glycidyl methacrylate) (EMAGMA),

1 soybean oil (SBO) or Tertbutylperoxy 2-ethylhexyl carbonate (TBEC) peroxide). The
 2 addition of EMAGMA increases phase compatibilization between the samples both
 3 with and without the TBEC. The authors claim that the peroxide decomposition and
 4 the radical reactions mainly take place in the PLA phase. Adding EMAGMA to the
 5 blends decreases the initial size of the soft phase and thus increases the interfacial
 6 area (Figure 17) where diffusion of the peroxide between the phases can take place.
 7 This phenomenon results from the inhibition of coalescence due to the addition of
 8 compatibilizer (Figure 17).



9

10 *Figure 17 Schematic representation of physical compatibilization of PLA and EPDM with EMAGMA and possible*
 11 *chemical reactions and (a) coalescence of dispersed particles without compatibilizer and (b) inhibition of*
 12 *coalescence with compatibilizer and possible agglomeration (59)*

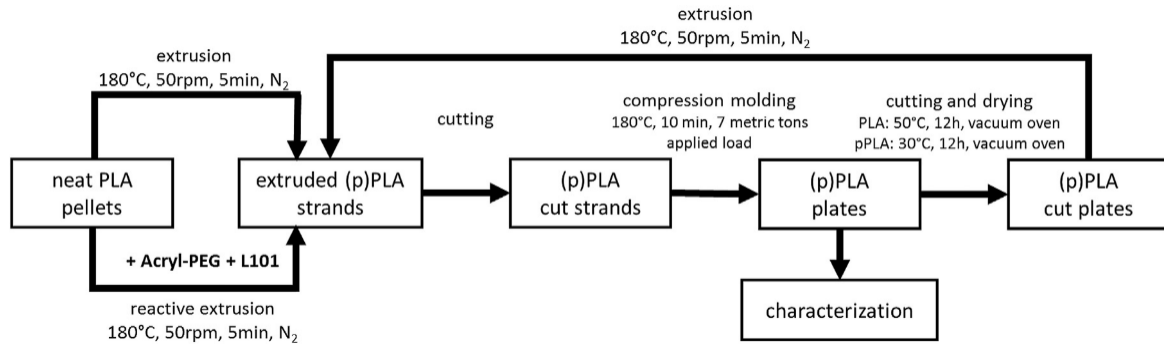
13 The Young's modulus as well as the tensile strength decrease with increasing content
 14 of soft phase independent of TBEC content in the blends. The addition of peroxide
 15 increases the elongation at break compared to the reference samples. The elongation
 16 at break, at first increases with an increasing content of SBO of up to 20 wt % and
 17 then decreases for 30 wt % SBO in the soft phase. This increases the viscosity ratio
 18 *i.e.* the ratio between the viscosity of the dispersed phase (η_D) and the continuous
 19 phase (η_C), which favors droplet breakup of the soft phase leading to smaller particles
 20 and a higher elongation at break. However, while SBO can contribute to the EPDM
 21 crosslinking as a small multifunctional crosslinking agent, it can also decrease the
 22 crosslinking efficiency of EPDM by reacting with the free radicals without bonding to
 23 the EPDM phase. Favorable elongation at break were obtained for an optimum SBO
 24 content of about 20 wt % inside the soft phase.(59)

1 In order to compatibilize oligo(lactic acid) (OLA) with cellulose acetate (AC), plasticized
2 copolymers were prepared by reacting EJ400, a diepoxide, with the OLA and AC via
3 reactive extrusion (60). Initially two different compatibilizers containing 14 wt. % (C1)
4 and 30 wt. % OLA (C2) were prepared. A ratio 4 / 1 (wt / wt) of pAC / compatibilizer
5 blends were prepared beforehand at 230 °C and then blended with PLA at 197 °C in
6 a second step. A consistent increase in torque with respect to the pAC can be
7 observed and can be attributed to the capability of the partially unreacted EJ400 to
8 further react with the pAC at 230 °C determining some occurrence chemical
9 crosslinking which was confirmed by extraction with a solution of acetone / water (90
10 / 10), resulting in a residue of 8 and 11 wt% for the blend pAC/C1 and pAC/Clab1,
11 respectively (60). Also because the OLA has one reactive site, a brush-type structure
12 is expected, due to the ring opening of the diepoxide. The mechanical properties of
13 the blends containing 85 % PLA show a decrease of Young's Modulus, when the
14 amount of C1 compatibilizer is increased. In blends containing only C1, Young's
15 Modulus is increased while tensile strength is decreased, attributed to the formation
16 of interfacial interactions due to compatibilization (60).

17 The use of OLA was also studied by Garcia-Sanoguera *et al.*(61) in order to
18 characterize the mechanical properties of polylactide blends. Therefore, PLA was
19 blended with 10 wt% of OLA and various amounts of DCP (0.1 or 0.3 phr) or
20 maleinized linseed oil (MLO) (3 or 6 phr). The results showed that with 0.3 phr of DCP
21 the PLA/OLA blend exhibited an impact strength of 52 kJ/m² which represents 25%
22 increase compared to neat PLA (61). On the other hand, the addition of MLO also
23 provided an enhanced impact strength to the PLA/OLA blend *i.e.* 60 kJ/m². However
24 both strategies led to a significant decrease of the crystallinity compared to neat PLA
25 (61).

26 Addiego *et al.* studied plasticization of PLA with Acryl-PEG and the effect of
27 reprocessing on the blends (62–64). Different blends were produced by REX: one
28 blank (containing no acrylated poly(ethylene glycol) (acryl-PEG)) and one containing
29 PLA / Acryl-PEG / L101 (79 / 20 / 1 wt%) (62–64). Then recycling-like drill were
30 performed. In a first study, it was done via cycles of extrusion and injection molding
31 (62) and a second work studied cutting / extrusion / compression-molding sequence
32 (CM)(63) (Figure 18). In the first work, the molecular weights of both PLA and
33 plasticized PLA (pPLA) decreases after reprocessing which is due to chain scission

1 (62). However, this effect is more pronounced for regular PLA, as for pPLA the formed
 2 shorter chains may act as plasticizers by increasing the chain mobility. For pPLA the
 3 ultimate strain (ϵ_u) increased from $\epsilon_u = 91\%$ to $\epsilon_u = 127\%$ after the fifth processing cycle
 4 (62).



5

6 *Figure 18 Processing and reprocessing procedures of (p)PLA including the main experimental conditions (63)*

7 In the second work, the specimens were analyzed and characterized after 1 (CM1), 3
 8 (CM3) and 5 (CM5) processing cycles. The plasticization of PLA decreased its tensile
 9 strength as a decrease of ultimate stress s_u from 71.9 MPa for PLA CM1 to 19.4 MPa
 10 for pPLA CM1, and the decrease of yield stress s_y from 77.9 MPa for PLA CM1 to 26.6
 11 MPa for pPLA CM1 was observed (63). The main decomposition mechanism of PLA
 12 is random chain scission, which lowers its molecular weight (from 289 kg/mol to 154
 13 kg/mol) and increases crystallization. However, for pPLA the decomposition
 14 mechanism is more complex. Indeed, the mechanical properties worsened (lower
 15 tensile ductility and decreased toughness) from the first processing to the third
 16 processing with the material becoming brittle. This can be explained via chain scission
 17 mechanisms of the polymer matrix where the polymer chains become shorter, due to
 18 transesterification, thus inducing higher crystallinity rates. This, in combination with
 19 the coupling of poly(acryl-PEG) phase size reduction and pore formation may
 20 decrease the physical interactions between the matrix and poly(acryl-PEG) which
 21 could be responsible for cracking. The authors note that at this stage plasticized PLA
 22 made by reactive extrusion cannot be repurposed (63).

23 The third study focused on the characterization of the formed chemical inclusions of
 24 PLA / acrylPEG / L101 (79 / 20 / 1 wt %).(64) The authors note that two reaction
 25 pathways are possible; the homopolymerization of acrylPEG or the grafting of
 26 acrylPEG onto PLA which could act as starting point for the polymerization of

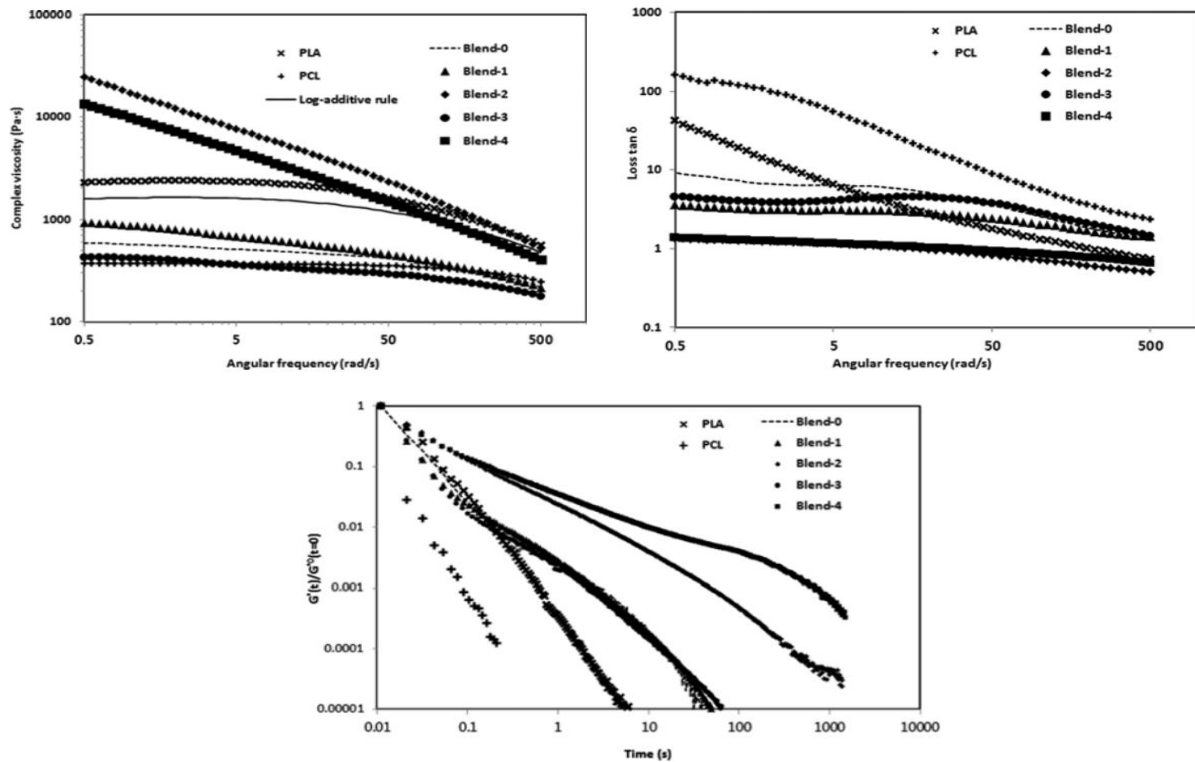
1 acryIPEG. The absence of two separate melting peaks in PLA/acryIPEG and pPLA
2 supports the assumption of a good miscibility between the plasticizer and the matrix
3 even after reactive plasticization. Grafted PLA / poly(acryIPEG) and plasticized PLA /
4 poly(acryIPEG) show higher elongation at break compared to PLA >16 % (this is due
5 to the limitation of the testing machine). Also the Young's modulus is decreased (7.5,
6 21 MPa for PLA / acryIPEG and pPLA, respectively) (64).

7 The same group also used myrcene (My) and limonene (LM) which are two bio-based
8 plasticizers to assess processability and performance using both reactive extrusion
9 and conventional blending (65). For the reactive extrusion, Luperox 101 was used to
10 initiate radical formation. Various compositions were tested: PLA / (LM or My) / L101
11 were processed at different % mass ratio (100/0/0, 80/20/0 and 79/20/1). In presence
12 of L101, two main reactions take place during the reactive extrusion: (i) the
13 polymerization of the plasticizer itself or (ii) PLA branching. However, there is no direct
14 proof of grafting of the plasticizers onto the PLA backbone. For the case of myrcene
15 there is radical homopolymerization that is shown by a slight increase of M_w *i.e.* $M_w =$
16 $229 \text{ kg}\cdot\text{mol}^{-1}$) for PLA / My / L101 compared to $M_w = 204 \text{ kg}\cdot\text{mol}^{-1}$ for PLA / My.(65)
17 The author noticed an increase of the extrusion force for PLA / My / L101 compared
18 to PLA / My as well as an increase of My inclusions size from PLA / My to PLA / My /
19 L101 that seemed to witness the polymerization of myrcene (65).

20 7) PLA / PCL blend compatibilization

21 Shin *et al.*(66) studied the viscoelastic properties of PLA / poly(ϵ -caprolactone) (PCL)
22 blends compatibilized by four different methods. The first two are based on reactive
23 extrusion. The first method (Blend-1) involving dicumyl peroxide (DCP) creates free
24 radicals on both PLA and PCL whereas the second one (Blend-2) uses Joncryl as
25 compatibilizer. Both Blend-3 and Blend-4 are prepared according to the same
26 extrusion parameters as Blend-1 and Blend-2. However, after extrusion, they were
27 subjected to an electron beam irradiation that facilitate cross-copolymerization at the
28 interface between PLA and PCL. The fourth method involved the use of a chain
29 extender, nine glycidyl methacrylate, as the reactive compatibilizer. Well
30 compatibilized blends could be distinguished using their viscoelastic properties. These
31 blends had similar or higher G' , G'' , and η^* values than those calculated using the log-
32 additive mixing rule, whereas poorly compatibilized blends showed negative
33 deviations of G' (except at low frequency), G'' , and η^* (Figure 19). In addition, poorly

1 compatibilized blends exhibited a plateau region in $\tan(\delta)$ curve and fast stress
2 relaxation process (Figure 19) (66).



3
4 Figure 19 Complex viscosities as a function of angular frequency, $\tan\delta$ curves as a function of angular frequency,
5 normalized transient stress relaxation moduli, $G^*(t)/G^*(t=0)$, (measured at 190°C) for PLA, PCL, and
6 compatibilized and non-compatibilized PLA/PCL (80/20) blends (66)

7 With the use of proper additives, degradation of PCL / PLA (90:10) blends can be
8 triggered by light irradiation *i.e.* it is also called photodegradation (67). The authors
9 highlighted that the blends compatibilized with DCP and containing TiO_2 exhibited an
10 enhanced photodegradation, 50% weight loss within 44 days in wet conditions and
11 30% weight loss within 77 days, compared to neat PLA. Therefore, it seems that Simon
12 *et al.* achieved the development of photodegradable polyester blend (67).

13 8) Other blend compatibilization

14 The improvement of mechanical properties of PLA / COPUP (castor oil-based
15 polyurethane pre-polymer) blends was performed by reacting isocyanide-terminated
16 COPUP with the hydroxyl groups of PLA (68). Firstly, isocyanide-terminated COPUP
17 was synthesized by reacting castor oil with methylene diphenyl diisocyanate (MDI).
18 The COPUP was then blended at different weight percentages (5, 10, 20, 30 %) with
19 PLA, the resulting blends were then subsequently injection molded (68). For the blend
20 containing 30 % of COPUP, the elongation at break increased by 401.3 % compared

1 to neat PLA while the tensile strength and Young's modulus decreased slightly with
2 61 (neat PLA) to 33 MPa (COPUP 30 %) and 2601 (neat PLA) to 1477 MPa
3 respectively (68).

4 Another study from Athanassiou *et al.*(69) focused on the use of extrusion,
5 compression molding and injection molding to produce blends of linear-PLLA with
6 different weight percent of star-PDLLA. The aim was to use the amorphous star-
7 PDLLA as plasticizer to improve the mechanical properties of linear-PLLA.
8 Subsequently the blends (0, 10 and 20 wt % of star-PDLLA) were injection-molded at
9 190 °C in a dumbbell shape for mechanical testing. Blending of star-PDLLA resulted
10 in less decomposition during processing compared to linear PLLA. This was observed
11 for injection molding and extrusion (69). Moreover, the T_g decreased with increasing
12 concentration of star-PDLLA, this would indicate that there is a plasticizing effect on
13 the linear-PLLA matrix. Increasing the weight percentage of star-PDLLA, increased
14 the toughness for both extruded/compressed and injected products (increase of 222
15 % and 265 %, respectively). While Young's modulus decreased slightly from 1.9 GPa
16 for injection molded PLA to 1.7 GPa for 20 % star-PDLLA (-10 %) and from 1.7 GPa
17 for EC (extrusion and compression molded PLA) to 1.5 GPa for 20 % EC star-PDLLA
18 (-12 %) (69).

19 The production of poly(lactic acid) and (poly(ω -hydroxytetradecanoic acid)) (PC14)
20 block copolymers was achieved by a transesterification reaction using $Ti(OBu)_4$ as
21 catalyst (70). The objective was to improve the elongation at break of PLA. Parameters
22 such as screw speed, residence time, reaction temperature and PLA / PC14 blend
23 ratio were varied in order to find the best conditions to improve the elongation at break
24 of the resulting material. Variation of the screw speed was investigated while keeping,
25 temperature (200°C), residence time (30 min), catalyst concentration (200 ppm
26 $Ti(OBu)_4$) and blend ratio (PLA / PC14 (90/10 w/w)) constant. It is shown that screw
27 speed higher than 150 rpm induces a decrease of the molecular weight due to chain
28 scission (70). Studies on the effect of reaction time indicated that; 15 min reaction time
29 yields the highest elongation at break, an increase of the residence time lowers the
30 molecular weight (280 kg/mol after 5 min down to 250 kg/mol after 15 min) (70) and
31 increase the elongation at break (50 % after 5 min up to 145 % after 15 min) (70).
32 Furthermore, PLA / PC14 blends prepared by REX (200°C, 150 rpm, 15 min residence

1 time) containing 20 % of PC14 exhibits an impact strength increased by 2.4 times
2 compare to neat PLA (70).

3 Mihai *et al.*(71) studied the behavior of plasticization of PLA using a bio-based
4 cardanol derivative. This derivative, made by epoxidation of cardanol, is grafted
5 through reactive extrusion and in that case, ethyltriphenyl phosphonium bromide
6 (ETPB) was used as catalyst. Different blends were elaborated by varying the amount
7 of ECard and ETPB. The absence of ETPB show incompatibility between PLA/ECard
8 as large domains (- 5 μm) are formed as seen by the SEM analyses. The reaction
9 between ETPB and PLA end groups allows better compatibilization, however the
10 addition of more than 0.02 phr of catalyst deteriorates the overall properties of PLA.
11 Thermal stability is affected only at temperatures above 270 °C which do not interfere
12 with the processing temperatures. The best results were obtained for PLA / Ecard /
13 ETPB (80 / 20 / 0.02 phr) which has a 49 % increase in elongation at break (71).

14 PLA / PBS blends were compatibilized in another work, by adding poly(propylene
15 carbonate) grafted maleic anhydride (gPPC) (72). Different blends were produced by
16 varying the content of gPPC to evaluate the different effects (72). Various
17 compounding conditions were assessed for each blend by changing the specific
18 mechanical energy (SME), which is defined as the energy given to the system during
19 the reactive extrusion. This value depends on the flow rate, screw speed, the motor
20 power, and torque (commonly used parameters). It was shown that high shear rates
21 combined to short residence times was able to allow chemical reaction while
22 preventing thermal decomposition of the reagents (72). Moreover, it promoted the
23 reduction of the droplets size in all the blend allowing energy dispersion. In some
24 cases, strain at break was increased up to 360 % compared to the neat blend (72).

25 A study reported the production of ternary blends PLA / PBS / ethylene-methyl
26 acrylate-glycidyl methacrylate (EGMA) which were then compression molded into
27 dumbbell shaped specimen (73). The goal of this paper was to study the influence of
28 EGMA on both PLA / PBS blends morphology and mechanical properties. It is shown
29 that the addition of 30 wt % of PBS in the PLA matrix does increase the elongation at
30 break ($\epsilon = 336 \%$) but result in a decrease in tensile strength ($\sigma = 40 \text{ MPa}$). When the
31 compatibilizer EGMA was added to a PLA/PBS blend, the tensile strengths decreased
32 from 37 to 24 MPa for samples 5 and 20 wt % EGMA, respectively. On the contrary,

1 the elongation at break of blends has a remarkable increase from 478 % for 5 wt %
2 EGMA to a maximal value of 549 % for 10 wt % EGMA and exhibits superior
3 stretchability of 83 times higher than that of neat PLA, which represents enhanced
4 ductility. With further increase of EGMA contents to 15 wt % and 20 wt %, the
5 elongations at break slightly drop to 417 and 324 %, respectively. With the
6 incorporation of 20 wt % EGMA, the impact strength was improved to 46.5 kJ/m² which
7 is approximately 20 times more than PLA (73).

8 Palai *et al.*(74) prepared blown films of PLA / TPS (thermoplasticized starch). Two
9 different starch sources were used: Cassava and Maize starch. TPS was obtained by
10 mixing the starch with 25 % glycerol and 5 % water in a Rheomix at 120 °C. The PLA
11 / TPS blends were prepared by reactive extrusion and compatibilized using glycidyl
12 methacrylate (GMA) by mixing the TPS with PLA, GMA and benzoyl peroxide as
13 radical initiator. Blends with a concentration of TPS from 5 to 30 % weight decreased
14 the tensile modulus both in transverse direction and machine direction having 50 %
15 value of virgin PLA for blends containing 30 % TPS. On the contrary, increasing the
16 TPS concentration, elongation at break increased up to 144 % for blends containing
17 30 % TPS. PLA containing thermoplasticized cassava starch display better tensile
18 properties compared to maize starch. This may be due to the higher crystallinity of
19 thermoplasticized cassava starch evidenced by FTIR and DSC analysis (74).

20 In a recent study, Fredi *et al.*(75) investigated the compatibilization with Joncryl ADR
21 4468 of PLA / poly(ethylene 2,5-furanoate) (PEF) blends that aimed to be used as
22 sustainable packaging. Several formulations were produced by melt compounding and
23 hot pressed to obtain polymer films. Joncryl was proved to effective both as a chain
24 extender and a compatibilizer leading to a more homogeneous PEF domain size in
25 the PLA matrix. However, 10 wt% of PEF (PLA-PEF10) were proved to increase the
26 crystallinity of the blend up to 28 % (+ 72% compared to neat PLA), the addition of 1
27 phr of Joncryl (PLA-PEF10-J1) had the opposite effect leading to a crystallinity of 11%
28 (- 34 % compared to neat PLA). (75) The mechanical characterization of the different
29 synthesized blends proved the positive effect of Joncryl. Indeed, the uncompatibilized
30 blend displayed mechanical properties that were lower to those of neat PLA. But the
31 PLA-PEF3-J1 blend (3 wt% of PEF, 1 phr of Joncryl) displayed highly improved strain
32 at break and tensile strength (+103 % and +42.5 % compared to neat PLA
33 respectively) even if the elastic modulus was slightly hindered (-11 % compared to

1 neat PLA). Finally, the authors proved that with only 1 wt% of PEF both UV- and
2 oxygen-barrier were enhanced which represent an interesting point in order to use
3 those blends in the packaging industry. Therefore, PLA-PEF blends compatibilized
4 with Joncryl represent interesting materials yet the ideal blend has not been found.
5 Indeed, the blends that displays the best gas barrier is not the one with the best
6 mechanical properties of the highest crystallinity.

7 All the studies of this part explore various way to compatibilize PLA-based blends and
8 focus mostly on the improvement of the mechanical properties of PLA. It would be
9 interesting to go further and study deeper both thermal properties and fire behavior of
10 the blends. It may open a wider range of application for the developed polymers.
11 Moreover, focusing on the development of bio-based compatibilizers for bio-blends
12 (*i.e.* PLA / biopolymer blends) would bring new insight on finding alternatives to
13 petroleum-based polymers.

14 3. Composite Compatibilization

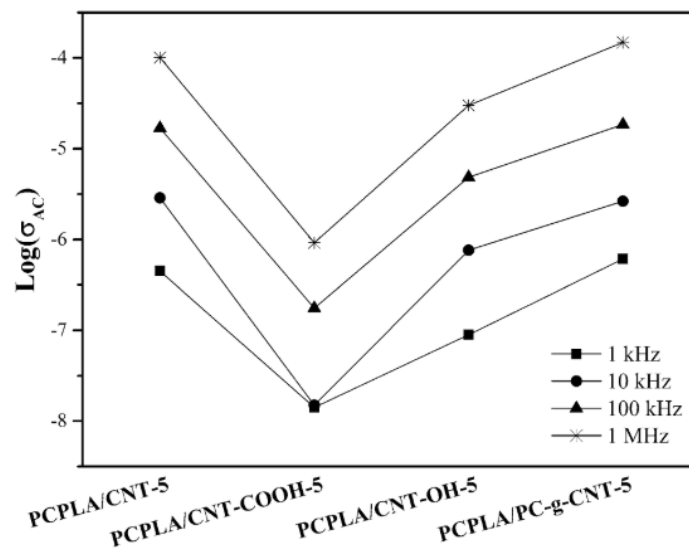
15 Currently most of the composites on the world market are based polymers arising from
16 petroleum based polymers *e.g.* polyethylene (PE), polypropylene (PP) and polyvinyl
17 chloride (PVC) (76). However, the interest to recycle these composites keeps growing
18 resulting in the need of greener products. Thus combining the creation of green
19 composites to mechanical properties (impact strength, ductility or tensile strength)
20 enhancement strategies, PLA can be mixed with fillers. Therefore research strategies
21 such as the use carbon derivatives (17,77–79), reusing food byproducts (76,80–84)
22 or wood derivatives have been employed (85–90).

23 1) PLA / Carbon fibers or carbon nanotubes composites

24 PLA-g-MAH was proved to be a good compatibilizer for PLA-based blends
25 (45,47,50,52,55,58,72) but it can also compatibilize PLA / natural fibers composites as
26 mentioned in Pérez-Fonseca *et al.*(17) review's or PLA / carbon fibers composites.
27 The grafting of PLA with MAH can be performed using dicumyl peroxide as an initiator
28 (77). The resulting compatibilized composites displayed improved mechanical
29 properties with a 150 % and 28 % enhancement in tensile modulus or impact strength
30 respectively. Moreover, the addition of 0-3 % wt PLA-g-MAH as compatibilizer
31 increased the crystallinity and displayed a surface resistivity of $10^{-3} \Omega \cdot \text{cm}$ (77). PLA
32 properties were improved by the addition of carbon nanotubes (CNT) using PLA-g-

1 MAH (78). The latter was obtained) by REX using benzoyl peroxide (BPO) as a radical
2 initiator prior to be mixed with PLA. The obtained nanocomposite displayed an impact
3 strength enhanced by 274 % with 1 wt % of CNT and 3 wt % of PLA-g-MAH (78).
4 Moreover, the TGA results showed that the addition of CNT and PLA-g-MAH does not
5 affect the thermal properties of PLA (78).

6 Aytac *et al.*(79) studied the influence of 3 or 5 wt% of non-functionalized (MWCNT),
7 hydroxyl-functionalized (MWCNT-OH), carboxyl-functionalized (MWCNT-COOH) and
8 polycarbonate-grafted multi-walled carbon nanotube (PC-g-MWCNT) on the
9 properties of polycarbonate (PC) / PLA (70 / 30 wt%) blend (79). The results showed
10 that MWCNT-COOH contributes to enhance the mechanical properties of the PC /
11 PLA blend *i.e.* the elongation at break was increased up to 159% vs 7.6% for neat PLA
12 (79). On the other hand, the addition of 5 wt% of PC-g-MWCNT influenced the
13 electrical conductivity of the PC / PLA blend (Figure 20).



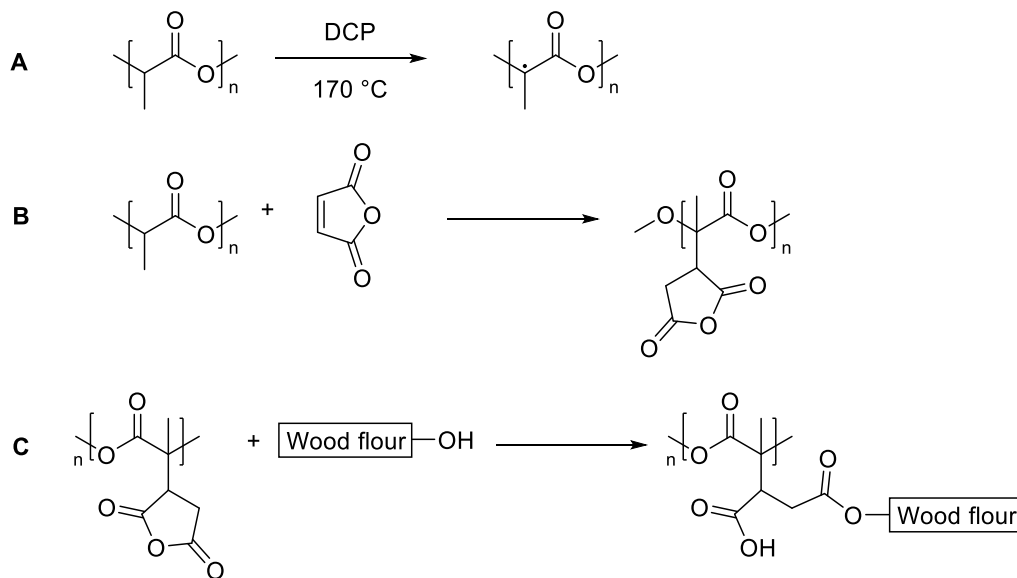
14
15 Figure 20 $\text{Log}(\sigma_{AC})$ of nanocomposites at different frequencies (79)

16 2) PLA / food industry byproduct composites

17 Different studies have focused on the production of biocomposites from the
18 combination of PLA with wastes from the agro-food industry, multi-functionalized
19 vegetable oils (80–82) or wood flour (76,83,84).

20 The composites prepared with wood fibers are well known under the name of wood-
21 plastics composites (WPCs), and a lot of applications with PP, PE and PVC have been
22 developed (83). Furthermore, since PLA displays some properties that are equivalent

1 to those of oil-based polymers, WPCs based on PLA and wood flour represent a
 2 promising biodegradable material with good mechanical properties for industrial
 3 applications e.g. food packaging. Gu *et al.*(83) developed PLA / wood flour (WF)
 4 composites modified with MAH by a one-step REX process. As mentioned before,
 5 MAH acts as a compatibilizer and provides an efficient grafting and crosslink between
 6 the three components of the composite (Figure 21). It was observed that 1 wt % of
 7 MAH in the composites increase the mechanical strength up to 144 % whereas the
 8 tensile strength is increased by 44 %. However, according to thermal analysis, the
 9 addition of MAH and dicumyl peroxide (initiator), during the REX process catalyzes
 10 decomposition of PLA (83).



11

12

Figure 21 Mechanism of chemical reaction among PLA, wood flour and MAH (83)

13 The development of PLA / WF composites was also studied by Zhang *et al.*(76) with
 14 benzoyl peroxide (BPO) as the initiator and methyl acrylate (MA) as the compatibilizer.
 15 After grafting wood flour with MA, WF-g-polymethyl acrylate (PMA) was used as a filler
 16 to improve the interactions between PLA and WF (76). An enhanced interfacial
 17 compatibility of the composites treated with MA and an improved water resistance
 18 were observed. However, the thermal stability of the compatibilized composites was
 19 slightly lower than that of pure PLA (76). Another type of compatibilizer based on
 20 methylenediphenyl diisocyanate (MDI) combined to MAH was studied by Seo *et al.*(84)
 21 and used with PLA / polybutylene succinate (PBS) / WF composites. The DSC
 22 thermograms showed that MDI contributes to the increase in T_g of the composites

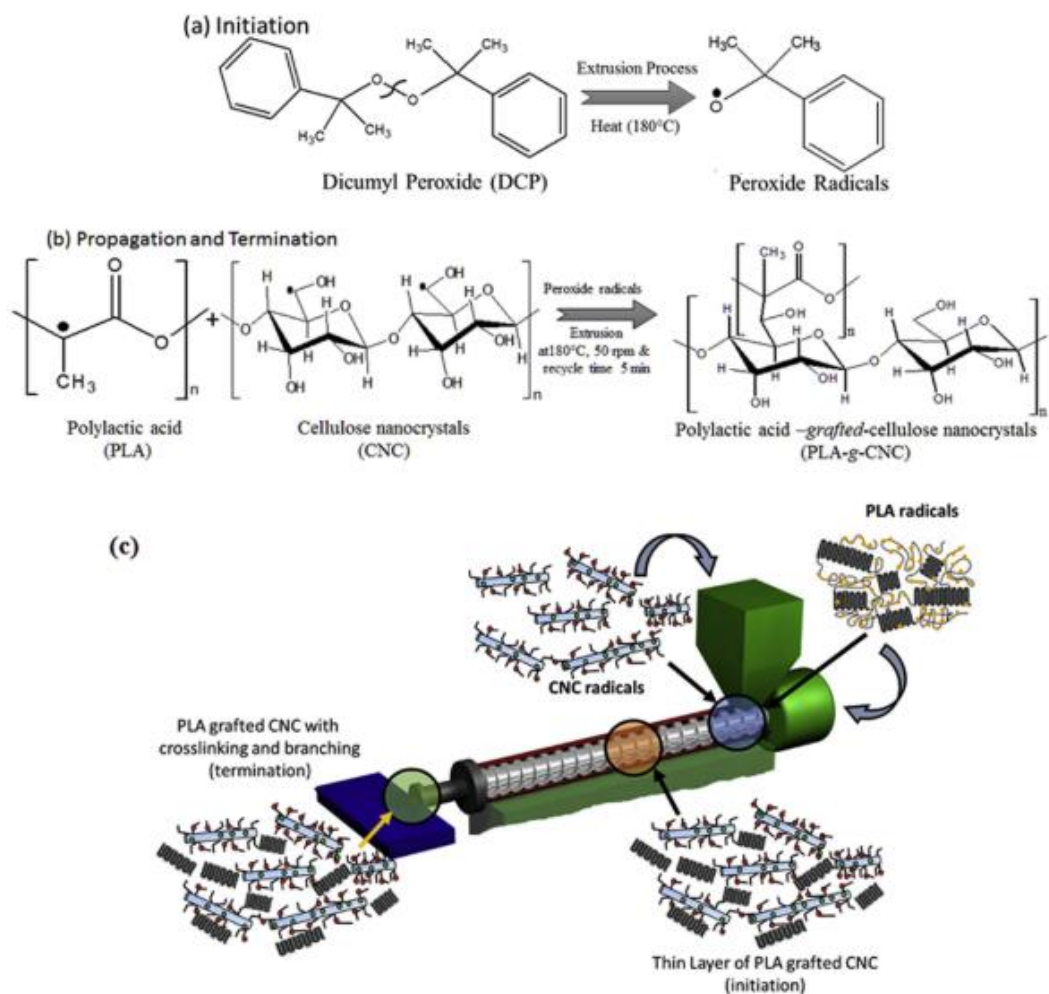
1 (84). Moreover, the composites containing both MDI and MAH displayed the most
2 enhanced thermal stability (84).

3 Quiles-Carrillo *et al.*(80–82) published two studies using food industry by-product : one
4 on PLA / almond shell flour (ASF) compatibilized with maleinized linseed oil (MLO)
5 and one relating to the compatibilization of PLA / orange peel flour (OPF) by acrylated
6 epoxidized soybean oil (AESO). The addition of high amounts of ASF in the PLA matrix
7 enhanced the hardness of the resulting bio-composites (81). Through a plasticizing
8 effect and grafting, MLO was able to improve the compatibility between PLA and ASF
9 (81). Therefore, the mechanical, thermal and thermomechanical properties of PLA /
10 ASF composites displayed strong enhancements compared to the uncompatibilized
11 composite (81). Indeed, with a MLO content of 10 parts per hundred resin, T_{deg} of PLA
12 / ASF composite was measured around 327°C with a residue of 0.7 % (81). In
13 comparison, the PLA / OPF composites containing 10 % of OPF and compatibilized
14 with AESO displayed a decomposition temperature of 330°C with a residue of almost
15 11 % (80). Both decomposition temperatures of the composites are close to that of
16 neat PLA but the residue is higher especially for PLA / OPF compatibilized with AESO
17 (80,81). Another food industry recoverable waste, walnut shell flour (WSF), was used
18 to develop a PLA / PCL / WSF composite compatibilized with MLO (82). However,
19 these composites displayed an improved ductility (elongation at break up to 19 vs 9 %
20 for neat PLA) (82) especially with low levels of WSF (10-20 %) (82), due to the
21 presence of PCL, and minimal losses in terms of mechanical toughness (shore
22 hardness around 74-78 vs 81 for neat PLA) (82) and mechanical stress *i.e.* impact
23 strength comparable to neat PLA when WSF content less than 30 % (82), the TGA
24 analysis showed lower decomposition temperatures compared to neat PLA but higher
25 residues (~10 %) (82).

26 3) Biobased nanocomposites (PLA / CNC or SNC, PLA / CNF)

27 Arising from renewable biomass sources, cellulose nanocrystals (CNC) are
28 manufactured by extracting the crystalline part of cellulose. CNCs display improved
29 mechanical properties including high tensile strength and elastic modulus (140-220
30 GPa) making them an attractive material for PLA-based nanocomposites, however the
31 compatibility between PLA and CNCs needs to be improved. Dhar *et al.*(85,86)
32 investigated a single step REX process designed to produce PLA grafted cellulose
33 nanocrystal (PLA-g-CNC) (Figure 22). The aim of this work was to develop

1 nanocomposite films for packaging application. The grafting of PLA on CNC was
 2 performed via REX make the hydrophobic PLA and the hydrophilic CNC compatible.

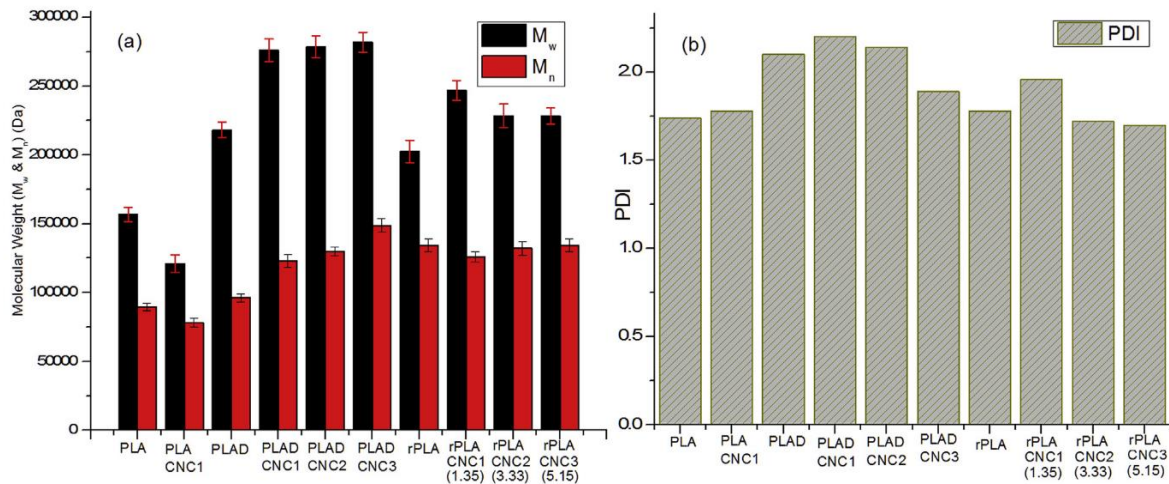


3
 4 Figure 22 (a) Mechanism of thermal decomposition of the DCP into peroxide radicals during extrusion at $T = 180^\circ\text{C}$ (initiation step), (b) Generation of CNC and PLA radicals followed by reactive extrusion at screw speed $\frac{1}{4}$
 5 50 rpm and recycle time $\frac{1}{4}$ 2 min (propagation step) leading to the formation of PLA grafted CNC structures
 6 (termination step). (c) Pictorial representation of the grafting mechanism of initiation, propagation and termination
 7 of the reactive extrusion process for PLA-g-CNC along the different zones of the extruder (85)
 8

9 One of the first study showed that the recycling of PLA-g-CNC nanocomposites was
 10 possible without significant breakage in the molecular structure of PLA *i.e.* no
 11 significant reduction of M_w was observed (Figure 23). Moreover, the M_w and M_n of PLA-
 12 g-CNC were significantly increased by the chain extension and the formation of
 13 branched structure. It was also proven that the presence of C-C bonds with the CNCs
 14 improved thermal properties and mechanical properties of the PLA-g-CNC
 15 composites. The tensile strength of the composite was increased by 41 % and Young's
 16 modulus enhanced by 490 % (85). Another study showed that PLA chains grafted onto

1 CNCs were responsible for the formation of high molecular mass ($M_w \approx 150\text{--}245$ kDa)
 2 cross-linked structure (86). The obtained polymers displayed an improved
 3 processability as well as enhancement in the structural and barrier properties that
 4 present interests for potential applications in the packaging industry (86).

5



6

7 Figure 23 (a) Molecular weight distribution, weight average (M_w) and number average (M_n) and (b) polydispersity
 8 index (PDI) of extruded PLA, reactively extruded PLA/CNC nanocomposites (PLAD, PLAD/CNC1, PLAD/CNC2 &
 9 PLAD/CNC3) and reprocessed PLA-g-CNC gels (rPLA, rPLA/CNC1(1.35), rPLA/CNC2(3.33) & rPLA/CNC3(5.15))
 10 (85)

11 The use of cellulose nanocrystals to reinforce PLA-based nanocomposites was also
 12 reported by Frone *et al.*(91) and Phuong *et al.*(92) PLA / polycarbonate (PC) blends
 13 can be modified with regenerated cellulose fibers to produce reinforced composites.
 14 Phuong *et al.* conducted the extrusion of a PLA / PC polymer reinforced with fibers in
 15 the presence of triacetine and tetrabutylammonium tetraphenylborate, as the
 16 transesterification catalysts (92) Infrared analysis showed that the catalyzed process
 17 allowed the grafting of PLA and PC onto cellulose fibers. Moreover, TGA analysis
 18 results displayed an improved thermal resistance for the composites resulting from the
 19 catalyzed process. These enhanced thermal properties were due to the grafting of
 20 PLA and PC onto cellulose fibers. Indeed, new chemical bonds were created between
 21 the matrix and the regenerated cellulose, displaying a compatibilizing effect on the
 22 resulting composite (92). More recently, Frone *et al.* reported the development of a
 23 single step process using dicumyl peroxide (DCP) as a cross-linking agent. They
 24 compared the extrusion technique to compression molding and 3D printing. First, the
 25 cross-linking agent promoted a better dispersion of CNC in the PLA/PHB matrix.

1 Moreover, the nanocomposites treated with DCP displayed the best thermal stability
2 as well as the highest maximum decomposition temperature (91). The results of the
3 DSC analysis show that CNC and DCP improved recrystallization. The
4 nanocomposites obtained by REX had an increased crystallinity due to the process
5 itself and an increased storage modulus. According to their study, Frone *et al.* discover
6 that filament of PLA / PHB nanocomposite meet the standards required in the 3D
7 printing applications, especially in terms of strength and thermal stability (91).

8 Silk nanocrystals (SNCs) were observed to thermally stabilize PLA when submitted to
9 multiple extrusion processes (93). Moreover, SNCs help to strengthen PLA and
10 contains serine groups which may form radical if initiated. Tesfaye *et al.*(93) used the
11 peroxide-initiated REX process to perform the grafting of SNCs onto PLA. They
12 obtained cross-linked PLA grafted SNCs. The existing of a bond between PLA and
13 SNCs were evidenced by ¹H NMR. The rheological properties of the composite e.g.
14 zero shear viscosity, storage modulus, crossover point were all improved by the
15 addition of SNC increasing the ability of PLA to endure reprocessing (93).

16 Cellulose nanofibers (CNF), arising from renewable resources, are used as
17 reinforcement for biopolymers such as PLA. Li *et al.*(94) studied the grafting of PLA
18 onto CNF with the help of DCP (Figure 24) which led to an improvement of the
19 interfacial interactions between the polymer matrix and the reinforcement fibers.
20 Therefore, compared with uncompatibilized PLA / CNF nanocomposites, the PLA
21 grafted CNF (PLA-g-CNF) displayed enhanced mechanical properties as well as a
22 higher crystallinity rate (40% vs 35%). Indeed, the tensile modulus of PLA-g-CNF
23 produced with 1 phr of DCP was increased by 1,400 MPa and its tensile strength by
24 12 MPa. It also has to be noticed that these values were much higher than those of
25 neat PLA. Thus, it seems that the addition of DCP to PLA / CNF composites is a way
26 to improve their mechanical properties which is viable from an industrial point of view
27 (94).

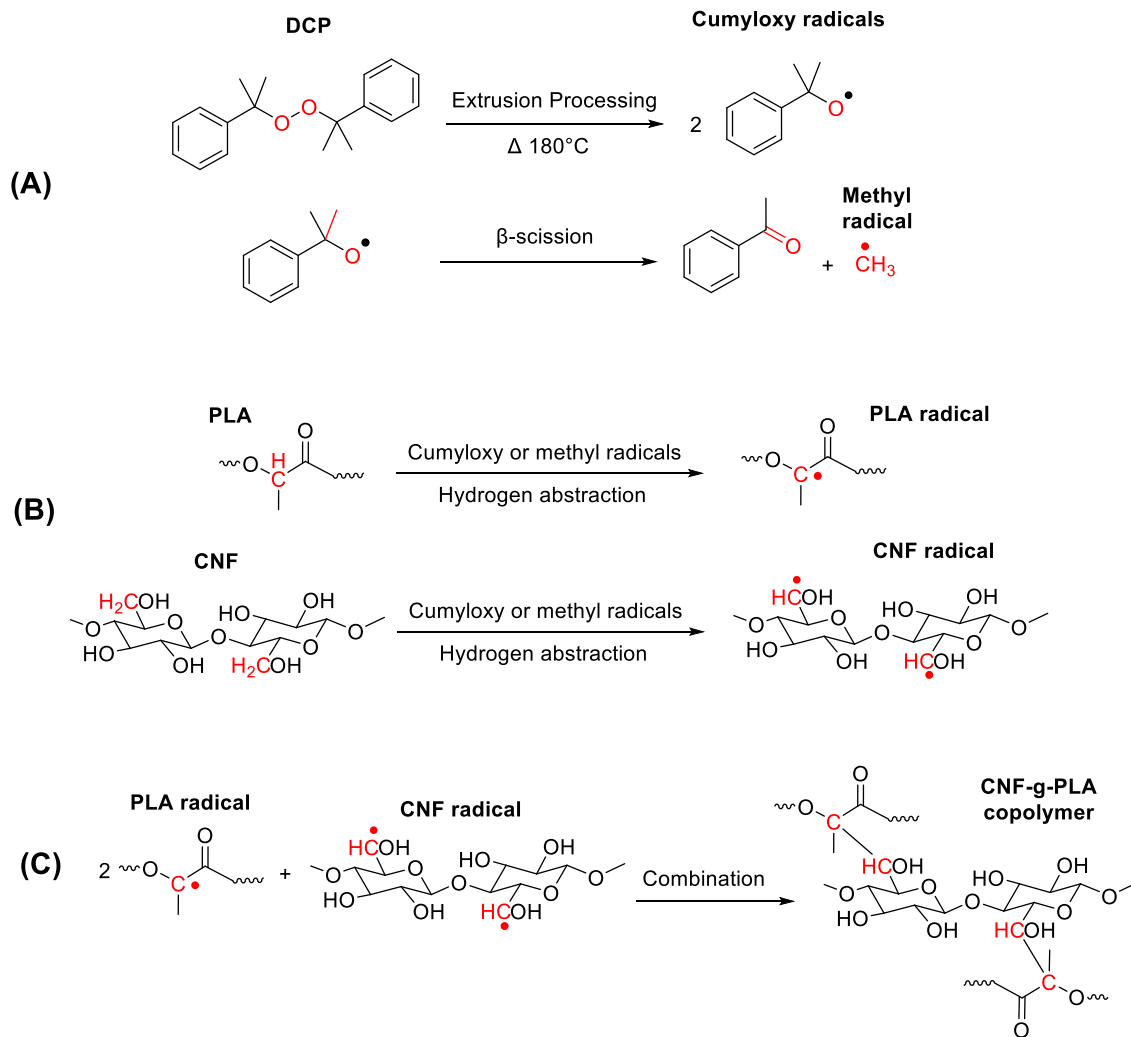
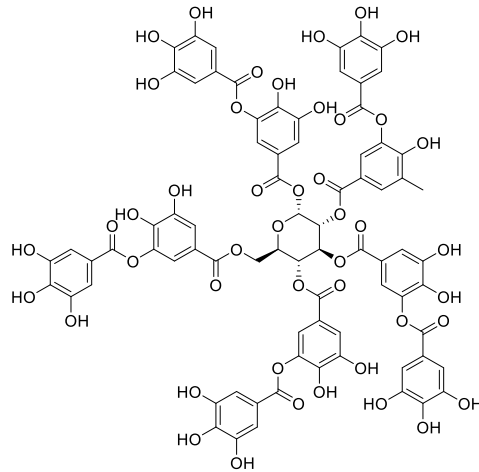


Figure 24 Possible reaction mechanism of DCP-initiated grafting of PLA onto CNF (94)

4) PLA / lignin or tannin composites

It has been proved that phenolic compounds usually display interesting properties including anti-UV capacity, thermal stability and flame retardancy (87,88). Especially, condensed tannins are abundant in bark and one of the most important phenolic compounds after cellulose, hemicellulose and lignin (87–90). Both tannin and lignin are bio-based and contain hydroxyl groups that can react with carboxyl terminal group of PLA. Thus, there has been great interest in producing biocomposites based on PLA and lignin or tannin. Zhou *et al.*(87,88) published the compatibilization of PLA and tannin via a one-step REX process (88) (Figure 26) and also worked on the interfacial improvement of PLA / tannin acetate (AT) biocomposites (87). The PLA / tannin composites were compatibilized with the help of promoters such as MDI or 3-aminopropytriethoxysilane (APS) which led to the formation of cross-linked tannin as well as tannin grafted PLA (88). The obtained composites displayed improved tensile

1 strength (60 vs 50 MPa for neat PLA) and Young's modulus (55 vs 47 MPa) resulting
2 from enhanced interfacial interactions between PLA and tannin (88). Moreover, the
3 use of MDI helped to obtain higher melting temperature and onset of thermal
4 decomposition compared to composites prepared with APS. However, the onset
5 decomposition temperature of the composites prepared with MDI was slightly lower
6 than that of neat PLA (319 vs 323 °C) (88). It can be noticed that the addition of tannin
7 to PLA led to a char formation at temperatures around 350 °C (88).



8

9 *Figure 25 Tannic acid, a specific compound from the tannin family; is widely applied to any*

10 *large [polyphenolic](#) compound containing sufficient [hydroxyls](#) and other suitable groups (such as [carboxyls](#))*

11 In another work from Zhou *et al.*(87) the REX process was used to compatibilize PLA
12 / AT biocomposites with dicumyl peroxide (DCP). They achieved good interfacial
13 interactions between AT and PLA as the onset decomposition temperature of the
14 composite was comparable to that of neat PLA (87). It appears that the free radical
15 compatibilization using DCP is more efficient for PLA / tannin composites.
16 Compatibilized PLA / AT composites also displayed an enhanced hydrophobicity and,
17 thus, may be use in the packaging industry (87).

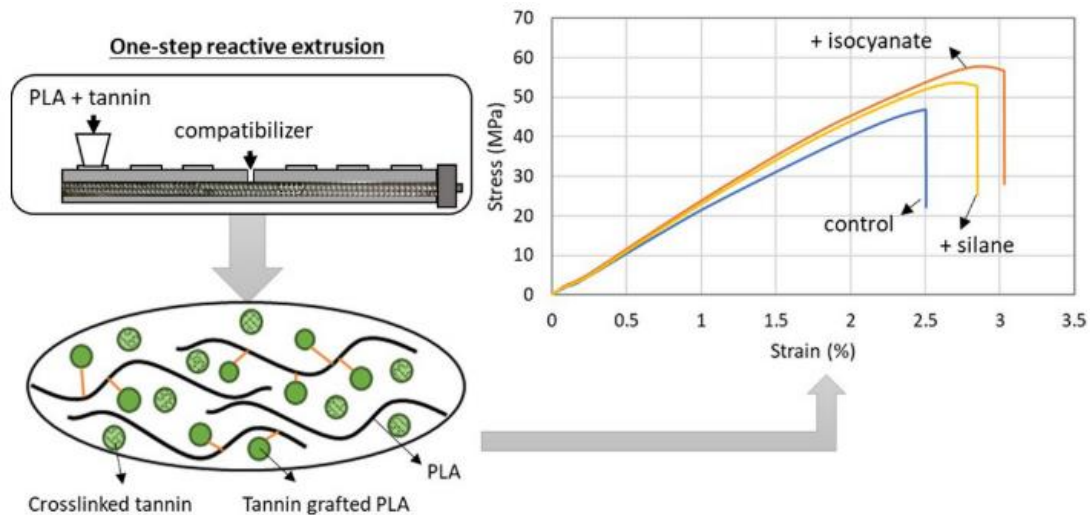


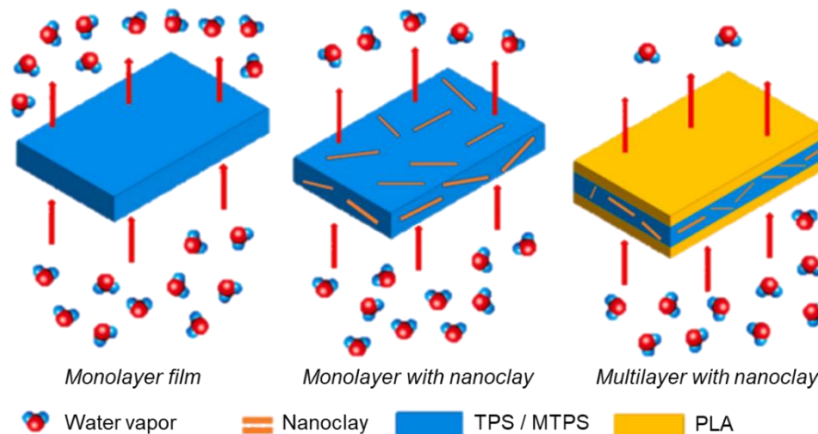
Figure 26 Production of tannin-grafted PLA via REX (88)

1
2
3 As already mentioned, lignin can also be added to PLA to produce biocomposites
4 (89,90). Weng *et al.*(89) evaluated the properties of PLA / lignin composites with and
5 without a silane coupling agent of γ -(2,3-epoxypropoxy) propyl trimethoxysilane
6 (KH560). The results showed a better adhesion between PLA and lignin in the
7 composites thanks to KH560 that acted as a compatibilizer. The TGA of PLA / LG
8 composites compatibilized and uncompatibilized displayed interesting results. The
9 compatibilized composites containing 5 % of lignin started to degrade at lower
10 temperature compared to neat PLA ($T_{5\%} = 297$ vs 327°C for neat PLA) but it has a
11 higher carbon residue (6 vs 1 %) (89). In their work, Abdelwahab *et al.*(90) used
12 organosolv lignin (OL) that is lignin pretreated with organic solvent to design a PLA-
13 based composite that may become an alternative to EPDM elastomer. OL displays a
14 higher number of functional groups as well as a lower glass transition temperature
15 compared to untreated lignin (90). This research focused on the toughening of PLA
16 with OL in the presence of poly(vinyl acetate) (PVAc) and glycidyl-methacrylate
17 monomer (GMA). The addition of PVAc enhanced the miscibility between PLA and OL
18 which was confirmed by a single T_g at the DSC analysis (90). The lower T_g of the
19 composites was an indicator of an enhanced flexibility and molecular mobility. The
20 composite PLA / PVAc / OL / GMA (40 / 22.2 / 21 / 16.8 wt.%) composite with displayed
21 the best mechanical properties : a high impact strength of ~ 900 J/m and elongation at
22 break of 340 % however its thermal properties were lower compared to neat PLA (90).

5) PLA / thermoplastic starch composites

The blending of PLA with thermoplastic starch was studied by different groups (95,96). Bher *et al.*(95) produced PLA / thermoplastic cassava starch (TPCS) functionalized with graphene (GRH) nanoplatelets nanocomposites using REX. The compatibilization between TPCS and PLA was promoted by the incorporation of MAH and a peroxide initiator during the extrusion process. Compared to neat PLA, PLA-g-TPCS-GRH displayed a toughness enhanced by 900 % and an increased elongation at break (95). Moreover, the thermal properties of PLA-g-TPCS-GRH were similar to those of neat PLA. It was illustrated by the values of onset decomposition temperature of 309°C vs 319°C (95).

PLA / thermoplastic starch (TPS) filled with nanoclays were developed by Mekonnen *et al.*(96) in order to obtain multilayer films (Figure 27) that display improved barrier properties to both gas and moisture. Therefore, TPS was maleated to obtain maleated TPS (MTPS). It helped to improve the interfacial interactions between TPS and both nanoclays and PLA. In comparison to neat PLA, the obtained multilayer film displayed an oxygen permeability decreased from 0.260 down to 0.008 cm³.m/m².day.Pa and a water vapor permeation at 7 days of 1.10⁻¹³ kg.m/s.m².Pa which is 10 times lower than the one of neat TPS.



19

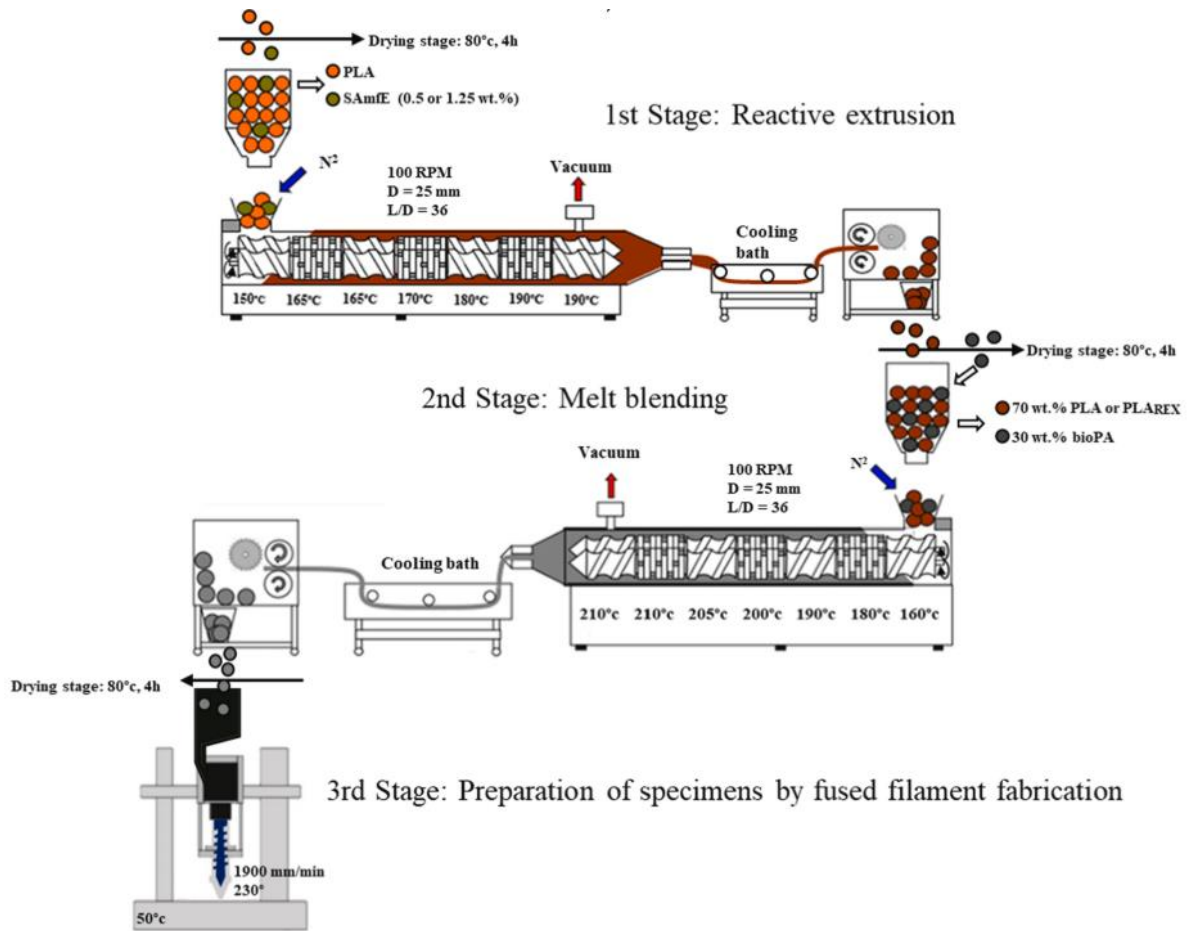
20 *Figure 27 Illustration of proposed permeation mechanism through TPS / MTPS and TPS / MTPS with nanoclays*
21 *and PLA coating (96)*

22 6) Other composites

23 PLA was blended with other polymers and the addition of fillers or nanofillers to the
24 blend in order to produce composites or nanocomposites that overcome PLA's
25 weaknesses was studied. In particular the use of clays is present in some studies

1 (97,98). Cailloux *et al.*(97) used organically modified montmorillonite (o-MMT) to
2 reinforce PLA via REX with and without SAMfE. Through REX, a good distribution of
3 o-MMT in the PLA matrix was achieved and the SAMfE molecules helped to get a
4 better clay delamination and intercalation resulting in improved interactions in the
5 polymer matrix (97). The addition of o-MMT to PLA increase the onset decomposition
6 temperature of the resulting composite of 10 °C compared to neat PLA (98). This study
7 of Carrasco *et al.*(98) highlight the thermal stability enhancement properties of
8 nanoparticles. Moreover, they investigated the kinetics of the thermal decomposition
9 of PLA and PLA/o-MMT produced by REX. The TGA results confirmed the protective
10 effect of nanoparticles against thermal decomposition (98).

11 The same group, in previous works, showed that PLA / BioPA blends with 30 wt%
12 presented a brittle-to-ductile transition (99) as well as a higher activation energy of
13 thermal decomposition (204 kJ/mol) (100). However, the immiscibility between PLA
14 and PA required the use of a compatibilizer. Therefore, SAMfE was used to modify the
15 rheological properties of PLA by REX in order to compatibilize PLA / polyamide 10.10
16 (BioPA) blends (70:30 wt%)(101) that were used to fabricate microfibrillated
17 composites by fused filament fabrication (Figure 28). The authors observed that the
18 addition of 1.25 wt% of SAMfE helped to influence the morphology of the PA
19 microfibers, witnessing the compatibilizing effect of SAMfE. Moreover, the
20 compatibilized blends seems to display an enhanced fracture toughness at high strain
21 rates. Indeed the fracture parameters determined by applying LEFM (Linear Elastic
22 Fracture Mechanics) showed that despite of a comparable K_{Ic} , the G_c (4.8 vs 3 kJ/m²)
23 and w_f (7.8 vs 1.5 kJ/m²) of the blend containing 1.25 wt% of SAMfE were higher than
24 those of neat PLA (101). To go further in the research it would be interesting to design
25 a process that only use the extruder of the 3D printer to perform the reactive extrusion,
26 the melt blending and the 3D printing.



1

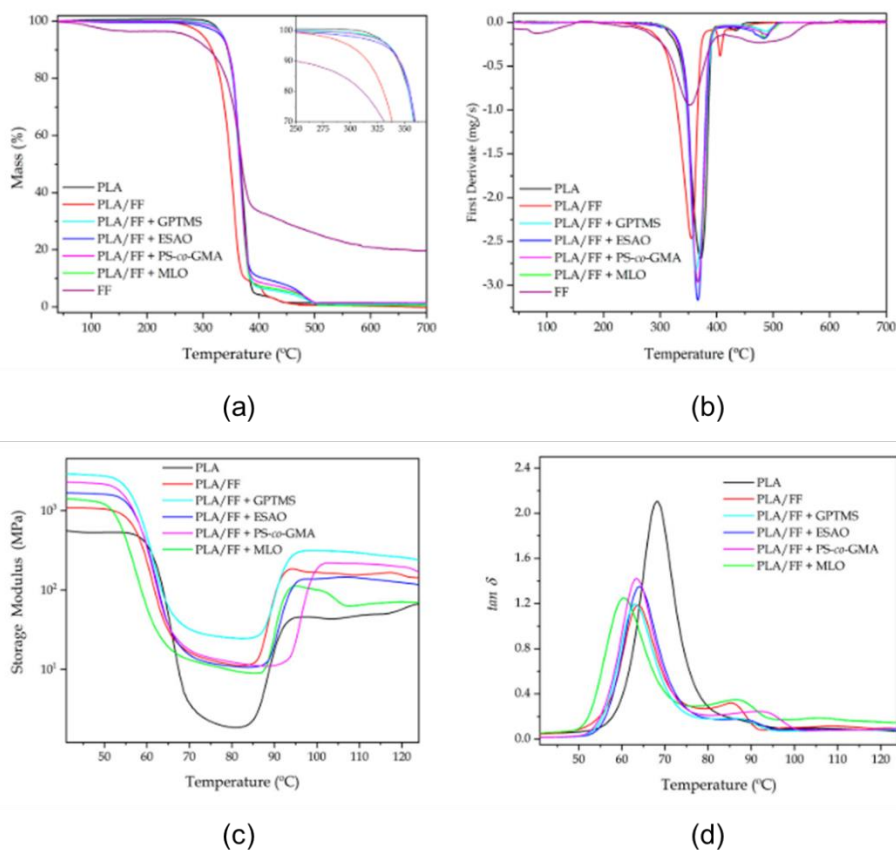
2 Figure 28 Schematic diagram of the manufacturing process including main manufacturing conditions per stages
3 (101)

4 Talc is a commonly used filler in numerous industries. When added to PLA, lamellar
5 talc allows the polymer to meet the requirement of the packaging industry for hot food
6 solutions and of other consumable goods that need an improved thermal stability in
7 terms of melt behavior and crystallinity (102). Barletta *et al.*(102) used modified
8 lamellar talc with maleic anhydride (MAH) and glycidyl methacrylate (GMA) as
9 compatibilizer to produce PLA/talc biocomposites via REX. The resulting compound
10 had an improved processability without a worsening effect on the biocomposites
11 properties compared to neat PLA (102). Also using talc as a filler, Nanthananon *et*
12 *al.*(103) developed, via REX, hybrid composites of talc reinforced PLA and short-fibers
13 with and without compatibilization. As expected, interfacial interactions between PLA
14 and fibers were better in the presence of compatibilizer which led to improved
15 properties of the resulting composite (103).

16 Zhang *et al.*(104) studied the role of Joncryl ADR 4468, MDI type TPU elastomer and
17 micro-sized talc on both mechanical and crystalline properties of PLA-based

1 composites. Joncryl acted as a chain extender (CE) introducing crosslinking and
2 grafting which lead to an improved rigidity of the composite as well as an enhanced
3 strength. Moreover, because of its miscibility with PLA, the TPU introduce both
4 toughness and ductility of the resulting composite. Finally, their work highlighted the
5 fact that talc helped to increase by 20% the crystallinity compared to neat PLA and it
6 showed that the cold crystallization temperature was increased by 10°C (104).
7 Therefore, it seems that this combination of additives can be used in order to develop
8 PLA-based composites with enhanced strength, toughness, crystallinity and faster
9 cold crystallization (104).

10 Flaxseed fibers (FFs) derived from linen waste may be used as a reinforcement agent
11 for polymers like PLA. Torres-Giner *et al.*(105) incorporated alkali-pretreated FFs into
12 PLA via REX and studied the influence of different compatibilization strategies on the
13 resulting composites. A multi-functional epoxy-based styrene-acrylic oligomer
14 (ESAO), a random copolymer of poly(styrene-co-glycidyl methacrylate) (PS-co-GMA),
15 and maleinized linseed oil (MLO) were used as coupling agents. The PLA/FFs
16 composite compatibilized with MLO displayed improved mechanical and thermal
17 properties and the highest ductility (Figure 29) whereas the composites compatibilized
18 with the petroleum-based additives *e.g.* ESAO and PS-co-GMA, showed the highest
19 mechanical resistance and toughness improvement and also the highest thermal
20 stability (Figure 29) (105). Even though, the oil-based compatibilizers bring better
21 mechanical properties to the PLA/FFs composites, the one compatibilized with MLO
22 fully arise from bio-based raw materials (105).



1

2 *Figure 29 (a) Thermogravimetric analysis (TGA) curves with inset zooming the onset of degradation; and (b) first*
 3 *derivate thermogravimetric (DTG) and evolution as a function of temperature of the (c) storage modulus and (d)*
 4 *dynamic damping factor ($\tan \delta$) of the poly(lactic acid) (PLA)/flaxseed fiber (FF) pieces compatibilized with (3-*
 5 *glycidylxypropyl) trimethoxysilane (GPTMS), epoxy-based styrene-acrylic oligomer (ESAO), poly(styrene-co-*
 6 *glycidyl methacrylate) (PS-co-GMA), and maleinized linseed oil (MLO) (105)*

7 Polysaccharides are widely used in both food and pharmaceutical industries. Among
 8 them, agar which is synthesized by marine algae and its extraction generate seaweed
 9 wastes (SWW) have been incorporated to PLA via REX (106). to produce
 10 biocomposites. The addition of MAH and DCP was proven to give composites with
 11 improved properties as the additives have a compatibilizing effect. (106) At low content,
 12 SWW acts as nucleating agent and led to PLA with the highest crystalline phase (6.5
 13 vs 3.2 % for neat PLA) (106). However, the better thermal properties are obtained from
 14 the composites with the highest amorphous phase. Moreover, PLA has a
 15 decomposition temperature of 346°C, that was shifted to 379°C for composites
 16 containing 20 % of SWW and 5 % of compatibilizer (106). SWW could be used as an
 17 environmentally friendly alternative to produce biocomposites at lower costs.

18 The effect of chitosan – a polysaccharide arising from chitin, which is a biopolymer
 19 used in the packaging industry – has been used in PLA/poly(butylene succinate)

1 (PBS) blend (107). Functionalized chitosan (FCH) and DCP were added during the
2 REX process. The obtained nanobiocomposite displayed a UV-blocking effect that
3 may be suitable for packaging applications (107).

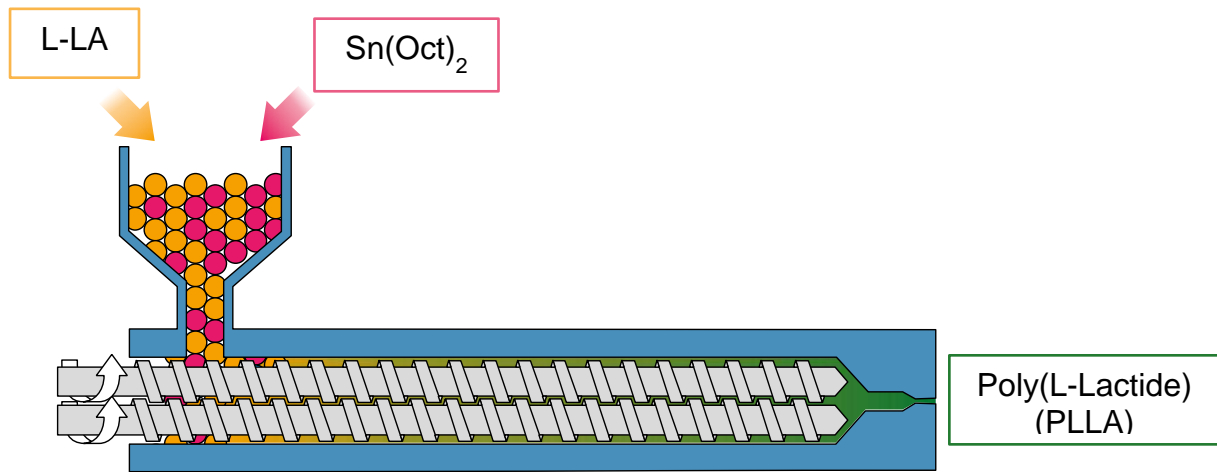
4 Polyhedral oligomeric silsesquioxane (POSS) are organic/inorganic hybrid
5 nanoparticles with $[RSiO_{3/2}]$ general formula, where R may be a reactive group that
6 can be varied. Liu *et al.*(108) prepared PLA / aliphatic poly(carbonate)(PPC) /
7 polyethylene glycol-polyhedral oligomeric silsesquioxane (PEG-POSS) composites
8 via REX with $SnOct_2$ as catalyst. PEG-POSS has a hydrophobic structure and
9 hydrophilic side chains (PEG-chains). As PPC is an amorphous polymer, its addition
10 to PLA lead to a decrease in the crystalline fraction of the composite however, the use
11 of PEG-POSS was able to enhance the crystallinity through transesterification
12 reactions between PLA and PPC. PLA water barrier properties were improved by the
13 addition of 20 % PPC and 4 % of PEG-POSS; indeed, the resulting composites
14 displayed a contact angle superior to 90° (108).

15 II. Ring-opening polymerization of lactide via reactive 16 extrusion

17 All published works summarized in the previous sections of this review focused on the
18 chemical modification of PLA via REX. In the present section, we will present the
19 research works related to the production and modification of PLA by Ring-Opening
20 Polymerization (ROP) of lactide under reactive extrusion.

21 The protocol that allowed the production of poly(L-Lactide) (PLA) by ROP of L-Lactide
22 (L-LA) via reactive extrusion (REX), was developed for the first time in 2000 by
23 Jacobsen *et al.*(5,6) The ROP of L-LA was promoted by mixing the monomer with an
24 equimolar quantity of tin(II) octoate ($Sn(Oct)_2$) and triphenylphosphine ($P(Ph)_3$) (Figure
25 30) (5,6,109). $Sn(Oct)_2$ is a metal-based catalyst which is FDA-approved as a food
26 additive, which allows PLA to be involved in applications in the food packaging
27 industry (8). $P(Ph)_3$ is added to prevent intramolecular transesterification reaction, also
28 called back-biting, a well-known secondary reactions occurring during the ROP of
29 cyclic esters and leading to the formation of cyclic polymers (109). The molar ratio
30 between L-LA and the catalyst may be adjusted depending on the targeted molecular
31 weights of the resulting polymers. In this study, the optimal ratio was found to be 5000
32 equivalents of monomer vs. tin. Reaction conducted at $185^\circ C$ with a screw speed of

1 100 rpm lead to a production of PLA with high molecular weight reaching 70 000 g/mol
2 along with nearly quantitative conversion (ca. 98 %) within 7 minutes (4,110–112).



3

4

Figure 30 Reactive extrusion process

5 In a recent study, Fernandez *et al.*(113) work on the synthesis of PLA by reactive
6 extrusion at a pilot plant scale. More precisely, the authors investigated the use of two
7 initiators, 1,12-dodecanediol (DDD) and di(trimethylol propane) (DTMP), to synthesize
8 high molecular weight PLLA. To do so, they used a twin-screw extruder in which L-
9 Lactide was added with Sn(Oct)₂, P(Ph)₃ and DDD (PLA_DDD) or DTMP
10 (PLA_DTMP).(113) The resulting PLA_DDD and PLA_DTMP reached high average-
11 weight molecular weights (M_w) *i.e.* 183 and 217 kDa with \bar{D} values of 2.44 and 2.36
12 respectively.

13 Recently, Abhyankar *et al.*(114) investigated some alternative energy (AE) sources to
14 boost the ROP of lactide during the REX process. Microwaves and ultrasounds were
15 used in an empirical way but also by modelling the reaction. Both microwaves and
16 ultrasounds enhanced the process in terms of molecular weight and monomer
17 conversion in a specific range of temperature (160-180°C). Indeed, working at lower
18 temperature is tricky due to PLA melting point which is about 170°C and the polymer
19 matrix risks to degrade when working at higher temperatures. The REX process
20 assisted with ultrasounds provide polymers with molecular weights increased up to
21 120 % in comparison to the REX process without ultrasounds (30,100 vs 13,700
22 g/mol). In both cases, a mathematical modelling of the process has been developed.
23 However it still needs to be refined as it predicted molecular weight that were three

1 times higher than the empirical results for some experiments of REX assisted by
2 ultrasounds (115).

3 REX was also used for the production of PLA macrocycles that display increased glass
4 transition temperature and smaller hydrodynamic volume compared to linear PLA.
5 These macrocycles may find interest in the medical field for drug delivery systems
6 (116). Although performing the ROP of lactide during the REX process is known and
7 well documented in the literature, it remains a challenge especially for the production
8 of PLA-based copolymers. Indeed, during the copolymerization, there is a competition
9 between both monomers (lactide and its comonomer) to access the reactive sites of
10 the catalyst. This competition leads to longer reaction time and sometimes inhibits the
11 copolymerization reaction. Finally, REX may be used to incorporate nanofillers and
12 flame retardant as it allows to polymerize lactide while performing the dispersion of
13 fillers (5,117).

14 1. PLA arising from other catalysts

15 In 2015, Bonnet *et al.*(116) reported the production of macrocyclic poly(L-lactide) via
16 reactive extrusion in one step synthesis using $\text{Ln}(\text{BH}_4)_3(\text{THF})_3$ ($\text{Ln} = \text{La}, \text{Nd}, \text{Sm}$) as
17 catalysts. These macrocycles arise from the intramolecular transesterification
18 reactions that occur during the ring-opening polymerization. It is noteworthy that they
19 can be produced by operating at lower temperature (130°C) than the usual ROP of L-
20 lactide via REX (usually at 185°C). Cyclic polyesters are polymers of high interest as
21 they have potential applications in the biomedical field. The authors pointed out that
22 their metal-based catalysts involved in this work displayed low toxicities which confirms
23 that PLA macrocycles are appropriate for such applications (116). It was further shown
24 that linear and macrocyclic PLA of same molecular weights exhibit slight differences
25 in terms of crystallinity (59 vs 50 %) or glass transition temperature (53 vs 56°C) (118).
26 Moreover, the melting temperature of macrocyclic PLA was found to be lower than its
27 linear analog (163 vs 171 °C) (118). The tensile tests also show differences that were
28 attributed to the constrained network implied by the macrocyclic topology. Indeed at
29 70°C PLA displays a higher deformation capacity than macrocyclic PLA which was
30 attributed to the possible macrocycles entangled (118).

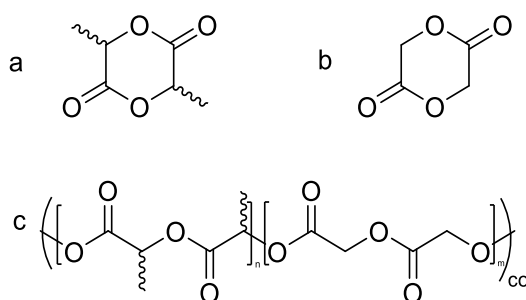
31 The same group used a titanium oxo-cluster to synthesize a hybrid PLA via REX (119).
32 The oxo-cluster acted both as a catalyst and as crosslinking agent allowing to obtain

1 PLA with M_n of about 58 000 g.mol⁻¹ (119). The EPMA (electron probe microanalyser)
2 analysis highlighted a good dispersion of the filler into the polymer matrix. Moreover,
3 the hybrid PLA displayed a superior dimensional stability than the commercial one.
4 Indeed, the dimensional stability tests under heat showed an almost unchanged shape
5 for hybrid PLA after 10 h at 150°C, whereas the commercial PLA sample was distorted
6 (119).

7 Raquez *et al.*(120) developed a greener magnesium-based catalyst (*i.e.* magnesium
8 (II) N-heterocyclic carbene) in order to allow the continuous polymerization of lactide
9 via REX. They proved that their new catalyst, used in a microcompounder, was able
10 to provided PLA with high molecular weight (47,500 g/mol), low polydispersity index,
11 no epimerization and a conversion of lactide of 80% at a temperature of 170°C (120).
12 Reactions conducted at 190°C led to lower molecular weight PLA with high dispersity
13 (above 2) as long as epimerization rates up to 15%. The authors believe that
14 magnesium (II) N-heterocyclic carbene is a promising catalyst in order to improve the
15 eco-friendliness of the continuous synthesis of PLA via reactive extrusion (120).

16 2. Copolymers

17 As a biodegradable and biocompatible polymer PLA is considered as a material of
18 huge interest for the medical and pharmaceutical fields.(12) Régibeau *et al.*(11)
19 presented in 2020 a synthesis of a medical grade of poly(D,L-lactide-co-glycolide)
20 (PLGA) (Figure 31) via the ROP of lactide and glycolide during the REX process. The
21 optimization of both screw and barrel designs allowed them to get 95 % conversion
22 within 10 min, affording polymers with molecular weights up to 50 000 g/mol (11).



24 Figure 31 Chemical structure of D,L-lactide (a), glycolide (b) and PLGA (c) (11)

25 Another cyclic polyester that is commonly polymerized by ROP promoted by Sn(Oct)₂
26 is ϵ -caprolactone (ϵ -CL) (4). Thus, poly(L-lactide-co- ϵ -caprolactone) can also be
27 produced by REX. The process is described by Nishida *et al.*(121) who designed a

1 three steps process including two REX separated by a mixing step . L-LA and Sn(Oct)₂
2 were extruded into a mixing hopper where the mixture was stirred with ε-CL prior to
3 be extruded. The resulting random copolymer displayed mechanical properties that
4 were lower than those of neat PLA e.g. the tensile strength was reduced of 50 to 20
5 MPa and the tensile elastic modulus dropped from 2500 MPa to 1500 MPa. In fact,
6 this decrease was inversely proportional to the ε-CL of the copolymer (121). These
7 poly(L-lactide-co-ε-caprolactone) copolymers with high ε-CL content can find their
8 utility in the medical or pharmaceutical field, as the biodegradability can be modulated
9 with the CL content and the type of copolymer formed (block, gradient or statistical).

10 A block copolymer PLA-b-PE was synthesized by Núñez et al.(55). To do so, an
11 intermediate product (PE-OH) was synthesized by coordination-insertion
12 polymerization using the zirconocene Cp₂ZrCl₂ at 50°C in toluene. Then, the block
13 copolymer was obtained via ROP by reacting PE-OH with L-lactide and Sn(Oct)₂. The
14 resulting copolymer was used to compatibilize a blend of PLA and PE.

15 Another type of block copolymer that is PLA-co-poly(propylene adipate) (PPAd) was
16 developed by Terzopoulou *et al.*(122) in order to tune the degradation properties of
17 PLA. After the polymerization of L-lactide with PPAd oligomers by REX at 180°C
18 during 20 minutes, the obtained PLA / PPAd copolymers reached number average
19 molecular weights up to 63,000 g/mol however the PPAd was inserted into the
20 copolymer, the lower the molecular weight was (122). Indeed, PPAd acted as a
21 macroinitiator which lead to an increased number of growing chains resulting in lower
22 molecular weight. Moreover, the incorporation of PPAD into the PLA backbone
23 contributed to increase the hydrolysis rate with and without enzyme of the copolymer
24 in comparison with neat PLA (Figure 32).

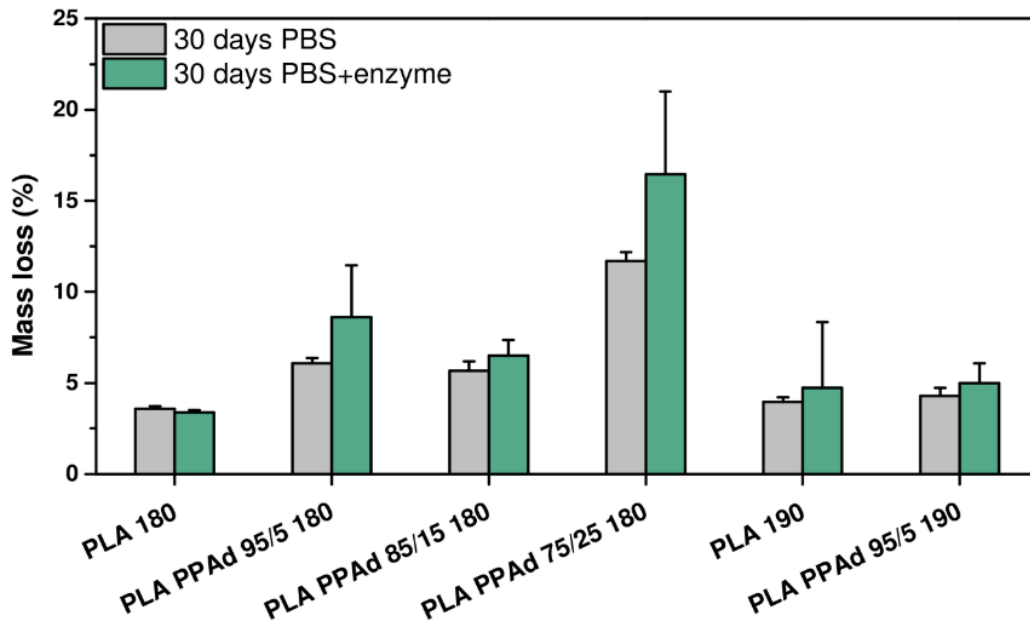


Figure 32 Effect of the presence of enzymes in the hydrolysis of the samples for 30 days(122)

3. Nanocomposites and complexed PLA

The incorporation of nanofillers e.g. silica, layered silicates, POSS and graphite (117), to the polymer matrix during the ROP of lactide via REX is often used to enhance PLA properties in terms of crystallinity, stiffness or thermal stability as described in the following papers (117,123).

The addition of graphite nanoplatelets (GNP) during the ROP of L-LA via REX was performed by Fina *et al.*(117) In particular the effect of the addition of molecules containing a pyrene end group and a poly(D-lactide) (PDLA) chain (Pyr-D) was studied (Figure 33). In the presence of PDLA, the L-lactic acid segment of PLLA will strongly interact with the D-lactic acid segments resulting in the formation of stereocomplexes (124,125). The PLA/GNP nanocomposites were found to be both thermally and electrically conductive. Moreover, the presence of stereo complexed regions increased the thermal conductivity of the PLA-based nanocomposites (117).

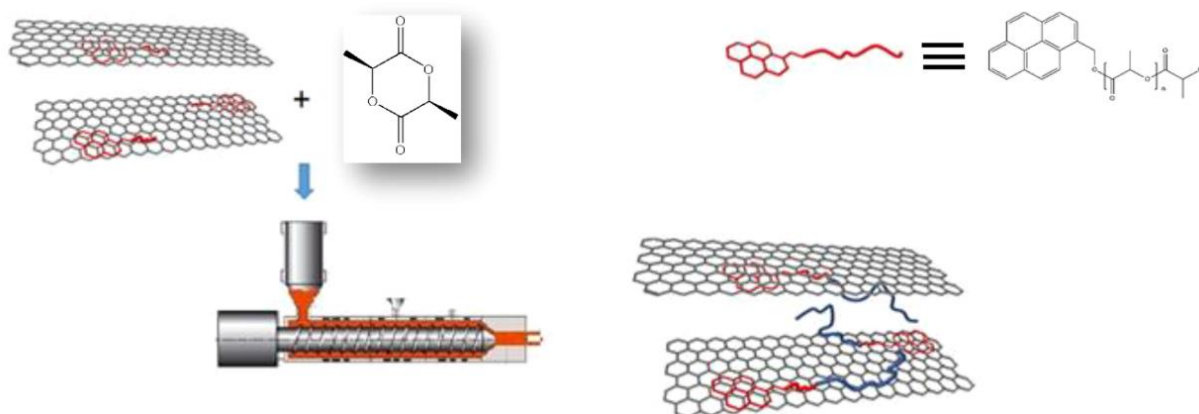


Figure 33 Scheme of the nanocomposites preparation procedure(117)

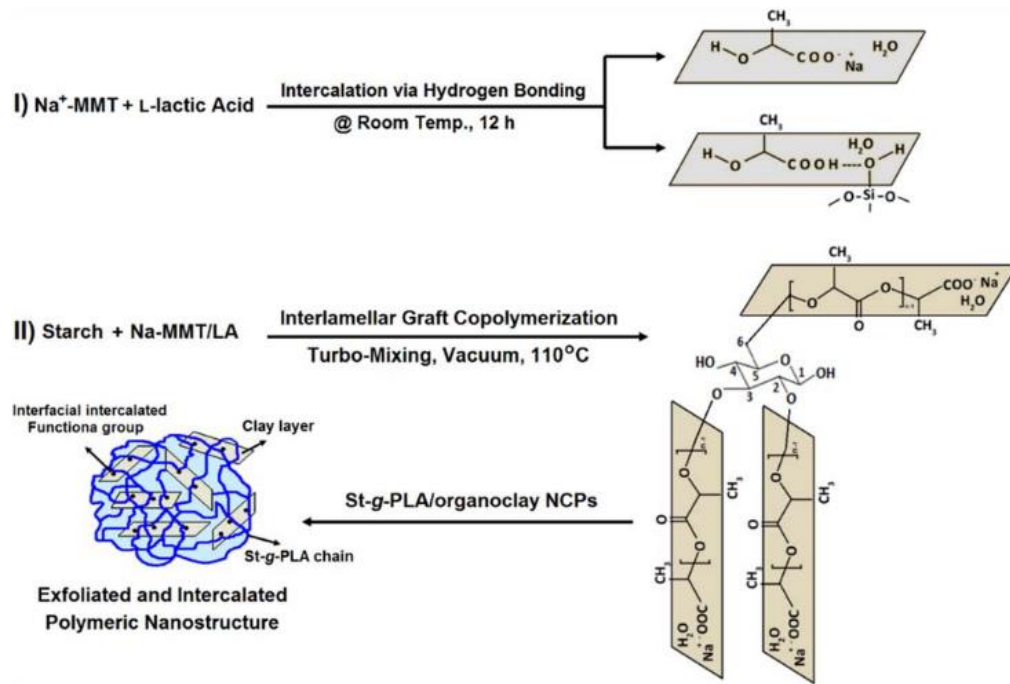
1
2
3 Zhen *et al.*(123) synthesized aminated benzoic acid intercalated layered double
4 hydroxides (AB-LDH). The latter was feed with L-LA and zinc lactate as the catalyst in
5 an extruder to obtain PLA / AB-LDH nanocomposites. Thanks to an orthogonal design
6 of experiment, they determined the optimum process conditions which were 2 wt % of
7 catalyst, 0.3 wt % of AB-LDH, a polymerization temperature of 170°C and a screw
8 speed of 20 rpm. AB-LDH act as nucleating agent which lead to an increase in PLA
9 nucleation density and crystallinity. Moreover, studies on the thermal decomposition
10 kinetics shows that, compared to neat PLA, the composite's thermal decomposition
11 activation energy is increased (34 kJ/mol vs 22 kJ/mol for neat PLA) (123) and the
12 thermal stability of PLA is improved. Indeed, the decomposition temperature of the
13 nanocomposite lies between 250°C and 300°C depending on the heating rates
14 whereas it is between 240°C and 280°C for neat PLA (123).

15 The addition of organically modified clay during the ROP of L-LA via REX was
16 performed by Nishida *et al.*(126). They observed that the obtained PLA / clay
17 nanocomposites had an intercalative morphology that affected the NMR parameters:
18 T_{1C} (overall carbon relaxation time) and T_{1H} (overall proton relaxation time). Indeed,
19 the nanocomposite had a different behavior resulting in decreased T_{1H} values above
20 room temperature (126). T_{1H} can be used as an indicator of the nanofiller dispersion
21 into the polymer matrix (127). Indeed, the paramagnetic Fe^{3+} from the clay acts as
22 relaxation sinks for proton leading to shortened relaxation time (127). Therefore, using
23 these data, calculations can be done to characterize the clay dispersion (127).
24 Moreover, the organoclay accelerate the relaxation time of ^{13}C nuclei especially for
25 temperatures above the T_c (crystallization temperature) (126). The TGA results also

1 showed that the presence of montmorillonite increased the decomposition
2 temperature (T_{dec}) compared to neat PLA (278°C vs 260°C) (126).

3 Salimi *et al.*(128) mixed starch (St) with LA and montmorillonite (MMT), an organoclay.
4 Their goal was to enhance the adhesion between both phases of the composite
5 leading to a potential candidate for petroleum-based plastics substitution. The first step
6 consisted in mechanical stirring followed by reactive extrusion in order to increase the
7 degree of grafting (Figure 34). The obtained St-g-PLA copolymers and St-g-PLA /
8 MMT nanocomposites were designed to produce films. Compared to St-g-PLA, the
9 nanocomposite displays higher thermal stability as proven by the TGA analysis. The
10 thermograms appeared to be shifted from 10-20°C to the right (128). Moreover, the
11 addition of 5 % of MMT enhanced St-g-PLA mechanical properties in terms of
12 elongation at break (5.2 vs 3.6 %), tensile strength (82.4 vs 52.4 N/mm²) and Young's
13 modulus (531 vs 140 N/mm²) (128).

14 Li *et al.*(129) prepared PLA-Y-cyclodextrin inclusion complexes from multi-branched
15 PLA (PLA-IC-PLA) starting from L-lactide. The thermal analysis (TGA, DSC) showed
16 that PLA-IC-PLA displayed a lower T_g as well as a 3 % higher crystallinity whereas the
17 TG curves showed similar profiles (129). Moreover, the branching brought better
18 mechanical properties to PLA-IC-PLA with a slightly higher elongation at break and an
19 improved impact strength (7 vs 5 kJ/m²). PLA-IC-PLA has an enhanced hydrophilicity
20 compared to neat PLA. This branched complexed polymer may have a potential use
21 in biomedical materials (129).



1

2 Figure 34 Schematic representation of the St-g-PLA/organoclay nanocomposite synthesis via a shear mixer and
 3 reactive extrusion(128)

4 4. Flame Retardancy

5 The flame retardancy of PLA is a challenging subject, however PLA has to be flame-
 6 retarded for being involved in long-lasting applications such as in automotive, aircraft
 7 or electronic fields.

8 Another example of using carbon as nanofiller in PLA nanocomposite is the work of
 9 Bourbigot *et al.*(110) The REX process of PLA / multi-wall carbon nanotubes (MWNT)
 10 (1 wt% of fillers) provided materials with an acceptable dispersion, *i.e.* the dispersion
 11 of MWNT particles in the polymer matrix was satisfactory and good enough to provide
 12 fire retardancy. PLA nanocomposites had an enhanced thermal stability compared to
 13 neat PLA. Indeed, the fire tests that were conducted on the resulting polymer also
 14 showed an enhanced flame retardancy that was determined by mass loss calorimetry.
 15 However, it could have been higher with a better dispersion of the nanofillers in the
 16 polymer matrix (110). The influence of MWNT on the thermal stability of PLA was also
 17 assessed by Gallos *et al.*(112) in 2014 where nanocomposites were produced by REX
 18 during the polymerization poly-L,D-lactide stereocomplexes. An improvement of the
 19 thermal stability was highlighted by TGA analysis. The first decomposition step of
 20 PDLLA-MWNT nanocomposite occurs at 209°C vs 170°C for PDLLA. However this
 21 improvement was reduced in the presence of α -tropolone, which is the component

1 used to deactivate the catalyst ($\text{Sn}(\text{Oct})_2$) (112). Indeed, the first decomposition step
2 of PDLLA-MWNT nanocomposite containing α -tropolone occurs at 193°C. Moreover,
3 the formation of a char layer was observed during fire test (mass loss calorimetry
4 experiment). The role of this layer is to reduce the volatile escaping to the flame and
5 acts as a thermal insulator during a certain period of time (110).

6 Flame retarded materials can also be obtained by the addition of intumescent
7 additives. Upon heating, an insulative, expanded charred coating will develop at the
8 surface of the polymer and provide low flammability (111). An intumescent
9 stereocomplexed PLA was successfully obtained when a combination of ammonium
10 polyphosphate (APP), melamine and organoclay were mixed with L-LA, D-LA and
11 $\text{Sn}(\text{Oct})_2 / \text{PPh}_3$ (1:1 mol%) in a twin-screw extruder (111). More precisely, 20 g of L-
12 LA were first added with the $\text{Sn}(\text{Oct})_2 / \text{PPh}_3$ mixture and the polymerization was
13 followed with the evolution of the torque. When it reached a plateau, half of the
14 synthesized PLLA was removed from the extruder and 10 g of D-LA with the $\text{Sn}(\text{Oct})_2$
15 / PPh_3 mixture were added. Finally, α -tropolone was used to deactivate the catalyst
16 and both APP, melamine and organoclay were added (111). This provided materials
17 with significantly improved fire properties compared to neat PLA (111). APP and
18 melamine are conventional flame retardants which, with nanoclay, reacts upon heating
19 and lead to the formation of a char. The mass loss calorimeter results shown a
20 significant reduction of the pHRR (peak heat release rate) of flame retarded PDLLA
21 (50 vs 250 kW/m² for PDLLA) (111).

22 However, the above-mentioned methods present some drawbacks that are the
23 potential leaching and migration of the additives. Thus, a solution to these problem is
24 the incorporation of fire-retardant (FR) moieties directly in the PLA backbone which
25 was investigated by Mincheva's *et al.*(130). A three-steps process (Figure 35) was
26 developed including the synthesis of a [9,10-dihydro-oxa-10-phosphaphenanthrene-
27 10-oxide]-based initiator (DOPO-diamine) that was used during the ROP of L-LA in
28 bulk. DOPO-PLA was coupled with hexamethylene diisocyanate (HDI) leading to the
29 formation of DOPO-PLA-PU which were mixed with commercial PLA. Compared to
30 commercial PLA, DOPO-PLA-PU exhibited enhanced fire properties at the cone
31 calorimeter and UL-94 tests. The pHRR (peak heat release rate) was reduced by 35
32 % and the THR (total heat release) was reduced by 36 % compared to neat PLA (130).

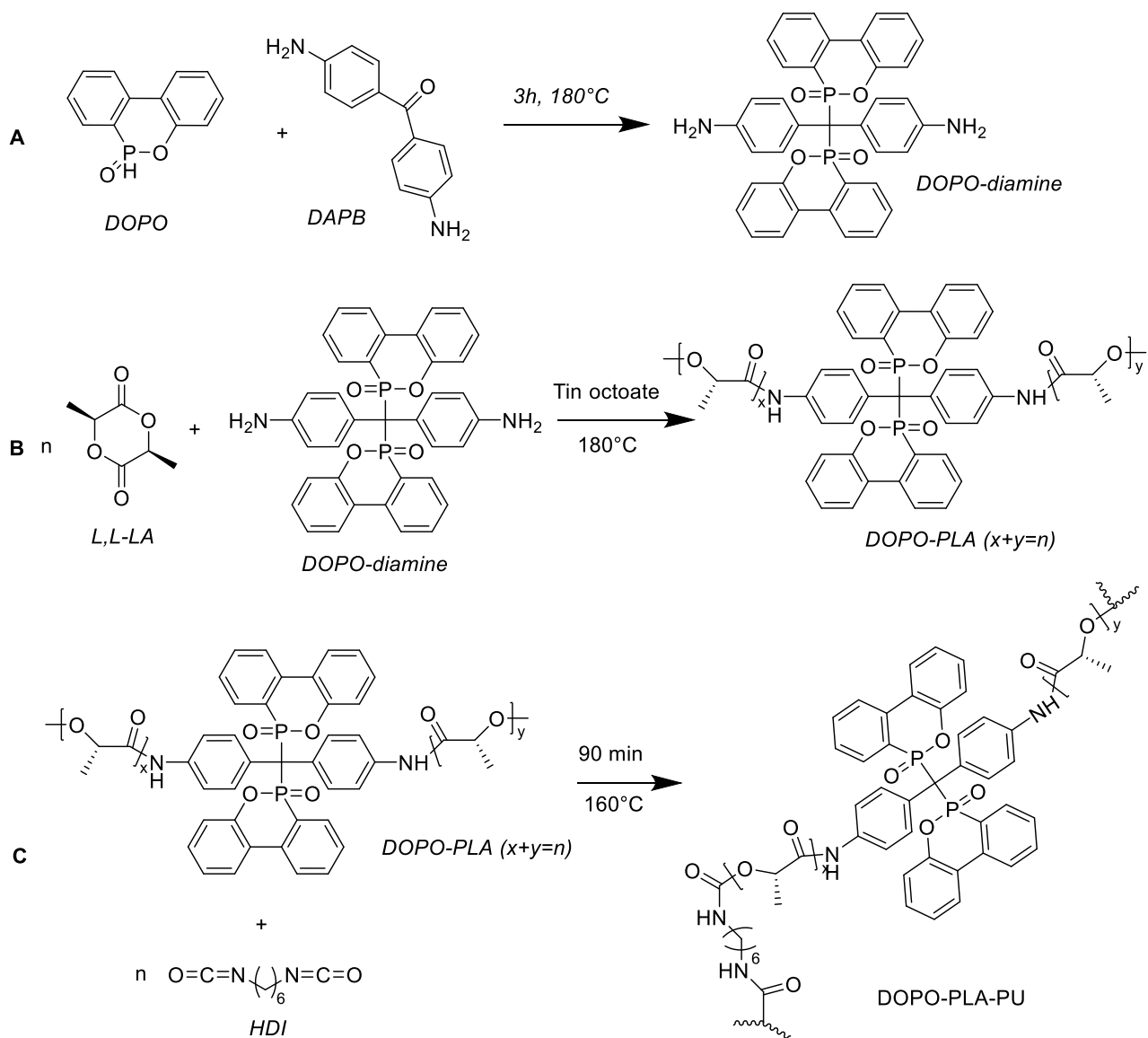


Figure 35 Three-step synthetic pathway to 9,10-dihydro-oxa-10-phosphaphenanthrene-10-oxide (DOPO)-poly(lactic acid) (PLA) PUs: (A) Synthesis of DOPO-diamine; (B) DOPO-initiated bulk ring-opening polymerization (ROP) of L,L-lactide (L,L-LA); (C) chain coupling reaction (130)

1 Conclusion

2 Many pathways have been developed to synthesize PLA with improved thermo-
3 mechanical properties. One of the most common strategy involves the blending of
4 commercial PLA with other polymers and compatibilizing agents. The development of
5 PLA-based composites is also a well-studied route. It usually involves peroxides to
6 create radicals allowing the grafting of molecules onto PLA backbone. Most of the
7 studies exploring these strategies explore the use of petroleum-based polymers or
8 non-sustainable additives. However, one of the challenges in the chemical
9 modification of PLA is to improve its mechanical properties while retaining its
10 biodegradability. Therefore, sustainable modification routes of PLA have focused on
11 the use of biosourced additives such as functionalized vegetable oil or food industry
12 byproducts flour e.g. walnut shell, almond shell, orange peel. However,
13 complementary studies assessing the sustainability of the obtained PLA-based blends
14 or composites would be required. The chemical modification of PLA starting from L-
15 lactide allows the insertion of a comonomer or moiety into the PLA backbone which
16 can prevent potential leaching or migration of the active functionality. This route may
17 offer a wider range of possibilities for the modification of PLA but is highly challenging.
18 This route offers possibilities to design specific comonomer to give a targeted property
19 to resulting PLA. The thermal, mechanical and rheological properties enhancement of
20 PLA can be performed with the addition of additives during the reactive extrusion
21 process, opening perspectives for the incorporation of additives, and in particular
22 flame retardants, the fireproofing of PLA still being a challenge. However, the number
23 of steps needed may prevent it from being compatible with an industrial process. A
24 new area of research would be to design a single-step reactive extrusion process that
25 will allow the incorporation of functional moieties in the PLLA backbone during the
26 ring-opening polymerization of L-LA. It could be, for example, used to develop a flame
27 retardant biopolymer, which would therefore be used for long lasting applications in
28 the automotive industry. In both fields *i.e.* modification of commercial PLA and
29 modification of PLA during its synthesis, the sustainability of the modified PLA should
30 be targeted and assessed. Indeed, neat PLA is considered as a green alternative to
31 petroleum-based polymer since it is compostable. Therefore, modified PLA should
32 keep this feature. To do so, new bio-based and compostable additives should be
33 designed. Moreover, in this pandemic context, functionalization of PLA with

- 1 antibacterial groups would enlarge its range of use *e.g.* as a virucidal or bactericidal
- 2 sustainable coating in the medical field.
- 3 This work has received funding from the French Research Agency (PLARE, ANR-20-
- 4 CE93-0004)
- 5

Bibliography

1. Plastics - the Facts 2021. <https://plasticseurope.org/resources/market-data/>, Consult 10012022.
2. Geyer R, Jambeck JR, Law KL. Production, use, and fate of all plastics ever made. *Sci Adv*. 2017 Jul 19;3(7).
3. Nikolaivits E, Pantelic B, Azeem M, Taxeidis G, Babu R, Topakas E, et al. Progressing Plastics Circularity: A Review of Mechano-Biocatalytic Approaches for Waste Plastic (Re)valorization. *Front Bioeng Biotechnol*. 2021 Jun 22;9(June):1–31.
4. Raquez J-M, Ramy-Ratiarison R, Murariu M, Dubois P. CHAPTER 4. Reactive Extrusion of PLA-based Materials: from Synthesis to Reactive Melt-blending. In: *Processing, Characterization and Physical Properties of PLA*. 2014. p. 99–123.
5. Jacobsen S, Fritz HG, Degée P, Dubois P, Jérôme R. Single-step reactive extrusion of PLLA in a corotating twin-screw extruder promoted by 2-ethylhexanoic acid tin(II) salt and triphenylphosphine. *Polymer (Guildf)*. 2000;41(9):3395–403.
6. Jacobsen S, Fritz HG, Degée P, Dubois P, Jérôme R. New developments on the ring opening polymerisation of polylactide. *Ind Crops Prod*. 2000;11(2–3):265–75.
7. Karamanlioglu M, Preziosi R, Robson GD. Abiotic and biotic environmental degradation of the bioplastic polymer poly(lactic acid): A review. *Polym Degrad Stab*. 2017;137:122–30.
8. Jem KJ, Tan B. The development and challenges of poly (lactic acid) and poly (glycolic acid). *Adv Ind Eng Polym Res*. 2020;3(2):60–70.
9. Bourbigot S, Fontaine G. Flame retardancy of polylactide: An overview. Vol. 1, *Polymer Chemistry*. 2010. p. 1413–22.
10. Ku Marsilla KI, Verbeek CJR. Modification of poly(lactic acid) using itaconic anhydride by reactive extrusion. *Eur Polym J*. 2015;67:213–23.
11. Régibeau N, Hurlet J, Tilkin RG, Lombart F, Heinrichs B, Grandfils C. Synthesis

- 1 of medical grade PLLA, PDLLA, and PLGA by a reactive extrusion
2 polymerization. *Mater Today Commun.* 2020 Sep;24(May):101208.
- 3 12. Vlachopoulos A, Karlioti G, Balla E, Daniilidis V, Kalamas T, Stefanidou M, et al.
4 Poly(Lactic Acid)-Based Microparticles for Drug Delivery Applications: An
5 Overview of Recent Advances. *Pharmaceutics.* 2022;14(2):1–37.
- 6 13. Balla E, Daniilidis V, Karlioti G, Kalamas T, Stefanidou M, Bikiaris ND, et al.
7 Poly(lactic acid): A versatile biobased polymer for the future with multifunctional
8 properties-from monomer synthesis, polymerization techniques and molecular
9 weight increase to PLA applications. *Polymers (Basel).* 2021;13(11).
- 10 14. Castellón SM, Standau T, Altstädt V, Bonten C. Modification of different
11 polylactides by reactive extrusion to enhance their melt properties. *AIP Conf*
12 *Proc.* 2020;2289(November).
- 13 15. Liu P, Wu J, Yang G, Shao H. Comparison of static mixing reaction and reactive
14 extrusion technique for ring-opening polymerization of L-lactide. *Mater Lett.*
15 2017;186(September 2016):372–4.
- 16 16. Standau T, Goettermann S, Weinmann S, Bonten C, Altstädt V, Di Maio E.
17 Autoclave foaming of chemically modified polylactide. *J Cell Plast.*
18 2017;53(5):481–9.
- 19 17. González-López ME, Robledo-Ortíz JR, Manríquez-González R, Silva-Guzmán
20 JA, Pérez-Fonseca AA. Polylactic acid functionalization with maleic anhydride
21 and its use as coupling agent in natural fiber biocomposites: a review. *Compos*
22 *Interfaces.* 2018;25(5–7):515–38.
- 23 18. Rolere S, Monge S, Rakotonirina MD, Guillaneuf Y, Gigmes D, Robin J.
24 Chemical modification of poly(lactic acid) induced by thermal decomposition of
25 N -acetoxy-phthalimide during extrusion. *J Polym Sci Part A Polym Chem.* 2019
26 Jan 15;57(2):120–9.
- 27 19. Rolere S, Monge S, Rakotonirina MD, Guillaneuf Y, Gigmes D, Robin JJ.
28 Functionalization of poly(lactide) with N-phenyl maleimide using N-acetoxy-
29 phthalimide during reactive extrusion. *J Polym Sci Part A Polym Chem.*
30 2019;57(8):917–28.

- 1 20. Tiwary P, Kontopoulou M. Tuning the Rheological, Thermal, and Solid-State
2 Properties of Branched PLA by Free-Radical-Mediated Reactive Extrusion. ACS
3 Sustain Chem Eng. 2018;6(2):2197–206.
- 4 21. Tiwary P, Kontopoulou M. Rheological characterization of long-chain branched
5 poly(lactide) prepared by reactive extrusion in the presence of allylic and acrylic
6 coagents. Vol. 62, Journal of Rheology. 2018. p. 1071–82.
- 7 22. Tiwary P, Najafi N, Kontopoulou M. Advances in peroxide-initiated graft
8 modification of thermoplastic biopolyesters by reactive extrusion. Can J Chem
9 Eng. 2021 Sep 29;99(9):1870–84.
- 10 23. Frédéric B, Samira T, Mohamed T. Graft copolymers of
11 poly(Methylmethacrylate) and poly(Lactic Acid) or poly(3-Hydroxybutyrate):
12 Synthesis by reactive extrusion and characterization. Macromol React Eng.
13 2014;8(2):149–59.
- 14 24. Herskovitz JE, Goddard JM. Reactive Extrusion of Nonmigratory Antioxidant
15 Poly(lactic acid) Packaging. J Agric Food Chem. 2020;68(7):2164–73.
- 16 25. Khajeheian MB, Rosling A. Rheological and Thermal Properties of Peroxide-
17 Modified Poly(l-lactide)s for Blending Purposes. J Polym Environ. 2015 Mar
18 24;23(1):62–71.
- 19 26. Simmons H, Kontopoulou M. Hydrolytic degradation of branched PLA produced
20 by reactive extrusion. Polym Degrad Stab. 2018;158:228–37.
- 21 27. Reungdech W, Tachaboonyakiat W. Functionalization of polylactide with
22 multibranch poly(ethyleneimine) by in situ reactive extrusion. Polymer
23 (Guildf). 2022;246(March):124746.
- 24 28. Li P, Zhu X, Kong M, Lv Y, Huang Y, Yang Q, et al. Fully biodegradable
25 polylactide foams with ultrahigh expansion ratio and heat resistance for green
26 packaging. Int J Biol Macromol. 2021 Jul;183:222–34.
- 27 29. Tiwary P, Park CB, Kontopoulou M. Transition from microcellular to nanocellular
28 PLA foams by controlling viscosity, branching and crystallization. Eur Polym J.
29 2017;91(March):283–96.
- 30 30. Li P, Zhu X, Kong M, Lv Y, Yang Q, Huang Y, et al. High performance branched

- 1 poly(lactide) induced by reactive extrusion with low-content cyclic organic
2 peroxide and multifunctional acrylate coagents. *Polymer* (Guildf).
3 2020;205(July):122867.
- 4 31. Göttermann S, Standau T, Weinmann S, Altstädt V, Bonten C. Effect of chemical
5 modification on the thermal and rheological properties of polylactide. *Polym Eng*
6 *Sci.* 2017;57(11):1242–51.
- 7 32. Yamoum C, Maia J, Magaraphan R. Rheological and thermal behavior of PLA
8 modified by chemical crosslinking in the presence of ethoxylated bisphenol A
9 dimethacrylates. *Polym Adv Technol.* 2017;28(1):102–12.
- 10 33. Dörr D, Standau T, Castellón SM, Bonten C, Altstädt V. Rheology in the
11 presence of carbon dioxide (CO₂) to study the melt behavior of chemically
12 modified polylactide (PLA). *Polymers* (Basel). 2020;12(5):1–10.
- 13 34. Schneider J, Bourque K, Narayan R. Moisture curable toughened poly(lactide)
14 utilizing vinyltrimethoxysilane based crosslinks. *Express Polym Lett.*
15 2016;10(10):799–809.
- 16 35. Lee JC, Choi MC, Choi DH, Ha CS. Toughness enhancement of poly(lactic acid)
17 through hybridisation with epoxide-functionalised silane via reactive extrusion.
18 *Polym Degrad Stab.* 2019;160:195–202.
- 19 36. Lee JC, Choi DH, Choi JY, Ha CS. Poly(lactic acid)/Functionalized Silica Hybrids
20 by Reactive Extrusion: Thermal, Rheological, and Degradation Behavior.
21 *Macromol Res.* 2020;28(4):327–35.
- 22 37. Torres E, Gaona A, García-Bosch N, Muñoz M, Fombuena V, Moriana R, et al.
23 Improved Mechanical, Thermal, and Hydrophobic Properties of PLA Modified
24 with Alkoxysilanes by Reactive Extrusion Process. *Polymers* (Basel). 2021 Jul
25 27;13(15):2475.
- 26 38. Chen C-Q, Ke D-M, Zheng T-T, He G-J, Cao X-W, Liao X. An Ultraviolet-Induced
27 Reactive Extrusion To Control Chain Scission and Long-Chain Branching
28 Reactions of Polylactide. *Ind Eng Chem Res.* 2016 Jan 27;55(3):597–605.
- 29 39. Li S, He G, Liao X, Park CB, Yang Q, Li G. Introduction of a long-chain branching
30 structure by ultraviolet-induced reactive extrusion to improve cell morphology

- 1 and processing properties of polylactide foam. *RSC Adv.* 2017;7(11):6266–77.
- 2 40. Barletta M, Aversa C, Puopolo M. Recycling of PLA-based bioplastics: The role
3 of chain-extenders in twin-screw extrusion compounding and cast extrusion of
4 sheets. *J Appl Polym Sci.* 2020;137(42).
- 5 41. Cailloux J, Santana OO, Franco-Urquiza E, Bou JJ, Carrasco F, Maspoch ML.
6 Sheets of branched poly(lactic acid) obtained by one-step reactive extrusion–
7 calendering process: physical aging and fracture behavior. *J Mater Sci.* 2014
8 Jun 19;49(11):4093–107.
- 9 42. Carrasco F, Cailloux J, Sánchez-Jiménez PE, Maspoch ML. Improvement of the
10 thermal stability of branched poly(lactic acid) obtained by reactive extrusion.
11 *Polym Degrad Stab.* 2014;104(1):40–9.
- 12 43. Quiles-Carrillo L, Duart S, Montanes N, Torres-Giner S, Balart R. Enhancement
13 of the mechanical and thermal properties of injection-molded polylactide parts
14 by the addition of acrylated epoxidized soybean oil. *Mater Des.* 2018;140:54–
15 63.
- 16 44. Grigora ME, Terzopoulou Z, Tsongas K, Klonos P, Kalafatakis N, Bikiaris DN,
17 et al. Influence of reactive chain extension on the properties of 3d printed
18 poly(Lactic acid) constructs. *Polymers (Basel).* 2021;13(9):1–18.
- 19 45. Valerio O, Misra M, Mohanty AK. Sustainable biobased blends of poly(lactic
20 acid) (PLA) and poly(glycerol succinate-: Co -maleate) (PGSMA) with balanced
21 performance prepared by dynamic vulcanization. *RSC Adv.* 2017;7(61):38594–
22 603.
- 23 46. Rigoussen A, Verge P, Raquez JM, Habibi Y, Dubois P. In-depth investigation
24 on the effect and role of cardanol in the compatibilization of PLA/ABS immiscible
25 blends by reactive extrusion. *Eur Polym J.* 2017;93(April):272–83.
- 26 47. Carrasco F, Santana OO, Cailloux J, Sánchez-Soto M, Maspoch ML. Thermal
27 degradation of poly(lactic acid) and acrylonitrile-butadiene-styrene bioblends:
28 Elucidation of reaction mechanisms. *Thermochim Acta.*
29 2017;654(February):157–67.
- 30 48. Vadori R, Misra M, Mohanty AK. Sustainable biobased blends from the reactive

- 1 extrusion of polylactide and acrylonitrile butadiene styrene. *J Appl Polym Sci.*
2 2016 Dec 5;133(45).
- 3 49. Vadori R, Misra M, Mohanty AK. Statistical optimization of compatibilized blends
4 of poly(lactic acid) and acrylonitrile butadiene styrene. *J Appl Polym Sci.*
5 2017;134(9).
- 6 50. Carrasco F, Santana OO, Cailloux J, Sánchez-Soto M, Maspoch ML. Poly(lactic
7 acid) and acrylonitrile–butadiene–styrene blends: Influence of adding
8 ABS–g–MAH compatibilizer on the kinetics of the thermal degradation. Vol. 67,
9 *Polymer Testing.* 2018. p. 468–76.
- 10 51. Rigoussen A, Raquez JM, Dubois P, Verge P. A dual approach to compatibilize
11 PLA/ABS immiscible blends with epoxidized cardanol derivatives. *Eur Polym J.*
12 2019;114(December 2018):118–26.
- 13 52. Abt T, Kamrani MR, Cailloux J, Santana O, Sánchez-Soto M. Modification of
14 poly(lactic) acid by reactive extrusion and its melt blending with acrylonitrile–
15 butadiene–styrene. *Polym Int.* 2020;69(9):794–803.
- 16 53. Rasselet D, Caro-Bretelle AS, Taguet A, Lopez-Cuesta JM. Reactive
17 compatibilization of PLA/PA11 blends and their application in additive
18 manufacturing. *Materials (Basel).* 2019;12(3).
- 19 54. Walha F, Lamnawar K, Maazouz A, Jaziri M. Rheological, morphological and
20 mechanical studies of sustainably sourced polymer blends based on poly(lactic
21 acid) and polyamide 11. *Polymers (Basel).* 2016;8(3).
- 22 55. Gallego R, López-Quintana S, Basurto F, Núñez K, Villarreal N, Merino JC.
23 Synthesis of new compatibilizers to poly(lactic acid) blends. *Polym Eng Sci.*
24 2014 Mar;54(3):522–30.
- 25 56. Bäckström E, Odelius K, Hakkarainen M. Designed from Recycled: Turning
26 Polyethylene Waste to Covalently Attached Polylactide Plasticizers. *ACS*
27 *Sustain Chem Eng.* 2019;7(12):11004–13.
- 28 57. Quiles-Carrillo L, Montanes N, Lagaron JM, Balart R, Torres-Giner S. In Situ
29 Compatibilization of Biopolymer Ternary Blends by Reactive Extrusion with Low-
30 Functionality Epoxy-Based Styrene–Acrylic Oligomer. *J Polym Environ.*

- 1 2019;27(1):84–96.
- 2 58. Valerio O, Pin JM, Misra M, Mohanty AK. Synthesis of Glycerol-Based
3 Biopolyesters as Toughness Enhancers for Polylactic Acid Bioplastic through
4 Reactive Extrusion. *ACS Omega*. 2016 Dec 31;1(6):1284–95.
- 5 59. Piontek A, Vernaez O, Kabasci S. Compatibilization of Poly(Lactic Acid) (PLA)
6 and Bio-Based Ethylene-Propylene-Diene-Rubber (EPDM) via Reactive
7 Extrusion with Different Coagents. *Polymers (Basel)*. 2020 Mar 6;12(3):605.
- 8 60. Coltelli M, Mallegni N, Rizzo S, Fiori S, Signori F, Lazzeri A. Compatibilization
9 of Poly(Lactic Acid) (PLA)/Plasticized Cellulose Acetate Extruded Blends
10 through the Addition of Reactively Extruded Comb Copolymers. *Molecules*.
11 2021 Apr 1;26(7):2006.
- 12 61. Tejada-Oliveros R, Fiori S, Gomez-Caturla J, Lascano D, Montanes N, Quiles-
13 Carrillo L, et al. Development and Characterization of Polylactide Blends with
14 Improved Toughness by Reactive Extrusion with Lactic Acid Oligomers.
15 *Polymers (Basel)*. 2022;14(9):1874.
- 16 62. Brüster B, Montesinos A, Reumaux P, Pérez-Camargo RA, Mugica A, Zubitur
17 M, et al. Crystallization kinetics of polylactide: Reactive plasticization and
18 reprocessing effects. *Polym Degrad Stab*. 2018;148(November 2017):56–66.
- 19 63. Brüster B, Addiego F, Hassouna F, Ruch D, Raquez J-M, Dubois P. Thermo-
20 mechanical degradation of plasticized poly(lactide) after multiple reprocessing
21 to simulate recycling: Multi-scale analysis and underlying mechanisms. *Polym*
22 *Degrad Stab*. 2016 Sep;131:132–44.
- 23 64. Brüster B, Amozoqueño C, Grysan P, Peral I, Watts B, Raquez JM, et al.
24 Resolving Inclusion Structure and Deformation Mechanisms in Polylactide
25 Plasticized by Reactive Extrusion. *Macromol Mater Eng*. 2017;302(12):1–10.
- 26 65. Brüster B, Adjoua YO, Dieden R, Grysan P, Federico CE, Berthé V, et al.
27 Plasticization of polylactide with myrcene and limonene as bio-based
28 plasticizers: Conventional vs. reactive extrusion. *Polymers (Basel)*. 2019;11(8).
- 29 66. Shin BY, Han DH. Viscoelastic properties of PLA/PCL blends compatibilized
30 with different methods. *Korea Aust Rheol J*. 2017;29(4):295–302.

- 1 67. Davis BJ, Thapa K, Hartline MC, Fuchs WK, Blanton MD, Wiggins JS, et al.
2 Enhanced photodegradation of TiO₂-containing poly(ϵ -caprolactone)/poly(lactic
3 acid) blends. *J Polym Sci.* 2021 Nov 23;59(21):2479–91.
- 4 68. Gurunathan T, Chung JS, Nayak SK. Reactive Compatibilization of Biobased
5 Polyurethane Prepolymer Toughening Polylactide Prepared by Melt Blending. *J*
6 *Polym Environ.* 2016;24(4):287–97.
- 7 69. Scoponi G, Francini N, Athanassiou A. Production of Green Star/Linear PLA
8 Blends by Extrusion and Injection Molding: Tailoring Rheological and
9 Mechanical Performances of Conventional PLA. *Macromol Mater Eng.* 2021
10 May 17;306(5):2000805.
- 11 70. Spinella S, Cai J, Samuel C, Zhu J, McCallum SA, Habibi Y, et al.
12 Polylactide/Poly(ω -hydroxytetradecanoic acid) Reactive Blending: A Green
13 Renewable Approach to Improving Polylactide Properties. *Biomacromolecules.*
14 2015 Jun 8;16(6):1818–26.
- 15 71. Mihai I, Hassouna F, Fouquet T, Laachachi A, Raquez JM, Ibn El Ahrach H, et
16 al. Reactive plasticization of poly(lactide) with epoxy functionalized cardanol.
17 *Polym Eng Sci.* 2018;58:E64–72.
- 18 72. Calderón BA, McCaughey MS, Thompson CW, Barinelli VL, Sobkowicz MJ.
19 Evaluating the Influence of Specific Mechanical Energy on Biopolymer Blends
20 Prepared via High-Speed Reactive Extrusion. *ACS Appl Polym Mater.* 2019 Jun
21 14;1(6):1410–9.
- 22 73. Xue B, He H, Zhu Z, Li J, Huang Z, Wang G, et al. A Facile Fabrication of High
23 Toughness Poly(lactic Acid) via Reactive Extrusion with Poly(butylene
24 Succinate) and Ethylene-Methyl Acrylate-Glycidyl Methacrylate. *Polymers*
25 (Basel). 2018 Dec 17;10(12):1401.
- 26 74. Palai B, Biswal M, Mohanty S, Nayak SK. In situ reactive compatibilization of
27 polylactic acid (PLA) and thermoplastic starch (TPS) blends; synthesis and
28 evaluation of extrusion blown films thereof. *Ind Crops Prod.*
29 2019;141(February):111748.
- 30 75. Fredi G, Dorigato A, Dussin A, Xanthopoulou E, Bikiaris DN, Botta L, et al.

- 1 Compatibilization of Polylactide/Poly(ethylene 2,5-furanoate) (PLA/PEF) Blends
2 for Sustainable and Bioderived Packaging. *Molecules*. 2022;27(19):6371.
- 3 76. Zhang Y, Jiang Y, Liu X, Lv S, Cao J, Tan H, et al. Properties of grafted wood
4 flour filled poly (lactic acid) composites by reactive extrusion. *J Adhes Sci*
5 *Technol*. 2018;32(4):429–38.
- 6 77. Pan Y-J, Lin Z-I, Lou C-W, Huang C-L, Lee M-C, Liao J-M, et al. Polylactic
7 acid/carbon fiber composites: Effects of polylactic acid-g-maleic anhydride on
8 mechanical properties, thermal behavior, surface compatibility, and electrical
9 characteristics. *J Compos Mater*. 2018 Feb 8;52(3):405–16.
- 10 78. Verginio GEA, Montanheiro TL do A, Montagna LS, Marini J, Passador FR.
11 Effectiveness of the preparation of maleic anhydride grafted poly (lactic acid) by
12 reactive processing for poly (lactic acid)/carbon nanotubes nanocomposites. *J*
13 *Appl Polym Sci*. 2021;138(12):10–2.
- 14 79. Urtekin G, Aytac A. The effects of multi-walled carbon nanotube additives with
15 different functionalities on the properties of polycarbonate/poly (lactic acid)
16 blend. *J Polym Res*. 2021;28(5):1–13.
- 17 80. Quiles-Carrillo L, Montanes N, Lagaron JM, Balart R, Torres-Giner S. On the
18 use of acrylated epoxidized soybean oil as a reactive compatibilizer in injection-
19 molded compostable pieces consisting of polylactide filled with orange peel
20 flour. *Polym Int*. 2018;67(10):1341–51.
- 21 81. Quiles-Carrillo L, Montanes N, Sammon C, Balart R, Torres-Giner S.
22 Compatibilization of highly sustainable polylactide/almond shell flour composites
23 by reactive extrusion with maleinized linseed oil. *Ind Crops Prod*.
24 2018;111(March 2017):878–88.
- 25 82. Montava-Jordà S, Quiles-Carrillo L, Richart N, Torres-Giner S, Montanes N.
26 Enhanced Interfacial Adhesion of Polylactide/Poly(ϵ -caprolactone)/Walnut Shell
27 Flour Composites by Reactive Extrusion with Maleinized Linseed Oil. *Polymers*
28 (Basel). 2019 Apr 30;11(5):758.
- 29 83. Lv S, Gu J, Tan H, Zhang Y. Modification of wood flour/PLA composites by
30 reactive extrusion with maleic anhydride. *J Appl Polym Sci*. 2016;133(15):1–9.

- 1 84. Seo Y-R, Bae S-U, Gwon J, Wu Q, Kim B-J. Effects of Methylenediphenyl 4,4'-
2 Diisocyanate and Maleic Anhydride as Coupling Agents on the Properties of
3 Polylactic Acid/Polybutylene Succinate/Wood Flour Biocomposites by Reactive
4 Extrusion. *Materials (Basel)*. 2020 Apr 3;13(7):1660.
- 5 85. Dhar P, Tarafder D, Kumar A, Katiyar V. Thermally recyclable polylactic
6 acid/cellulose nanocrystal films through reactive extrusion process. *Polymer*
7 (Guildf). 2016;87:268–82.
- 8 86. Dhar P, Gaur SS, Soundararajan N, Gupta A, Bhasney SM, Milli M, et al.
9 Reactive Extrusion of Polylactic Acid/Cellulose Nanocrystal Films for Food
10 Packaging Applications: Influence of Filler Type on Thermomechanical,
11 Rheological, and Barrier Properties. *Ind Eng Chem Res*. 2017;56(16):4718–35.
- 12 87. Liao J, Brosse N, Hoppe S, Zhou X, Xi X, Du G, et al. Interfacial improvement
13 of poly (lactic acid)/tannin acetate composites via radical initiated
14 polymerization. *Ind Crops Prod*. 2021;159(July 2020):113068.
- 15 88. Liao J, Brosse N, Hoppe S, Du G, Zhou X, Pizzi A. One-step compatibilization
16 of poly(lactic acid) and tannin via reactive extrusion. *Mater Des*.
17 2020;191:108603.
- 18 89. Wang N, Zhang C, Zhu W, Weng Y. Improving interfacial adhesion of pla/lignin
19 composites by one-step solvent-free modification method. *J Renew Mater*.
20 2020;8(9):1139–49.
- 21 90. Abdelwahab MA, Jacob S, Misra M, Mohanty AK. Super-tough sustainable
22 biobased composites from polylactide bioplastic and lignin for bio-elastomer
23 application. *Polymer (Guildf)*. 2021;212(October 2020):123153.
- 24 91. Frone AN, Batalu D, Chiulan I, Oprea M, Gabor AR, Nicolae C, et al. Morpho-
25 Structural, Thermal and Mechanical Properties of PLA/PHB/Cellulose
26 Biodegradable Nanocomposites Obtained by Compression Molding, Extrusion,
27 and 3D Printing. *Nanomaterials*. 2019 Dec 24;10(1):51.
- 28 92. Phuong VT, Gigante V, Aliotta L, Coltelli MB, Cinelli P, Lazzeri A. Reactively
29 extruded ecocomposites based on poly(lactic acid)/bisphenol A polycarbonate
30 blends reinforced with regenerated cellulose microfibers. *Compos Sci Technol*.

- 1 2017;139:127–37.
- 2 93. Tesfaye M, Patwa R, Dhar P, Katiyar V. Nanosilk-Grafted Poly(lactic acid) Films:
3 Influence of Cross-Linking on Rheology and Thermal Stability. ACS Omega.
4 2017 Oct 31;2(10):7071–84.
- 5 94. Li FJ, Yu XT, Huang Z, Liu DF. Interfacial improvements in cellulose nanofibers
6 reinforced polylactide bionanocomposites prepared by in situ reactive extrusion.
7 Polym Adv Technol. 2021;32(6):2352–66.
- 8 95. Bher A, Unalan IU, Auras R, Rubino M, Schvezov CE. Toughening of poly(lactic
9 acid) and thermoplastic cassava starch reactive blends using graphene
10 nanoplatelets. Polymers (Basel). 2018;10(1):1–18.
- 11 96. Trinh BM, Chang CC, Mekonnen TH. Facile fabrication of thermoplastic
12 starch/poly (lactic acid) multilayer films with superior gas and moisture barrier
13 properties. Polymer (Guildf). 2021;223(January):123679.
- 14 97. Cailloux J, Hakim RN, Santana OO, Bou J, Abt T, Sánchez-Soto M, et al.
15 Reactive extrusion: A useful process to manufacture structurally modified
16 PLA/o-MMT composites. Compos Part A Appl Sci Manuf. 2016;88:106–15.
- 17 98. Carrasco F, Santana O, Cailloux J, Maspoch ML. Kinetics of the thermal
18 degradation of poly(lactic acid) obtained by reactive extrusion: Influence of the
19 addition of montmorillonite nanoparticles. Polym Test. 2015;48:69–81.
- 20 99. Cailloux J, Abt T, García-Masabet V, Santana O, Sánchez-Soto M, Carrasco F,
21 et al. Effect of the viscosity ratio on the PLA/PA10.10 bioblends morphology and
22 mechanical properties. Express Polym Lett. 2018;12(6):569–82.
- 23 100. Carrasco F, Pérez OS, Maspoch ML. Kinetics of the thermal degradation of
24 poly(Lactic acid) and polyamide bioblends. Polymers (Basel). 2021;13(22):1–
25 15.
- 26 101. Martinez-Orozco L, León N, Cailloux J, Sánchez-Soto M, Maspoch ML, Santana
27 O. EcoBlends'up: PLA/BioPA blends composites, microfibrillated “in situ”
28 through additive manufacturing. Theor Appl Fract Mech. 2022;118(December
29 2021).
- 30 102. Barletta M, Pizzi E, Puopolo M, Vesco S, Daneshvar-Fatah F. Thermal behavior

- 1 of extruded and injection-molded poly(lactic acid)–talc engineered
2 biocomposites: Effects of material design, thermal history, and shear stresses
3 during melt processing. *J Appl Polym Sci.* 2017;134(32):1–19.
- 4 103. Nanthananon P, Seadan M, Pivsa-Art S, Hamada H, Suttiruengwong S. Facile
5 preparation and characterization of short-fiber and talc reinforced Poly(lactic
6 acid) hybrid composite with in situ reactive compatibilizers. *Materials (Basel).*
7 2018;11(7):1–13.
- 8 104. Zhang L, Tian H, Chen J, Hao Y, Liu Y, Sun Y, et al. Insight into roles of different
9 types of additives on mechanical and crystalline properties of polylactic acid. *J*
10 *Appl Polym Sci.* 2022;139(11):1–10.
- 11 105. Agüero Á, Garcia-Sanoguera D, Lascano D, Rojas-Lema S, Ivorra-Martinez J,
12 Fenollar O, et al. Evaluation of different compatibilization strategies to improve
13 the performance of injection-molded green composite pieces made of
14 polylactide reinforced with short flaxseed fibers. *Polymers (Basel).*
15 2020;12(4):1–22.
- 16 106. Madera-Santana TJ, Freile-Pelegrín Y, Encinas JC, Ríos-Soberanis CR,
17 Quintana-Owen P. Biocomposites based on poly(lactic acid) and seaweed
18 wastes from agar extraction: Evaluation of physicochemical properties. *J Appl*
19 *Polym Sci.* 2015;132(31):1–8.
- 20 107. Monika, Pal AK, Bhasney SM, Bhagabati P, Katiyar V. Effect of Dicumyl
21 Peroxide on a Poly(lactic acid) (PLA)/Poly(butylene succinate)
22 (PBS)/Functionalized Chitosan-Based Nanobiocomposite for Packaging: A
23 Reactive Extrusion Study. *ACS Omega.* 2018 Oct 31;3(10):13298–312.
- 24 108. Chen Y, Liu S, Zhou Y, Zeng G, Liu W. Biodegradable PLA-based composites
25 modified by POSS particles. *Polym Technol Mater.* 2020;59(9):998–1009.
- 26 109. Degé PH, Dubois PH, Jacobsen S, Fritz HG, Jérôme R. Beneficial effect of
27 triphenylphosphine on the bulk polymerization of L, L-lactide promoted by 2-
28 ethylhexanoic acid tin (II) salt. *J Polym Sci Part A Polym Chem.*
29 1999;37(14):2413–20.
- 30 110. Bourbigot S, Fontaine G, Gallos A, Bellayer S. Reactive extrusion of PLA and of

- 1 PLA/carbon nanotubes nanocomposite: Processing, characterization and flame
2 retardancy. *Polym Adv Technol.* 2011;22(1):30–7.
- 3 111. Gallos A, Fontaine G, Bourbigot S. Reactive extrusion of intumescent
4 stereocomplexed poly-L,D-lactide: characterization and reaction to fire. *Polym*
5 *Adv Technol.* 2013 Jan;24(1):130–3.
- 6 112. Gallos A, Fontaine G, Serge B. Influence of MWNT and α -Tropolone on Thermal
7 Stability and Crystallinity Behavior of Stereocomplexed Poly-l,d-lactides. *Ind*
8 *Eng Chem Res.* 2014 Jun 4;53(22):9377–82.
- 9 113. Viamonte-Aristizábal S, García-Sancho A, Arrabal Campos FM, Martínez-Lao
10 JA, Fernández I. Synthesis of high molecular weight L-Poly(lactic acid (PLA) by
11 reactive extrusion at a pilot plant scale: Influence of 1,12-dodecanediol and
12 di(trimethylol propane) as initiators. *Eur Polym J.* 2021;161(June).
- 13 114. Dubey SP, Abhyankar HA, Marchante V, Brighton JL, Bergmann B, Trinh G, et
14 al. Microwave energy assisted synthesis of poly lactic acid via continuous
15 reactive extrusion: modelling of reaction kinetics. *RSC Adv.* 2017;7(30):18529–
16 38.
- 17 115. Dubey SP, Abhyankar HA, Marchante V, Brighton JL, Blackburn K, Temple C,
18 et al. Modelling and validation of synthesis of poly lactic acid using an alternative
19 energy source through a continuous reactive extrusion process. *Polymers*
20 *(Basel).* 2016;8(4).
- 21 116. Bonnet F, Stoffelbach F, Fontaine G, Bourbigot S. Continuous cyclo-
22 polymerisation of l-lactide by reactive extrusion using atoxic metal-based
23 catalysts: Easy access to well-defined polylactide macrocycles. *RSC Adv.*
24 2015;5(40):31303–10.
- 25 117. Fina A, Colonna S, Maddalena L, Tortello M, Monticelli O. Facile and Low
26 Environmental Impact Approach to Prepare Thermally Conductive
27 Nanocomposites Based on Polylactide and Graphite Nanoplatelets. *ACS*
28 *Sustain Chem Eng.* 2018;6(11):14340–7.
- 29 118. Louisy E, Fontaine G, Gaucher V, Bonnet F, Stoclet G. Comparative studies of
30 thermal and mechanical properties of macrocyclic versus linear polylactide.

- 1 Polym Bull. 2020;(0123456789).
- 2 119. Louisy E, Bellayer S, Fontaine G, Rozes L, Bonnet F. Novel hybrid poly(L-lactic
3 acid) from titanium oxo-cluster via reactive extrusion polymerization. Eur Polym
4 J. 2020;122(June):109238.
- 5 120. Mincheva R, Narayana Murthy Chilla S, Todd R, Guillerm B, De Winter J,
6 Gerbaux P, et al. Reactive Extrusion and Magnesium (II) N-Heterocyclic
7 Carbene Catalyst in Continuous PLA Production. Polymers (Basel). 2019 Dec
8 2;11(12):1987.
- 9 121. Nishida M, Nishimura Y, Tanaka T, Oonishi M, Kanematsu W. Solid state NMR
10 analysis of poly(L-lactide) random copolymer with poly(ϵ -caprolactone) and its
11 reactive extrusion process. Vol. 123, Journal of Applied Polymer Science. 2012.
12 p. 1865–73.
- 13 122. Terzopoulou Z, Zamboulis A, Bikiaris DN, Valera MA, Mangas A. Synthesis,
14 Properties, and Enzymatic Hydrolysis of Poly(lactic acid)-co-Poly(propylene
15 adipate) Block Copolymers Prepared by Reactive Extrusion. Polymers (Basel).
16 2021 Nov 26;13(23):4121.
- 17 123. Geng Z, Zhen W. Preparation, Performance, and Kinetics of Poly(Lactic-
18 Acid)/Amidated Benzoic Acid Intercalated Layered Double Hydroxides
19 Nanocomposites by Reactive Extrusion Process. Polym Compos.
20 2019;40(7):2668–80.
- 21 124. Tsuji H. Poly(lactic acid) stereocomplexes: A decade of progress. Adv Drug
22 Deliv Rev. 2016 Dec;107:97–135.
- 23 125. Gallos A. Polylactides stéréocomplexés et ignifugés : Élaboration par extrusion
24 réactive et caractérisations. 2011;
- 25 126. Nishida M, Tanaka T, Yamaguchi T, Suzuki K, Kanematsu W. Intercalative
26 polymerization of L-lactide with organically modified clay by a reactive extrusion
27 method and instrumental analyses of the poly(lactic acid)/clay nanocomposites.
28 J Appl Polym Sci. 2012 Jul 25;125(SUPPL. 1):2658–67.
- 29 127. Bourbigot S, Vanderhart DL, Gilman JW, Awad WH, Davis RD, Morgan AB, et
30 al. Investigation of nanodispersion in polystyrene-montmorillonite

- 1 nanocomposites by solid-state NMR. *J Polym Sci Part B Polym Phys.*
2 2003;41(24):3188–213.
- 3 128. Salimi K, Şen SC, Ersan HY, Pişkin E. Fabrication of starch- g -poly(l -lactic
4 acid) biocomposite films: Effects of the shear-mixing and reactive-extrusion
5 conditions. *J Appl Polym Sci.* 2017 Apr 5;134(13).
- 6 129. Li Y, Zhen W. Preparation and Performance of Poly(Lactic Acid)- γ -Cyclodextrin
7 Inclusion Complex-Poly(Lactic Acid) Multibranched Polymers by the Reactive
8 Extrusion Process. *Polym - Plast Technol Eng.* 2018;57(9):836–49.
- 9 130. Mincheva R, Guemiza H, Hidan C, Moins S, Coulembier O, Dubois P, et al.
10 Development of inherently flame-retardant phosphorylated pla by combination
11 of ring-opening polymerization and reactive extrusion. *Materials (Basel).*
12 2020;13(1):1–13.
- 13